Title
DIFFUSION OF LANTHANUM IN MOLTEN URANIUM

Author
Hovingh, Jack.

Publication Date
1973-02-01

DIFFUSION OF LANTHANUM IN MOLTEN URANIUM

Jack Hovingh
(M.S. thesis)

February 1973

Prepared for the U.S. Atomic Energy Commission
under Contract W-7405-ENG-48

LBL-1130
c.1

DISCLAIMER

DIFFUSION OF LANTHANUM IN MOLTEN URANIUM

Contents

DIFFUSION OF LANTHANUM IN MOLTEN URANIUM

Jack Hovingh

Inorganic Materials Research Division, Lawrence Berkeley Laboratory
and Department of Nuclear Engineering, College of Engineering;
University of California, Berkeley, California

and

Mechanical Engineering Department, Lawrence Livermore Laboratory

ABSTRACT

The diffusion coefficient and saturation concentration of lanthanum in molten uranium was measured using a capillary tube technique. Activated lanthanum was placed on top of a uranium ingot in a beryllia capillary tube. The capillary tube was heated to 1200°C, held at temperature for various diffusion times, and cooled. The lanthanum concentration was determined as a function of distance in the uranium from the lanthanum uranium interface by counting the photons emitted by the decay of the activated lanthanum.

The measured diffusion coefficient of lanthanum in molten uranium appears to be at least an order of magnitude less than predicted by theory. The measured saturation concentration of lanthanum in molten uranium appears to be several times higher than previously reported. The higher apparent saturation concentration may be caused by lanthanum seepage into a gap formed between the uranium ingot and the beryllia capillary tube during heating.

I. INTRODUCTION

Systematic measurements of the transport properties such as thermal conductivity, viscosity and diffusivity of simple liquid systems are needed to further our understanding of the liquid state. The interest in the diffusion of lanthanides in uranium is important in the melt refining of fission products from uranium,[1] since the fission product yield as a function of mass number has a maximum at 95 (molybdenum) and 140 (the lanthanides).[2] Since the lanthanides have high neutron capture cross sections, their removal is mandatory if uranium is to be recycled and reused as a thermal reactor fuel. The melt refining process is a pyrometallurgical method of reprocessing molten spent uranium in an oxide crucible such as urania, zirconia, or alumina. The fission products that are more stable than the oxide used are removed selectively from the melt. Elements such as the lanthanides react with the oxide crucible, while elements such as cesium, iodine and the rare gases volatize off. The rate of the melt refining process is dependent in part on the diffusion coefficient of the lanthanides in the uranium.

The purpose of this experiment is to measure the diffusion coefficient of lanthanum in molten uranium. Since liquid lanthanum is partially miscible in liquid uranium the diffusion coefficient can be measured by a simple capillary tube method.

Because of the high temperatures required ($> 1200°C$) and the agressive attack of most crucible materials by molten uranium, very few transport properties of molten uranium have been successfully measured. Smith,[1] using a 7 mm diameter capillary tube, measured a diffusion coefficient of cerium in molten uranium of 1×10^{-4} cm^2/sec at 1200°C. LeBorgne[3]

tried using a modified version of the capillary technique developed by Kitchener[4] to determine the diffusion coefficient of lanthanum in molten uranium. LeBorgne used a 3.2 mm diameter capillary tube and found the diffusion coefficient of lanthanum in molten uranium to be as low as 4.5×10^{-7} cm^2/sec. Upon sectioning a specimen, LeBorgne found large bubbles in the uranium near the lanthanum-uranium interface. It is believed that these bubbles may have caused the very low diffusion coefficients that he measured. In essence, this experiment is a repeat of LeBorgne's work, with the effort devoted to elimination of the bubbles.

The diffusion coefficient may be estimated by semitheoretical methods. Castleman and Conti[5] have arrived at an equation for the diffusion coefficients of liquid metals as a function of the melting points of the metal as

$$D = \frac{0.655\ T^{3/2}\ \sigma_{ij}}{M^{1/2}\left(\frac{\varepsilon_{ij}}{k} \times 10^{-3}\right)\Sigma} \qquad (1)$$

where M is the molecular weight of the solvent, T is the absolute diffusion temperature, Σ is a dimensionless force constant, σ_{ij} is the intermolecular separation where the Lennard-Jones potential is zero between unlike molecules, k is the Boltzmann constant, and ε_{ij} is the well depth of the Lennard-Jones potential for an interaction between unlike particles. The force constant can be determined from

$$\Sigma = \left[-(\sigma_{ij}/R_{ij})^7 + 2(\sigma_{ij}/R_{ij})^{13}\right]\Big|_{\bar{n},R_{ij}=R_{ab}} \qquad (2)$$

where σ_{ij}/R_{ab} can be determined from

$$(\sigma_{ij}/R_{ab})^{12}-(\sigma_{ij}/R_{ab})^{6} = 0.072\left(\frac{T^2}{T_m T_{m_s}}\right)^{1/2} - 0.25 \qquad (3)$$

with T_m and T_{m_s} the melting points of the solvent and the solute metals, and R_{ab} is the specific intermolecular distance for a molecular pair.

Castleman and Conti compute the well depth of the Lennard-Jones potential in terms of the melting point from

$$\varepsilon/k = 5.2\ T_m \qquad (4)$$

and

$$\varepsilon_{ij} = [\varepsilon_{ii}\ \varepsilon_{jj}]^{1/2} \qquad (5)$$

Bird et al.[6] give an expression for the intermolecular separation where the Lennard-Jones potential is zero for like molecules as

$$\sigma_{ii} = (1.82\ \frac{M}{\rho})\ 1/3 \qquad (6)$$

where ρ is the solid density of the metal. The above equation can be used to compute

$$\sigma_{ij} = \frac{1}{2}\ (\sigma_{ii} + \sigma_{jj}) \qquad (7)$$

The diffusion coefficient of lanthanum in molten uranium at 1200°C was found from Eq. (1) to be

$$D = 2.6 \times 10^{-5}\ cm^2/sec$$

Olander and Pasternak[7] calculated a diffusion coefficient for lanthanum in molten uranium of 1.5×10^{-5} cm^2/sec using the Stokes-Einstein equation. Using the modified rate method Olander and Pasternak[8,9]

calculated the diffusion coefficient for lanthanum in molten uranium as 2.5×10^{-5} cm^2/sec.

Thus the three different theoretical diffusion models estimate the diffusion coefficient of lanthanum in molten uranium as

$$1.5 \times 10^{-5} \leq D \leq 2.6 \times 10^{-5} \ cm^2/sec.$$

II. THEORETICAL ANALYSIS

A. Mathematical Model

The statement of conservation of matter which describes diffusion in a long capillary is

$$\frac{\partial c}{\partial t} = D \frac{\partial^2 c}{\partial x^2} \tag{8}$$

Equation (8) assumes a one-dimensional system and a constant diffusion coefficient.

B. Initial and Boundary Conditions

For the capillary tube the concentration of the diffusing medium is initially zero

$$C(x,0) = 0 \tag{9}$$

We will assume that the capillary tube is infinitely long which gives

$$C(x\to\infty,t)\to 0 \tag{10}$$

The final boundary condition assumes a fixed concentration of the diffusing solute at the lanthanum-uranium interface

$$C(0,t) = C_o \tag{11}$$

In the present case, C_o is the saturation concentration of lanthanum in uranium.

C. Solution of the Problem

For diffusion from a constant source into a semi-infinite medium, the ratio of the diffusing solute concentration at any point $x \geq 0$ in a solvent to that at the interface $x = 0$ is given by[10]

$$\frac{C(x,t)}{C_o} = \operatorname{erfc} \frac{x}{2\sqrt{Dt}} \tag{12}$$

III. EXPERIMENTAL APPARATUS

A. Furnace and Diffusion Apparatus

The vacuum system shown in Fig. 1 consists of a roughing pump and an ion pump to evacuate a 12 cubic feet bell jar. The experimental apparatus is shown in Fig. 2. The specimen holder consisting of a beryllia crucible in a molybdenum holder is similar to that used by LeBorgne in his diffusion experiments, and the support system is similar to that used by Finucane to measure the viscosity of uranium.[11] The water-cooled Brew furnace with tungsten mesh heating element and heat shields is regulated by a Powerstat connected to a 31.5 kva, 60 hertz, 3 phase transformer with a primary potential of 480 volts, secondary potential of 15 volts. The crucible holder temperature is measured by an optical pyrometer sighted through a right angle prism into a 3.2 mm diameter hole in the furnace bottom heat shield pack.

B. Counting System

The counting system shown in Fig. 3 is used to determine the concentration profile of the activated lanthanum in the uranium. The activated specimen is placed in a lead pig. The position of a specimen interface relative to the collimating slit in the pig can be adjusted vertically by turning a screw, and the change in position can be read directly on the measuring system. The position of the counting point from the interface can be determined within ± 0.3 millimeter.

The counting system consists of a Harshaw Type 6S812 1-1/2 inch diameter by 2-in.-thick thallium activated sodium iodide crystal optically coupled to a RCA 6342A multiplier phototube. The signal from the detector is fed into a RIDL Model 10-17 preamplifier. The

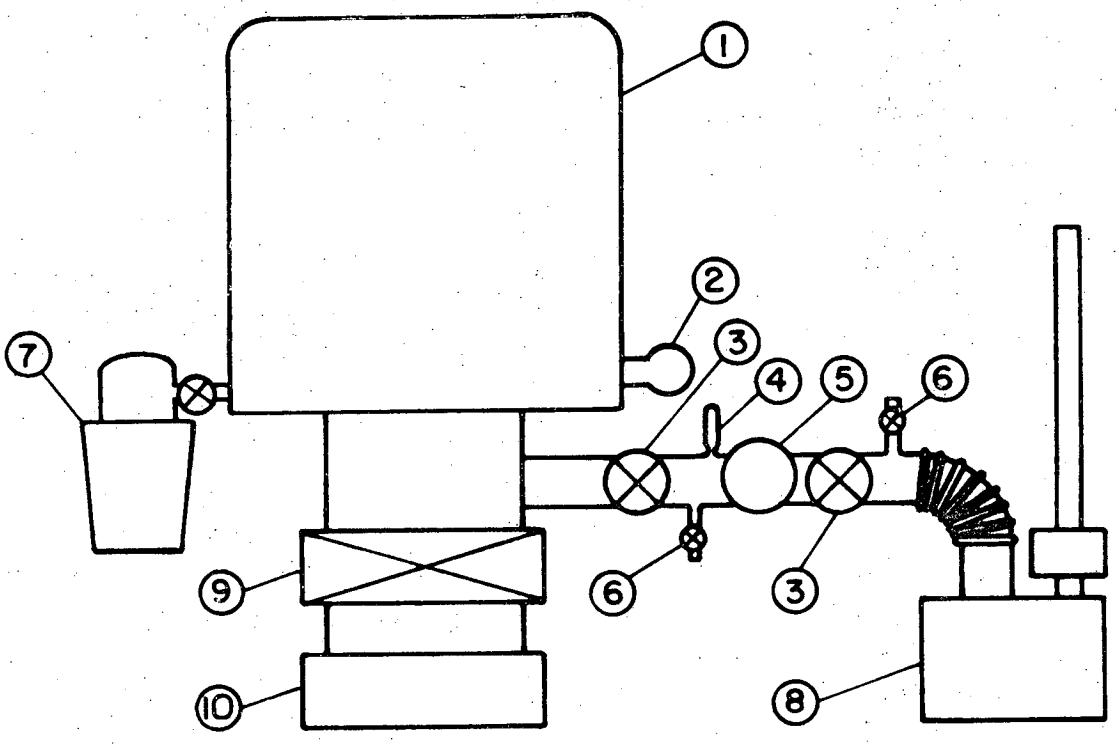

1 Stainless Steel Bell Jar
2 Ion Gauge
3 Roughing Valve
4 Thermocouple Gauge
5 Foreline Trap
6 Vacuum Release Valve
7 Sorption Pump and Valve
8 Roughing Pump
9 6" Gate Valve
10 200 L/S Ion Pump

XBL729-6921

Fig. 1. Vacuum System.

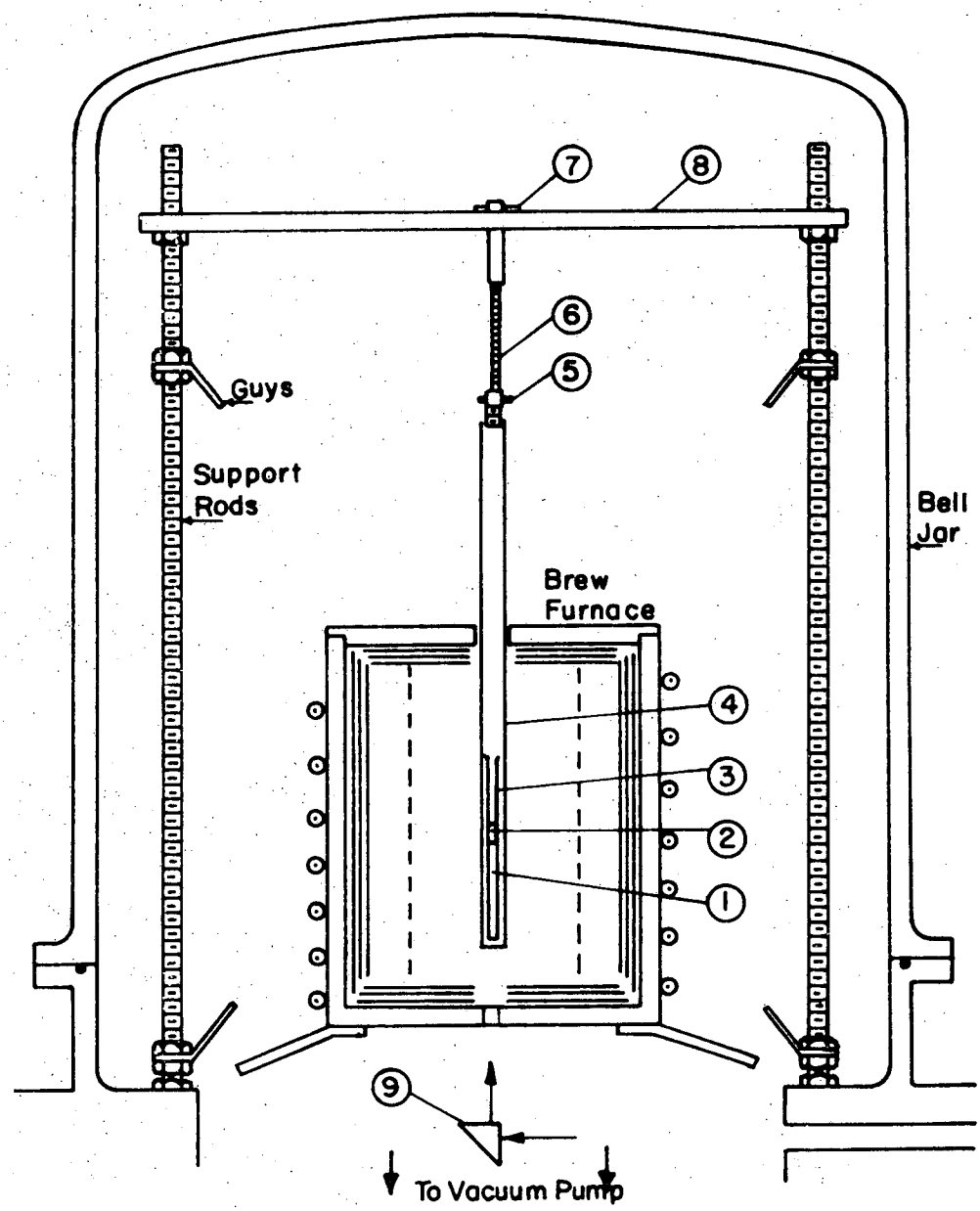

1 Molten Uranium
2 Molten Lanthanum
3 Beryllia Crucible
4 Molybdenum Holder
5 Stainless Steel Cap
6 Adjustable Support Rod
7 Support Pin
8 Stainless Steel Support Plate
9 Prism for Pyrometer Sighting

XBL729-6922

Fig. 2. New encapsulation scheme for containing molten activated lanthanum.

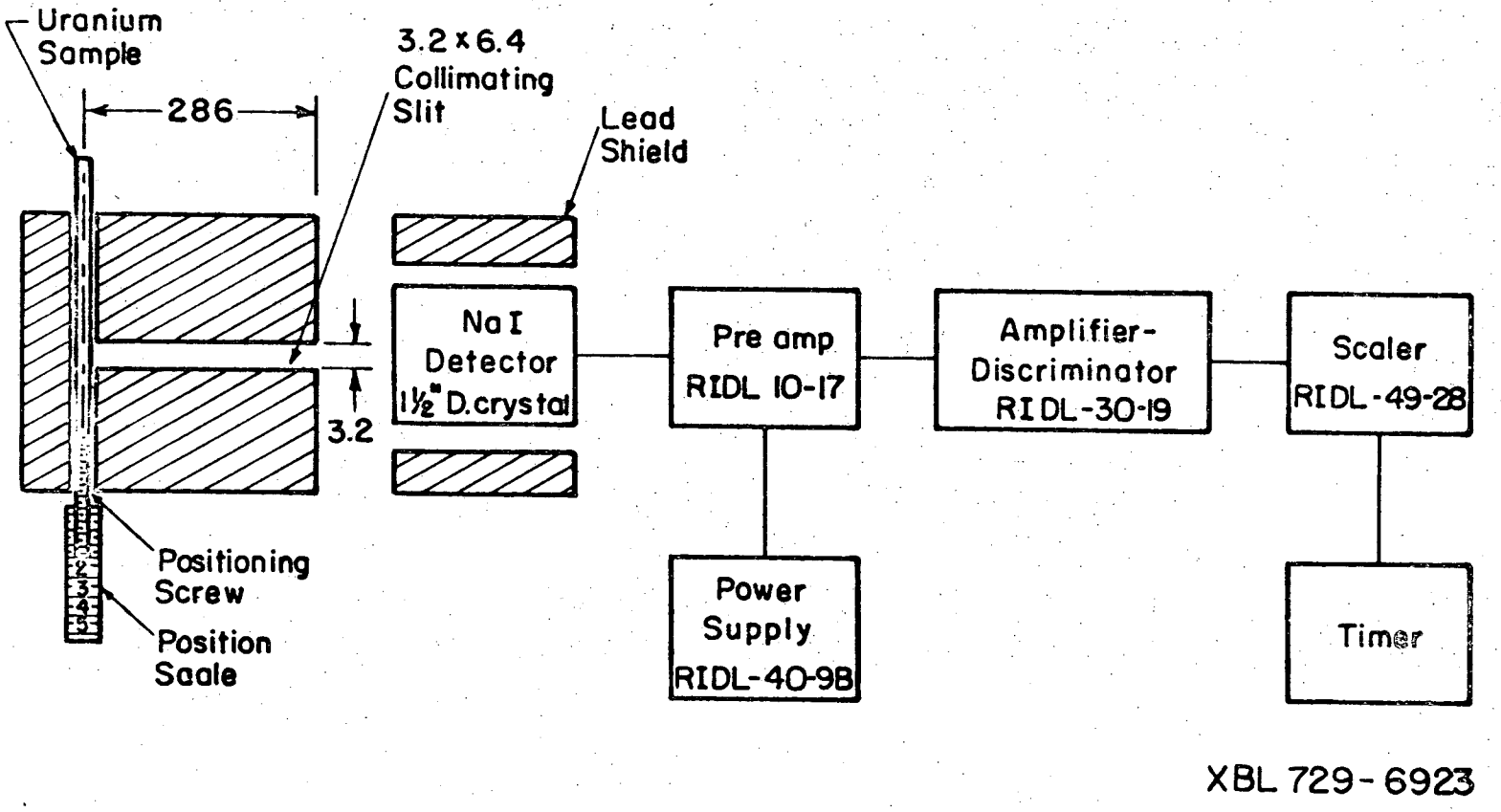

Fig. 3. Block diagram of the counting equipment. Dimensions in millimeters except as noted.

output is amplified by a RIDL Model 30-19 amplifier-discriminator. A RIDL Model 49-28 scaler connected to a timer is used to read the number of counts. A RIDL Model 40-9B power supply is used as a high voltage source in the counting circuit. The calibration of the counting system is discussed in Appendix VII.

C. Counting Procedure

The test assembly consisting of the uranium and activated lanthanum in the beryllia crucible held in a molybdenum crucible holder is placed in the lead counting pig. The positive measuring system is set to zero when the bottom of the molybdenum crucible holder is centered in the beam collimating slit. The assembly is counted for a set time and then the position is changed in one millimeter steps. Thus the lanthanum-140 activity which is proportional to the concentration of lanthanum in the uranium was obtained as a function of distance from the bottom of the test assembly.

IV. EXPERIMENTAL PROCEDURE

A. Melting Procedure

Several changes in the melting procedures used by LeBorgne were made for this experiment. The tantalum crucibles used by LeBorgne were eliminated because the molten uranium was found to leak out of them at temperatures of as low as 1200°C for times as short as 3 hours. The leakage mechanism was intergranular diffusion of the molten uranium through the tantalum.

An attempt was made to eliminate the bubbles which formed in the uranium by vibration of the molten uranium. However the vibration did not completely eliminate the bubbles. The bubbles were finally eliminated by multiple melts of each uranium ingot in beryllia crucibles, with cleaning of the ingot between each melt.

The as-received uranium rod was cleaned by clamping the specimen in a vise and filing until the surface was clean and shiny. The uranium was weighed and placed in a beryllia crucible. The distance from the mouth of the crucible to the top of the uranium rod was measured. The crucible was placed into the vacuum furnace and the system was evacuated to the 10^{-6} torr range. The furnace was brought up to 1300°C in slow steps such that the pressure in the bell jar did not exceed 5×10^{-5} torr. Heat up required about 3 hours. The crucible was held at about 1300°C for 3 hours before it was cooled down in the vacuum, and the system brought up to dry nitrogen.

The uranium was then removed from the beryllia crucible, cleaned and remelted. The number of times the uranium was melted was dependent upon the removal of the gases which caused bubbles in the uranium.

Bubble formation in the uranium ingot could be determined by the difference in height of the uranium in the beryllia crucible before and after melting.

The changes in melting procedures and the bubble formation in the uranium ingots are more fully discussed in Appendix VIII.

B. Diffusion Procedure

Two changes were made in LeBorgne's procedures for the diffusion runs. The first change involved the elimination of the flowing helium during diffusion. The helium flow rate could not be maintained at a constant level. The fluctuations in flow rate caused large fluctuations in the specimen temperature. The diffusion runs were conducted at a pressure of about 10^{-6} torr.

The welded capsule used to contain the lanthanum and uranium during the diffusion run was also eliminated. Instead a screw top capsule was used. This system contained the activity of the lanthanum without a visible oxide coating forming on the uranium-lanthanum interface.

The "gas free" uranium obtained from the melts described above was cleaned as before, weighed and placed in a beryllia crucible which had been baked out at 1300°C for 3 hours at a pressure of 10^{-5} to 10^{-6} torr. The uranium was held at 1300°C for 3 hours at a pressure of 10^{-5} to 10^{-6} torr and cooled down in the vacuum. The system was brought up to dry nitrogen and the uranium interface measured to insure no bubbles in the ingot. The beryllia crucible containing the uranium ingot was placed in a glove box flushed with dry nitrogen.

A 0.5 gram piece of 99.9% pure lanthanum metal was cleaned by filing while in the glove box and placed in a polyethylene snap-top irradiation capsule. The sample was irradiated for 30 min in the U. C. Berkeley TRIGA

reactor to generate approximately 20 mCi of lanthanum-140 by neutron capture in lanthanum-139.

After irradiation the activated lanthanum slug was returned to the glove box for opening and placed on the uranium ingot in the beryllia crucible. This assembly of the beryllia crucible, activated lanthanum and uranium ingot was placed in a molybdenum screw cap crucible holder. The assembly was counted in the lead collimator as a function of distance from the bottom of the assembly to estimate the lanthanum-uranium interface. The counter discriminator was set to count only photons with energies greater than 1.4 MeV.

The assembly was placed in the vacuum furnace and the system evacuated to the 10^{-6} torr range. The furnace was brought up to the desired temperature in a manner such that the bell jar pressure did not exceed 5×10^{-5} torr. To meet this requirement, the elapsed time between the melting of the lanthanum at 926°C and the melting of the uranium at 1132°C was about 60 minutes. The assembly was held at 1200°C for the desired diffusion time at a pressure between 10^{-5} and 10^{-6} torr, and cooled in vacuum. The vacuum system was brought up to dry nitrogen and the assembly counted as before. In all cases the elapsed time between the irradiation of the lanthanum and the diffusion counting was about 40 hours, or one half-life of lanthanum-140.

C. Summary of Procedures for Diffusion Runs

A summary of the melt and diffusion run pressures, temperatures, and times is given in Table I. Run #6 was a failure as the uranium diffused through the tantalum crucible during the lanthanum diffusion run.

Table I. Description of Diffusion Runs

Run	Melt	Temperature (°C)	Time at Temperature (min)	Pressure (torr)	Crucible* Bakeout	Comments
1	9	1300	180	1×10^{-6}	None	New Uranium and vibrated
	12	1304	180	2.2×10^{-6}	3 hr @ 1300°C	60 minutes**
		1220†	720†	2.9×10^{-6}		
2		1300	180	?	?	melted by LeBorgne #2 in Fig. 49
	15	1320	180	1×10^{-6}	3 hr @ 1330°C	
	16	1320	180	8×10^{-7}	3 hr @ 1310°C	71 minutes**
		1200†	480†	1×10^{-6}		
3		1300	180	?	?	melted by LeBorgne #4 in Fig. 49
	17	1315	180	1.1×10^{-6}	3.25 hr @ 1205°C	
	18	1320	180	8×10^{-7}	3 hr @ 1305°C	67 minutes**
		1200†	480†	1.2×10^{-6}		
4	19	1320	240	1×10^{-6}	None	New Uranium
	20	1323	180	1×10^{-6}	3 hr @ 1323°C	
	21	1312	180	8×10^{-7}	3 hr @ 1335°C	62 minutes**
		1216†	960†	9×10^{-7}		
5		1300	180	?	?	melted by LeBorgne #3 in Fig. 49
	13	1315	180	2×10^{-6}	3 hr @ 1302°C	
	14	1320	180	9×10^{-7}	3 hr @ 1305°C	
	22	1317	360	5×10^{-7}		remelt of melt 14
	23	1323	185	1.5×10^{-6}	3 hr @ 1310°C	60 minutes**
		1200†	240†	1.1×10^{-6}		
6	24	1315	180	6×10^{-7}	None	New Uranium
	25	1310	181	1×10^{-6}	None	Added scraps of Uranium
	26	1310	180	1×10^{-6}	3 hr @ 1325	
	27††	1220	23	2×10^{-6}	None	60 minutes** Uranium leaked through bottom of crucible
		1200†	240†	1.3×10^{-6}		

*Pressure between 10^{-4} to 10^{-6} torr

†Diffusion temperature and time

**Time between melting of lanthanum and melting of uranium

††Tantalum crucible

V. DATA

A. Pre-Diffusion Counting Profile

The count rate profile of each specimen with the activated lanthanum was determined by counting prior to the diffusion melts. The purpose of the pre-diffusion counting was to determine the uranium-lanthanum interface position, the length of the activated lanthanum prior to melting, the effective window width for the counting system, and the effect of scattering of the 1.6 MeV photons from the source on the measured count rates. The pre-diffusion counting profiles for runs 1 through 6 are shown in Appendices I through VI, respectively.

B. Post-Diffusion Counting Profiles

After the diffusion run, the counting profile of each specimen was determined using 10 minute count times at one millimeter intervals along the length of the specimen. The interface position, post-diffusion lanthanum length and the effective window width were determined from the counting profile. The post diffusion counting profile for runs 1 through 6 are shown in Appendices I through VI, respectively.

VI. DATA REDUCTION

A. Estimation of the Effective Counting Window Width, Lanthanum Length And the Location of the Lanthanum-Uranium Interface

The activity in the region containing activated lanthanum was plotted as a function of position. Since the activity of the lanthanum is much greater than the activity on either side of the lanthanum, the effect of the finite window width varies linearly from a maximum of the average over the lanthanum length to effectively zero a window width away from the highest and lowest position of the plateau of the maximum average counts over the activated lanthanum. The procedure for estimating the effective window width and lanthanum length is illustrated in Fig. 4. The length of the lanthanum and the effective window width can be estimated from

$$L = \frac{1}{2}(a+b) \tag{13}$$

$$w = \frac{1}{2}(a-b) \tag{14}$$

where w = effective window width

L = length of activated lanthanum

a = distance between intercepts of straight lines drawn through points adjacent to activated lanthanum extrapolated to zero count.

b = distance between intercepts of straight lines drawn through points adjacent to activated lanthanum extrapolated to maximum average counts plateau over the lanthanum.

The derivation of equations (13) and (14) is shown in Appendix IX.

The pre-diffusion and post-diffusion curves for estimating the effective window widths and lanthanum lengths for runs 1 through 6 are shown in Appendices I through VI, respectively. The position of the

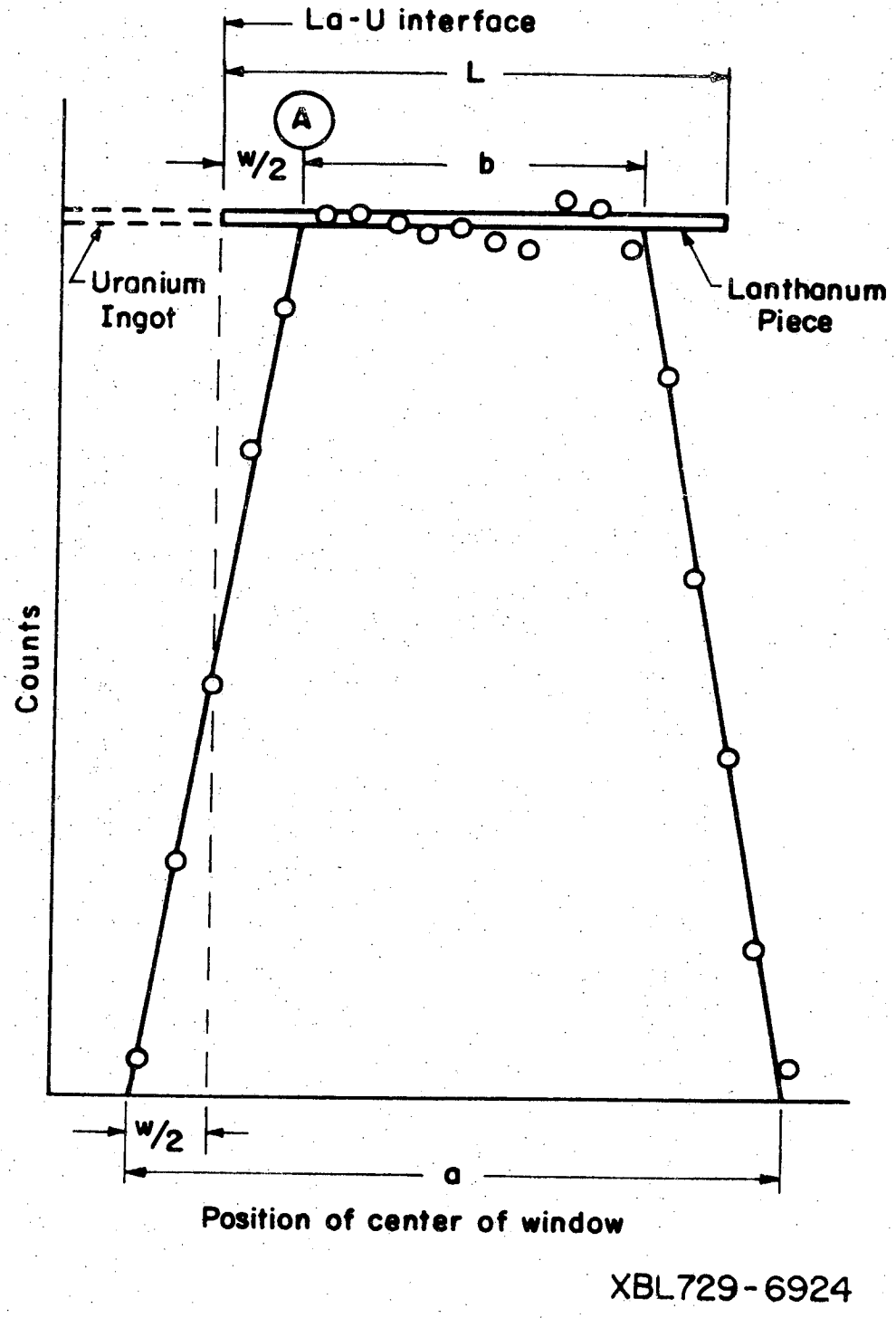

Fig. 4. Illustration of procedure to estimate lanthanum length and effective window width using counting data.

uranium-lanthanum interface can be estimated by subtracting half the estimated effective window width (w/2) from the position that the lines drawn through points adjacent to the uranium side of the activated lanthanum intercept the maximum average counts plateau over the activated lanthanum (point A in Fig. 4). This technique for estimating the position of the uranium-lanthanum interface is illustrated in Fig. 4. Note that the effective window width is assumed to be symmetric on both sides of the activated lanthanum.

B. Relation Between the Measured Count Rate and the Lanthanum Concentration

The relationship between the volumetric concentration of the lanthanum in the slice of metal which fills the window slit in the shielding pig to the detector and the measured count rate is needed to permit Eq. (12) to be used to determine the diffusion coefficient. The volumetric concentration and the measured count rate are related by

$$C = K(A-A_s-A_{bkg})F \tag{15}$$

where C is the molar concentration of lanthanum in uranium, A is the measured count rate at a distance x in the uranium measured from the lanthanum-uranium interface, A_s is the count rate at x due to scattering of 1.6 MeV photons from the activated lanthanum by uranium filling the window, A_{bkg} is the background count rate, F is the correction for the non-zero window width, and K is the counting instrument and geometry constant.

The scattering correction term A_s depends upon the window width w, the length of the lanthanum rod L, and the distance x. By considering

the attenuation of gamma rays in the ingot of uranium between tne interface and measurement point, the scattering correction is shown in Appendix X to be given by

$$\frac{A_s}{A^*} = \frac{k'}{w^2} e^{-\mu_u x} \ln\left[\left(\frac{x-1/2\ w+L}{x+1/2\ w+L}\right)\left(\frac{x+1/2\ w}{x-1/2\ w}\right)\right] \qquad (16)$$

where A^* is the count rate when lanthanum completely fills the window and k' is determined from the pre-diffusion data, i.e., before the lanthanum is melted. The background count rate A_{bkg} was subtracted from the measured A_s and A^* before applying Eq. (16) to determine k' using the pre-diffusion lanthanum length and effective slit width. This value of k' is used to obtain the scattering correction term in Eq. (15) for the post-diffusion count rates from Eq. (16) with the post-diffusion lanthanum length and effective window width. Note that as a result of the melting, the lanthanum rod fills the cross section of the capillary with a resultant decrease in length such that the post-diffusion lanthanum length is less than the pre-diffusion length. Also the meniscus between the uranium and the lanthanum is filled with lanthanum after the diffusion run resulting in a reduction in the sharp cut-off of the lanthanum slug and an apparent increase in the effective window width of the post-diffusion data compared with the pre-diffusion data.

The factor F which corrects for the non-zero width of the slit to the detector system is shown in Appendix XI to be

$$F(P,\eta) = \frac{2P\ \mathrm{erfc}\ (P\eta)}{\int_{P(\eta-1}^{P(\eta+1)} \mathrm{erfc}(u)\,du} \qquad (17)$$

where

$$P = \frac{w}{4\sqrt{Dt}} \tag{18}$$

$$\eta = \frac{2x}{w} \tag{19}$$

C. Approximate Determination of the Diffusion Coefficient

Consider two positions x_1 and x_2 in the post-diffusion uranium. From Eq. (12)

$$C_o = \frac{C(x_1,t)}{\operatorname{erfc} \frac{x_1}{2\sqrt{Dt}}} = \frac{C(x_2,t)}{\operatorname{erfc} \frac{x_2}{2\sqrt{Dt}}} \tag{20}$$

From Eq. (15) for the relationship between C and A and Eqs. (18) and (19) for the definitions of P and η, Eq. (20) becomes

$$\frac{(A_1-A_{s_1}-A_{bkg})F(P,\eta_1)}{\operatorname{erfc}(P\eta_1)} = \frac{(A_2-A_{s2}-A_{bkg})F(P,\eta_2)}{\operatorname{erfc}(P\eta_2)} \tag{21}$$

The measured count rates are corrected for scattering by using Eq. (16) and the background count rate is subtracted out. With η_1 and η_2 also known, Eq. (21) is solved numerically for P which gives a preliminary estimate of the diffusion coefficient by Eq. (18).

D. Determination of the Solubility of Lanthanum in Uranium

The solubility of lanthanum in uranium may be determined from the assumption that the uranium at the interface between the two partially miscible liquids is saturated with lanthanum. Using Eqs. (15) and (20), C_o is given by

$$C_o = \frac{K(A-A_s-A_{bkg})F(P,\eta)}{\text{erfc}(P\eta)} \tag{22}$$

If the window is placed so that it is entirely filled by the lanthanum, Eq. (15) becomes

$$C^* = K(A^*-A_{bkg}) \tag{23}$$

where A^* is the measured count rate under these conditions and C^* is the molar concentration of pure lanthanum

$$C^* = \frac{\rho_L}{M_L} \tag{24}$$

where ρ_L and M_L are the density and atomic weight, respectively, of lanthanum. Dividing Eq. (22) by Eq. (23)

$$\frac{C_o}{C^*} = \frac{(A-A_s-A_{bkg})F(P,\eta)}{(A^*-A_{bkg})\text{erfc}(P\eta)} \tag{25}$$

Let S be the solubility of lanthanum in liquid uranium expressed as a weight fraction. Then

$$C_o = \frac{S/M_L}{1/\rho_u} = \frac{\rho_u S}{M_L} \tag{26}$$

where the density of the lanthanum saturated uranium has been assumed equal to that of pure uranium. Substituting Eqs. (24) and (26) into Eq. (25) and solving for S yields

$$S = \frac{\rho_L}{\rho_u}\ \frac{C_o}{C^*}$$

$$= \frac{\rho_L}{\rho_u}\ \frac{(A-A_s-A_{bkg})F(P,\eta)}{(A^*-A_{bkg})\text{erfc}(P\eta)} \tag{27}$$

Thus a value of S may be inferred from the diffusion experiments by utilizing the data from the measured count rates at any distance x from the lanthanum-uranium interface.

E. Determination of the Diffusion Coefficient

The diffusion coefficient may be determined graphically using the data from a single experiment. Writing Eq. (12) as

$$\frac{C}{C_o} = \frac{C}{C^*}\,\frac{C^*}{C_o} = \operatorname{erfc}\,\frac{x}{2\sqrt{Dt}} \tag{28}$$

and using Eq. (15) for C, Eq. (23) for C^* and Eq. (26) with the experimentally determined value of S, the above equation becomes

$$\operatorname{erfc}^{-1}\left(\frac{[A(x)-A_s(x)-A_{bkg}]F(P,\eta)}{A^*-A_{bkg}}\cdot\frac{(\rho_L/\rho_u)}{S}\right) = \frac{x}{2\sqrt{Dt}} \tag{29}$$

where the preliminary estimate of D is used to compute the window correction factor $F(P,\eta)$, and $\operatorname{erfc}^{-1}(U) = z$ is the inverse complementary error function such that

$$U = \operatorname{erfc}(z) \tag{30}$$

The complementary error function is tabulated in Carslaw and Jaeger,[10] AMS 55,[12] or can be computed using the methods of Stegun and Zucker.[13] A plot of the experimentally determined left hand side of Eq. (29) as a function of the distance x from the uranium-lanthanum interface should give a straight line of slope $(2\sqrt{Dt})^{-1}$. Since the diffusion time t is known the diffusion coefficient D can be determined.

VII. RESULTS

The diffusion coefficients and solubility limits of lanthanum in molten uranium as determined from runs 1 through 5 are shown in Table II. Also included in Table II are LeBorgne's results for the diffusion of lanthanum in molten uranium and Smith's results for the diffusion of cerium in molten uranium.

Table II. Diffusion coefficient and solubility of lanthanum in molten uranium at 1200°C

Run	Diffusion coefficient (cm^2/sec)	Solubility weight fraction	Run time (min)
1	4.2×10^{-7}	0.15	720
2	4.2×10^{-6}	0.050	480
3	1.8×10^{-6}	0.066	480
4	5.1×10^{-7}	0.015	960
5	8.2×10^{-6}	0.053	240
LeBorgne	4.0×10^{-7}	0.01	1440
	5.0×10^{-7}	--	1440
Smith*	1.0×10^{-4}	0.01	26

*Cerium in molten uranium

VIII . DISCUSSION OF RESULTS

A. Diffusion Coefficient

The experimentally measured diffusion coefficient of lanthanum in molten uranium decreases with increasing diffusion time to a minimum of approximately 4×10^{-7} cm^2/sec after 10 hour diffusion times. As discussed in the introduction the semi-theoretically estimated diffusion coefficient of lanthanum in molten uranium ranges between

$$1.5 \times 10^{-5} < D < 2.6 \times 10^{-5} \ cm^2/sec$$

at 1200°C depending on the diffusion model selected. Thus the measured diffusion coefficient is roughly two orders of magnitude smaller than that predicted by theory.

B. Solubility Limit

The experimentally determined saturation concentration of lanthanum in molten uranium is from 2 to 20 times larger than the 0.0081 weight fraction reported by Haefling and Daane.[14] There does not appear to be a trend in the measured saturated concentration with diffusion time.

Two possible explanations exist for the larger measured saturation concentration than reported by Haefling and Daane and the decrease in the measured diffusion coefficient with diffusion time. One explanation is that during the heating for the diffusion run the lanthanum melts and flows down the gap caused by the difference in thermal expansions between the uranium ingot and the beryllia crucible. Another explanation is that the lanthanum undergoes a chemical reaction with the beryllia crucible such that the lanthanum is scavenged from the uranium and stored in the beryllia crucible as lanthana.

C. Lanthanum Penetration of the Uranium-Beryllia Gap

Eikenberry and Graman[15] have noted the formation of a gap between an uranium ingot and its graphite mold during the solidification of the uranium. During the cooling of the pre-diffusion melt of uranium in a beryllia crucible a gap may form at the uranium-crucible interface. This gap may allow seepage of the activated lanthanum between the solid uranium ingot and the crucible during the start-up of the diffusion run since the melting point of lanthanum is roughly 200°C less than that of the uranium. To prevent overloading the vacuum pump, approximately one hour was required to raise the temperature of the specimen from the melting point of lanthanum (926°C) to the melting point of uranium (1132°C). During this time seepage of the molten lanthanum into the uranium-beryllia gap could occur.

If the activated lanthanum is frozen into the gap during the cool-down of the diffusion run, the counting apparatus will measure the lanthanum activity in the gap with the result that the concentration of lanthanum in the uranium is apparently larger than actually exists. From Appendix XII the maximum probable gap width is approximately 0.07 millimeters which can result in an apparent saturation concentration of roughly twice that measured by Haefling and Daane.

Now assuming there is a gap effect the low density lanthanum may rise to the surface of the higher density uranium when the latter is liquified. Assuming that the lanthanum behaves as spherical balls in an infinite medium such as boundary layer effects along the crucible are negligible, the time required for the lanthanum balls to float to the uranium surface is given by

$$t = \frac{0.0235x}{r^2} \text{ seconds} \qquad (31)$$

where x is the distance of the lanthanum below the surface and r is the radius of the volume of the lanthanum. The terminal velocity of the volume is

$$v = 42.6\ r^2 \text{ cm/sec} \qquad (32)$$

For the diffusion runs the minimum velocity for all the lanthanum to rise to the surface from the bottom of the ingot is shown in Table III. Note that for velocities greater than 4 millimeters per hour the gap effect should disappear for all the runs assuming no diffusion of the lanthanum in the gap into the uranium and no reaction of the lanthanum with the beryllia crucible.

From Eq. (32), the radius required for the lanthanum volume to acquire a velocity greater than 4.0 millimeters per hour is roughly 0.016 millimeter, which is roughly 25% of the maximum probable gap width. Thus for a maximum probably gap the hydrodynamic flow should sweep the lanthanum from the gap such that no gap effect is apparent. However, assume that the 0.07 millimeter gap can behave as an infinite source of lanthanum for diffusion radially into the molten uranium, the time required to achieve an average concentration of lanthanum in a 3.18 millimeter diameter slug of molten uranium of 50% of the saturated concentration is

$$t = \frac{0.0015}{D} \text{ seconds}$$

where D is the diffusion coefficient in square centimeters per second. For

$$10^{-4} < D < 10^{-7} \text{ cm}^2/\text{sec}$$

Table III. Uranium ingot length and diffusion run time for diffusion runs 1 through 5

Run	Ingot length (mm)	Run time (hours)	Ingot length / Diffusion time (mm/hr)
1	35	12	2.92
2	20	8	2.50
3	20	8	2.50
4	30	16	1.88
5	15	4	3.75

then

$$15 \text{ second} < t < 4 \text{ hours}$$

Thus, for a gap of the size computed above the diffusion of lanthanum radially from the gap into the uranium could affect the results of the experiment even if the remainder of the lanthanum had floated to the top of the ingot.

In summary, the effect of a gap between the beryllia crucible and the uranium ingot on the experimental results may be to increase the apparent saturation concentration of the lanthanum in the molten uranium at the upper surface of the uranium ingot if all of the lanthanum has not floated to the top of the melt. If the lanthanum has floated to the surface of the melt, but the time required for the hydrodynamic movement was long such that diffusion of the lanthanum from the gap radially into the uranium melt could occur, the apparent diffusion coefficient measured would be larger, not smaller than the actual diffusion coefficient.

D. Reaction Between Lanthanum and Beryllia

Consider the chemical reaction

$$\frac{4}{3} La + 2BeO \rightarrow \frac{2}{3} La_2O_3 + 2Be$$

From Appendix XIII if the above reaction takes place between the beryllia crucible and the lanthanum, the lanthanum is not stable in solution in the uranium. Pulliam and Fitzsimmons[16] have observed the reduction of beryllia by lanthanum at 1200°C. From Appendix XIV the amount of lanthanum which diffuses into the beryllia crucible is small for times on the order of the diffusion run times, and the penetration distance of the lanthanum into the beryllia is short compared with the inner radius of the beryllia crucible.

Because the amount of lanthanum which diffuses into the beryllia crucible is small, this mechanism is probably not responsible for the apparent increase in the saturation concentration of lanthanum in molten uranium measured over that reported by Haefling and Daane. Also, since the diffusion coefficient of lanthanum into the beryllia crucible is much less than that of lanthanum through the molten uranium, the bulk of the transport will occur through the uranium. Thus the apparent low diffusion coefficient of lanthanum in molten uranium is not caused by scavenging of the lanthanum from the uranium by the beryllia crucible.

The net effect of both the gap and the reaction of the lanthanum with the beryllia crucible may be to increase the apparent saturation concentration of lanthanum in molten uranium. However the size of the apparent increase cannot be accounted for by the two mechanisms even if they are acting in accord. The effect of the two mechanisms on the diffusion coefficient may be compensatory, although the gap effect which would tend to increase the apparent diffusion coefficient appears to be more powerful than the effect of the reaction of the lanthanum with the beryllia crucible.

There is a trend that the magnitude of the diffusion coefficient given in Table II increases with a decrease in run time. The run with the shortest diffusion time (Run #5) gave the largest diffusion coefficient while the run with the longest diffusion time (Run #4) gave the lowest diffusion coefficient.

IX. RECOMMENDED CHANGES IN THE EXPERIMENTAL PROCEDURE FOR DETERMINING THE DIFFUSION OF LANTHANUM IN MOLTEN URANIUM

Two changes should be investigated in the experimental procedure for determining the diffusion of lanthanum in molten uranium. The first change involves the crucible material, while the second change involves the counting and melting technique.

Tungsten should be investigated as a crucible material for molten uranium. The use of tungsten would reduce the gap effect, and eliminate the possibiiity of a lanthanum-beryllia reaction. The entire crucible could be made from tungsten, or else a tungsten liner could be placed in the beryllia crucible. McIntosh and Bagley[17] report that the penetration of a tungsten crucible was 0.005 inch after 9 hours at 1300°C, and nil after 8 hours at 1250°C.

The gap effect in a beryllia crucible can be eliminated by dropping the lanthanum pellet on the uranium after the uranium has melted. This can be accomplished by supporting the lanthanum on a tantalum wire above the uranium at a distance such that the lanthanum temperature is less than, say, 600°C, and pulling the wire through a vacuum seal after the uranium melts. This technique does not allow the use of gamma counting to determine the pre-diffusion lanthanum interface.

A modification of the technique used for this experiment is to place the lead gamma shielding inside the vacuum vessel and measure the concentration of lanthanum at a fixed point above the base of the crucible as a function of time. This technique has the advantage that the counting data is taken during the diffusion run, resulting in higher count rates because of the reduced decay time of the activated lanthanum. The

lanthanum-uranium interface position can be determined by moving the crucible vertically with respect to the counting position by suspending the crucible holder on a wire attached to a micrometer vacuum feedthrough.

The diffusion coefficient obtained by counting the activated lanthanum at a given position as a function of time during the diffusion run should be checked against that obtained from a post-diffusion counting profile of the specimen as described in the Data section of this report. Also a post-diffusion profile of the lanthanum concentration as a function of position should be checked using an electron microprobe when the activity of the lanthanum has decreased to a reasonable level.

X. CONCLUSIONS

These experiments support LeBorgne's conclusion that the diffusion coefficient of lanthanum in molten uranium is much lower than that predicted by theory. This low diffusion coefficient and the measured viscosity of uranium by Finucane[11] greater than that predicted by theory indicates that the models used successfully for computing transport properties of many materials are not appropriate for computing the transport properties of the actinide metals.

The results of this experiment indicate that the saturated concentration of lanthanum in molten uranium may be several times higher than that measured by Haefling and Daane. However this higher saturation concentration may be caused by a gap forming between the uranium ingot and the beryllia crucible during heating, and the lanthanum seeping into the gap. Using tungsten crucibles and/or dropping the lanthanum slug on the molten uranium will eliminate the effects of a gap forming during heating. In situ counting may eliminate any problems associated with the effect of freezing the uranium on the lanthanum distribution in the ingot.

Finally, tantalum is not a satisfactory crucible for containing uranium at 1200°C. Diffusion of the molten uranium occurs through rather large thicknesses of tantalum in tens of minutes at 1200°C.

ACKNOWLEDGMENTS

This work has been supported by the U. S. Atomic Energy Commission through the Inorganic Materials Research Division of the Lawrence Berkeley Laboratory and the Mechanical Engineering Department of the Lawrence Livermore Laboratory.

I would like to thank Professor Donald R. Olander of the Department of Nuclear Engineering, University of California at Berkeley, for his assistance and advice during this research. Professor Olander's non-pedantic approach as a research director results in a stimulating atmosphere for study and research.

I would also like to thank Dr. Richard H. Jones of the Aerospace Corporation, Dr. Wigbert J. Siekhaus of the Lawrence Berkeley Laboratory and Mr. Han Chung Tsai of the Argonne National Laboratory for their technical assistance and discussions. A special thanks to Mr. William N. Ross and Mr. James N. Doggett of the Mechanical Engineering Department, Lawrence Livermore Laboratory for their interest and assistance. The secretarial personnel, Ms. Pamela D. Smith and Ms. Gladys M. Espindola, and the shop personnel, Mr. Dan E. Winterbauer and Mr. John Souza, of the Nuclear Engineering Department were most cooperative and helpful at all times.

Finally I would like to thank Ms. Gloria C. Pelatowski for drafting the figures and Ms. Shirley Ashley for the excellent job of interpreting my scribbles and translating them into typed pages.

APPENDIX I

Diffusion Run 1

Diffusion Time	12 hours
Diffusion Temperature	1220°C
Pre-Diffusion Interface	44.2 mm
Post-Diffusion Interface	43.2 mm
Pre-Diffusion Lanthanum Length	~10.7 mm
Post-Diffusion Lanthanum Length	4.8 mm
Pre-Diffusion Window Width	2.7 mm
Post-Diffusion Window Width	4.2 mm

Results:

Solubility (weight fraction)	0.15
Diffusion Coefficient	4.2×10^{-7} cm^2/sec

Note: Precount curve corrected for 1.7 mm air gap between lanthanum and uranium surface.

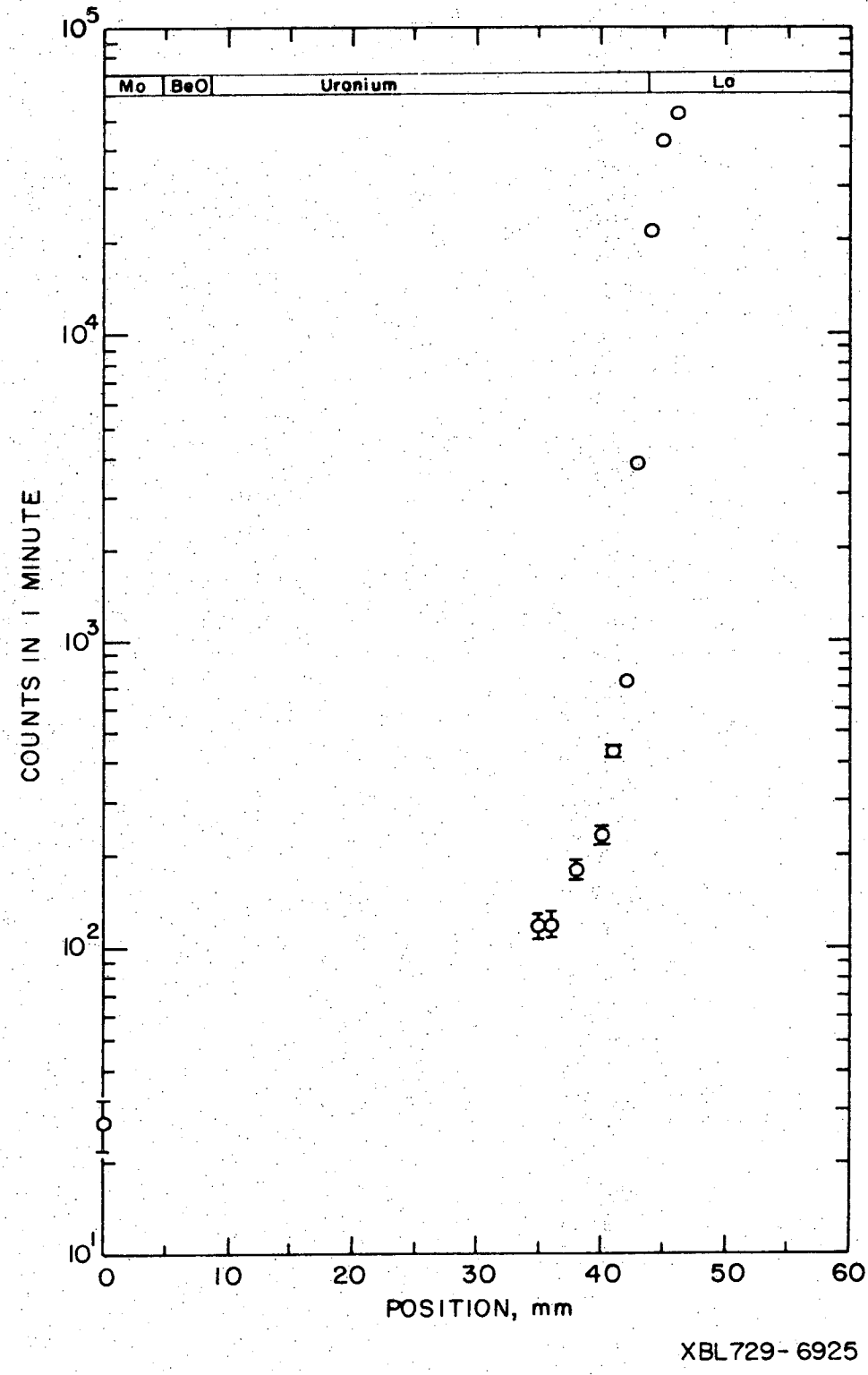

Fig. 5. Pre-diffusion count data for Run 1.

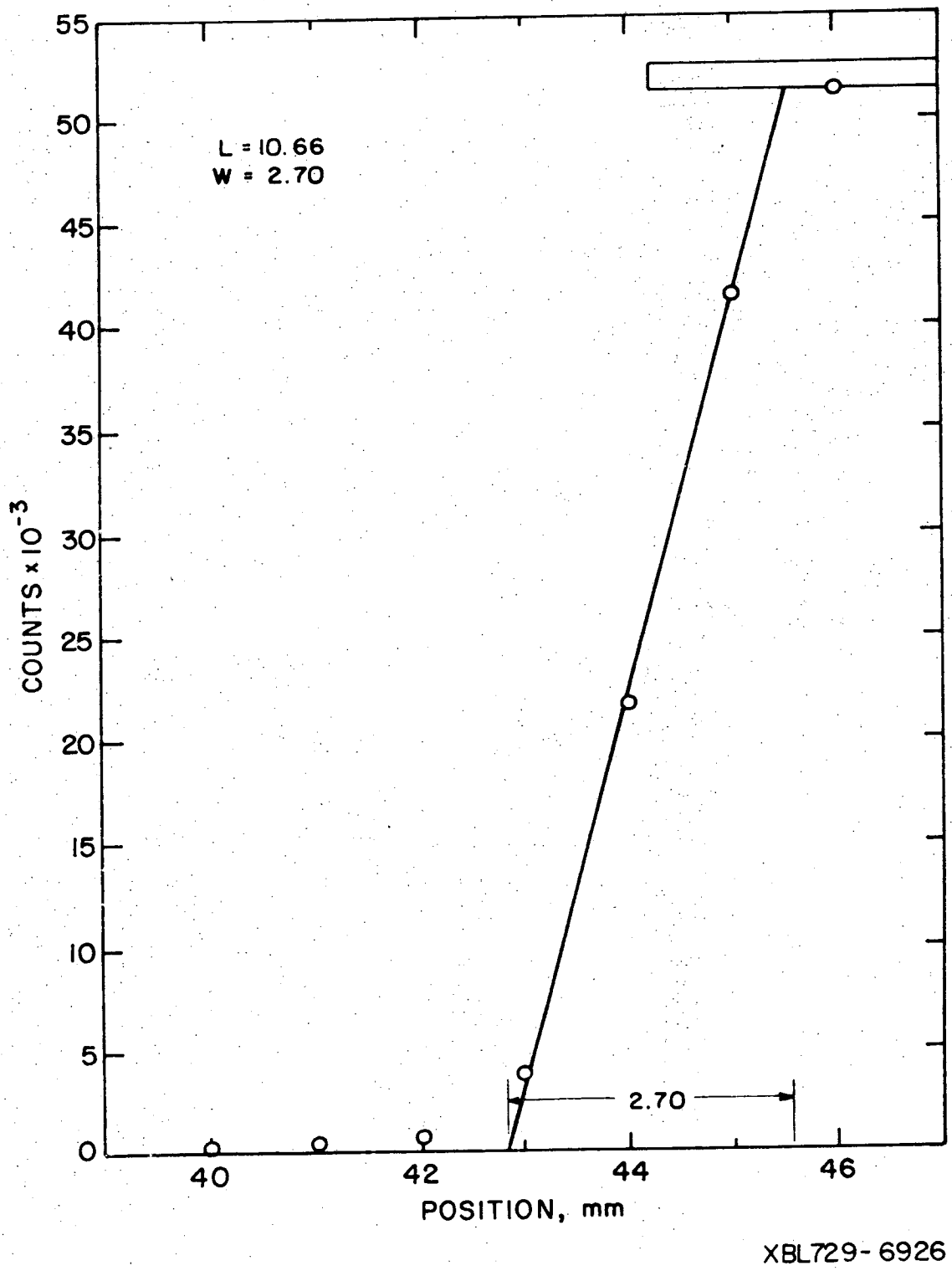

Fig. 6. Estimate of effective window width using pre-diffusion count data for Run 1.

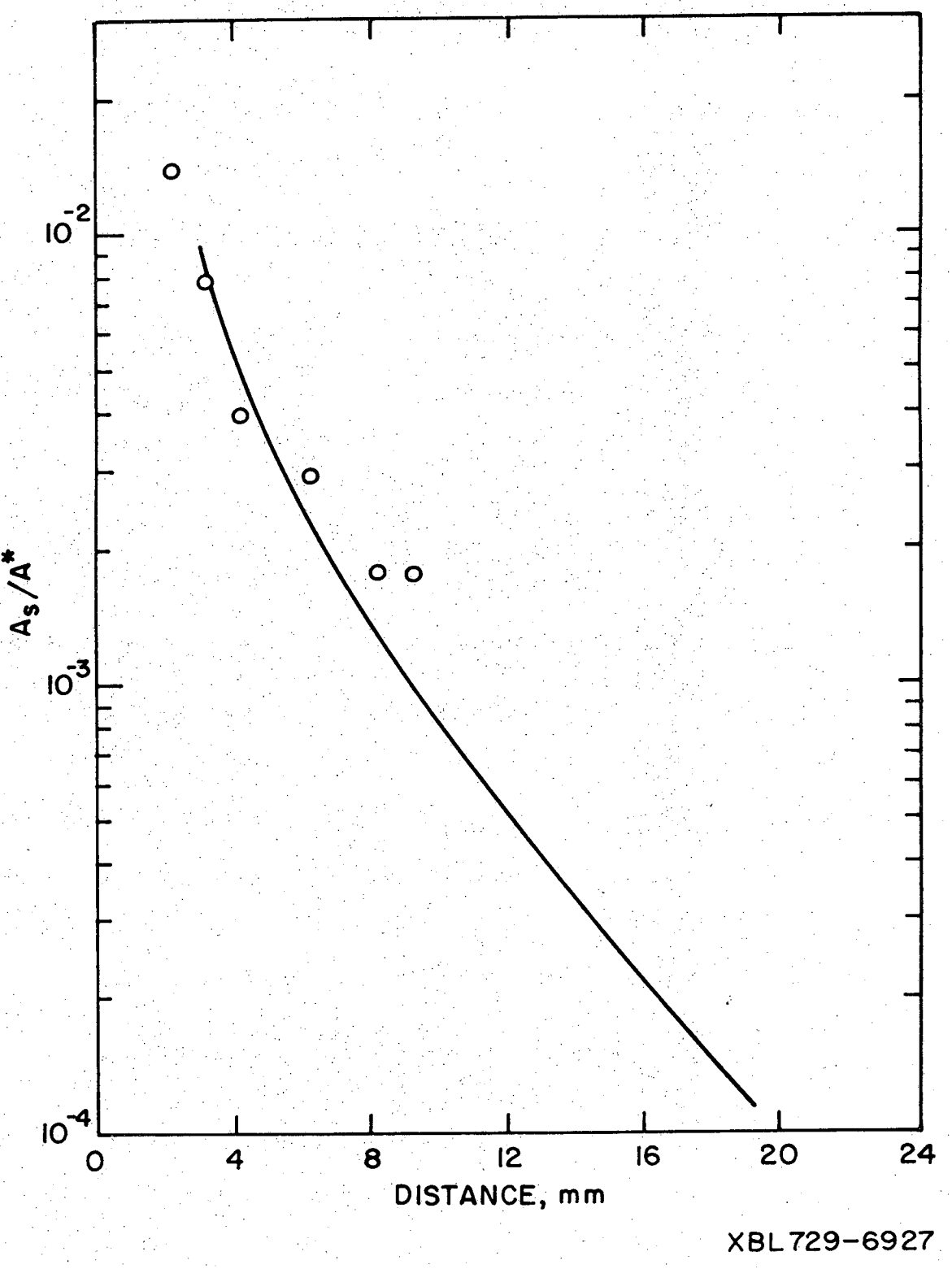

Fig. 7. Scattering correction normalized to maximum count rate of pure lanthenum from pre-diffusion count data for Run 1.

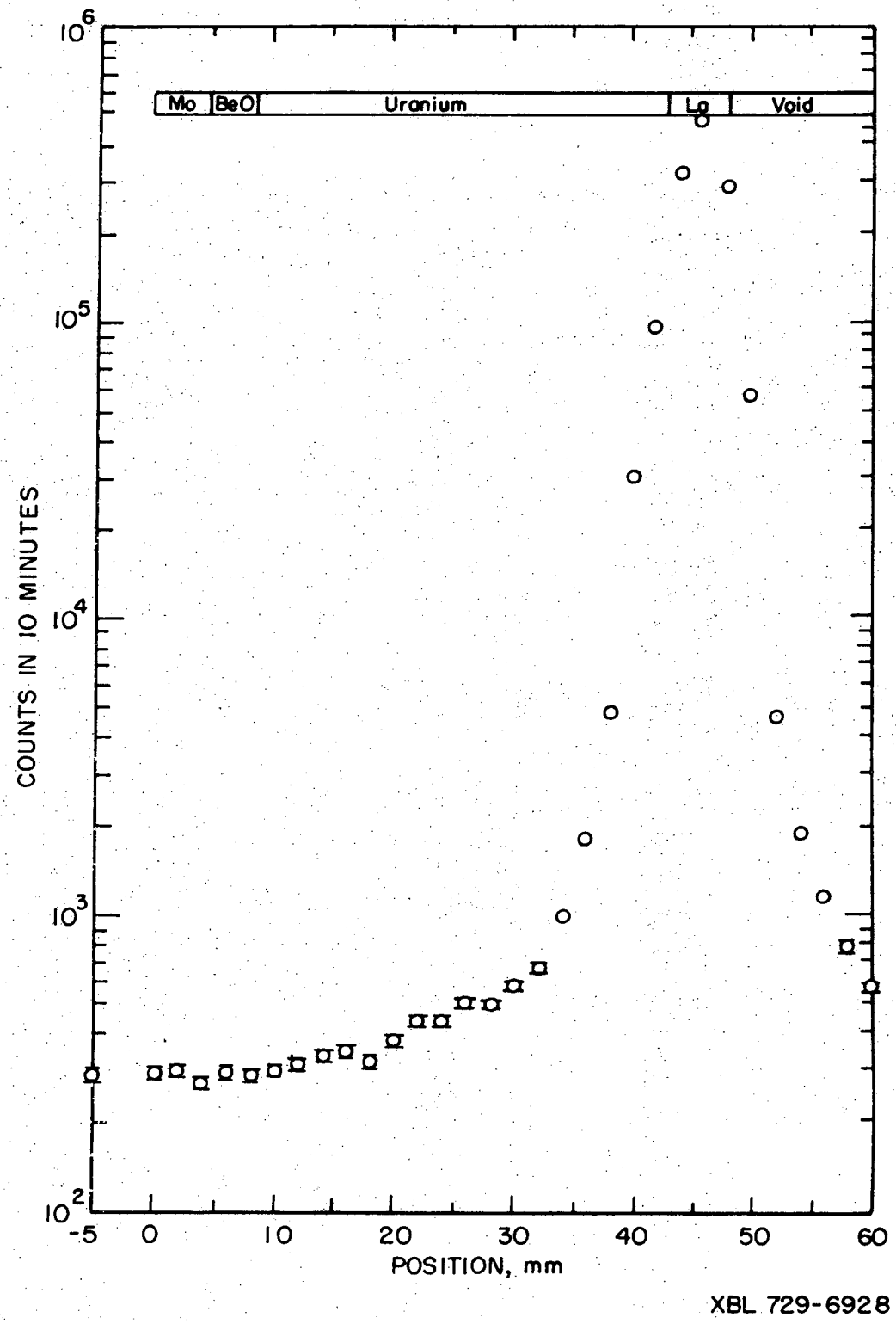

Fig. 8. Post-diffusion count data for Run 1.

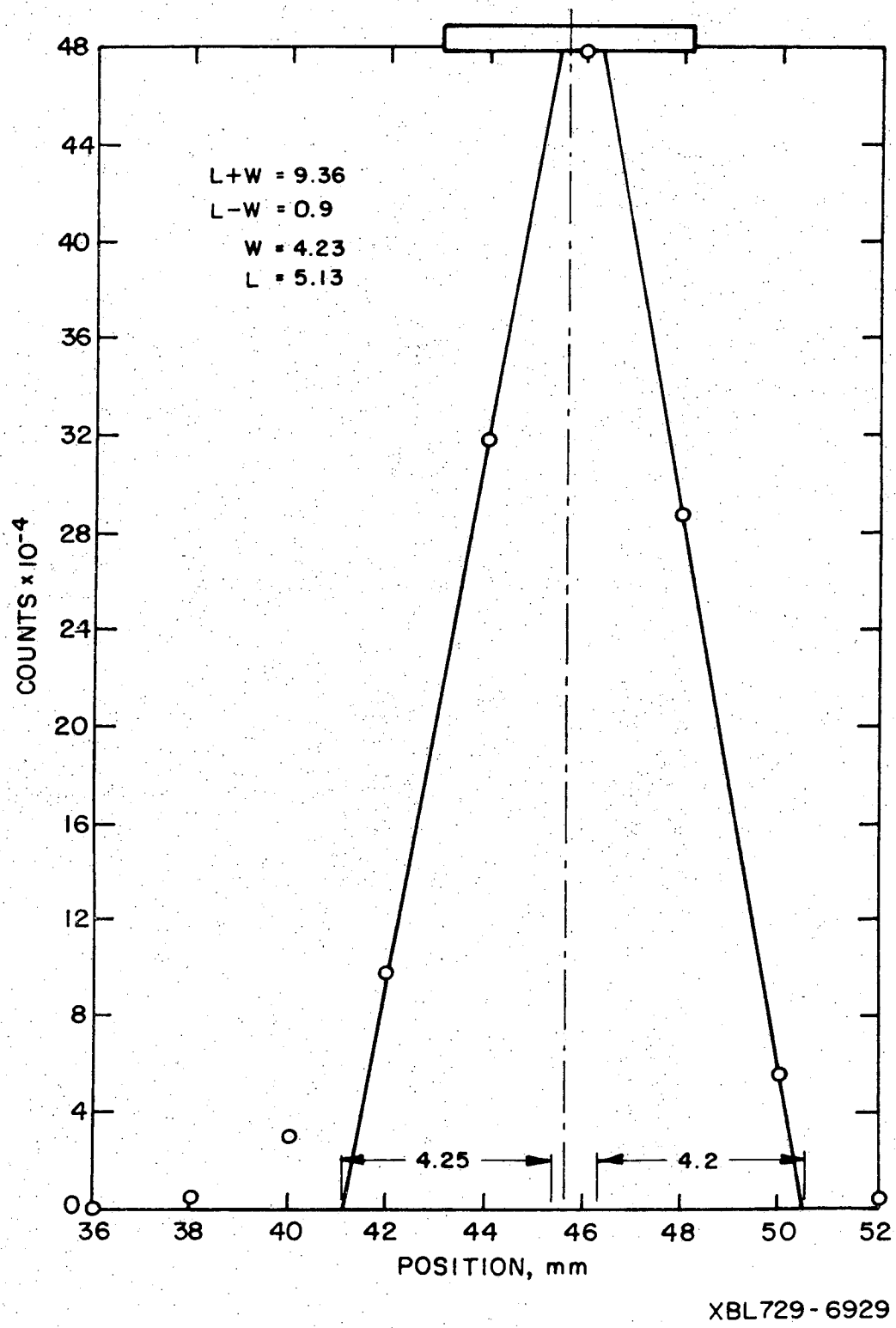

Fig. 9. Estimate of effective window width and lanthanum length using post-diffusion count data for Run 1.

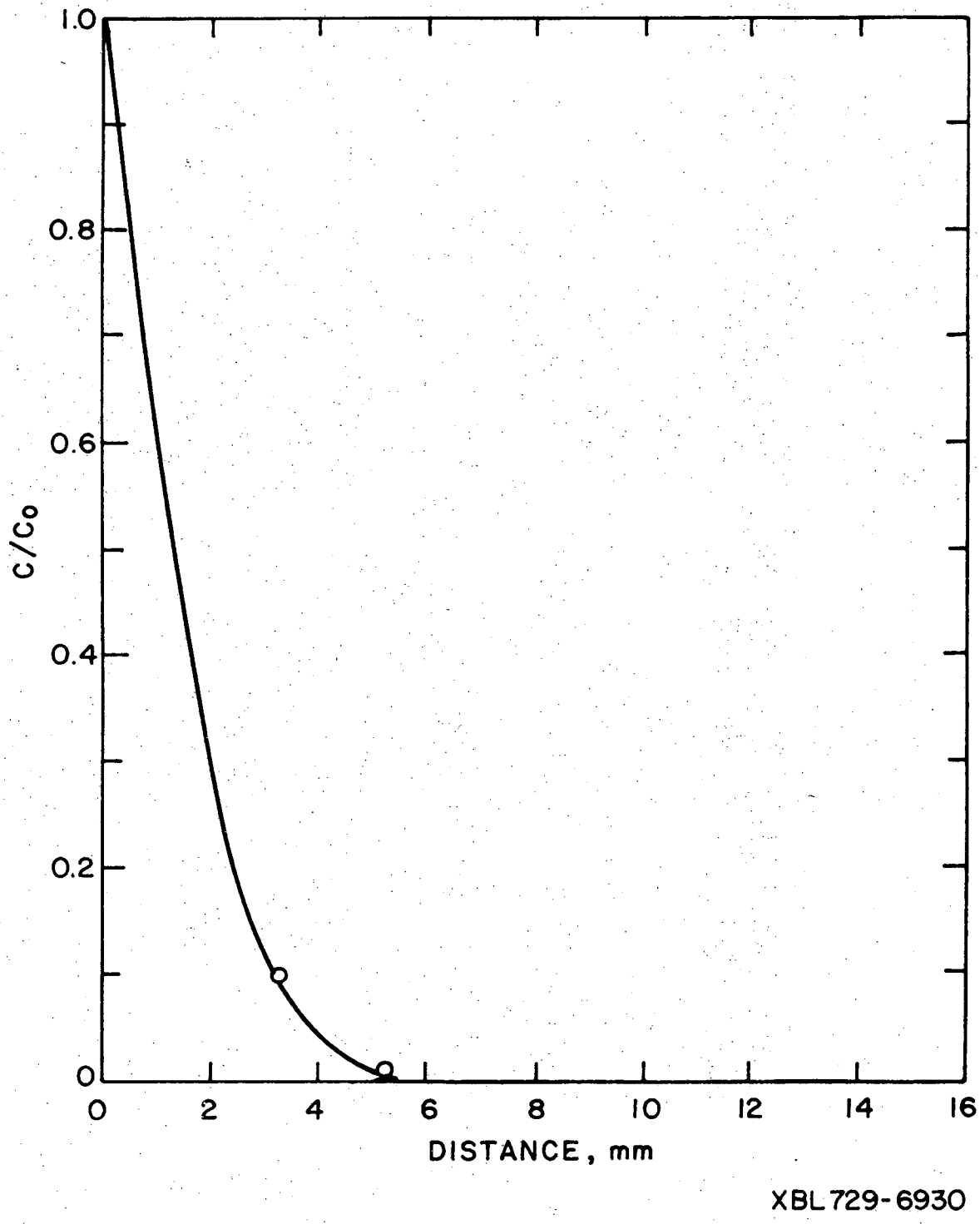

Fig. 10. Normalized concentration as a function of distance from interface for Run 1.

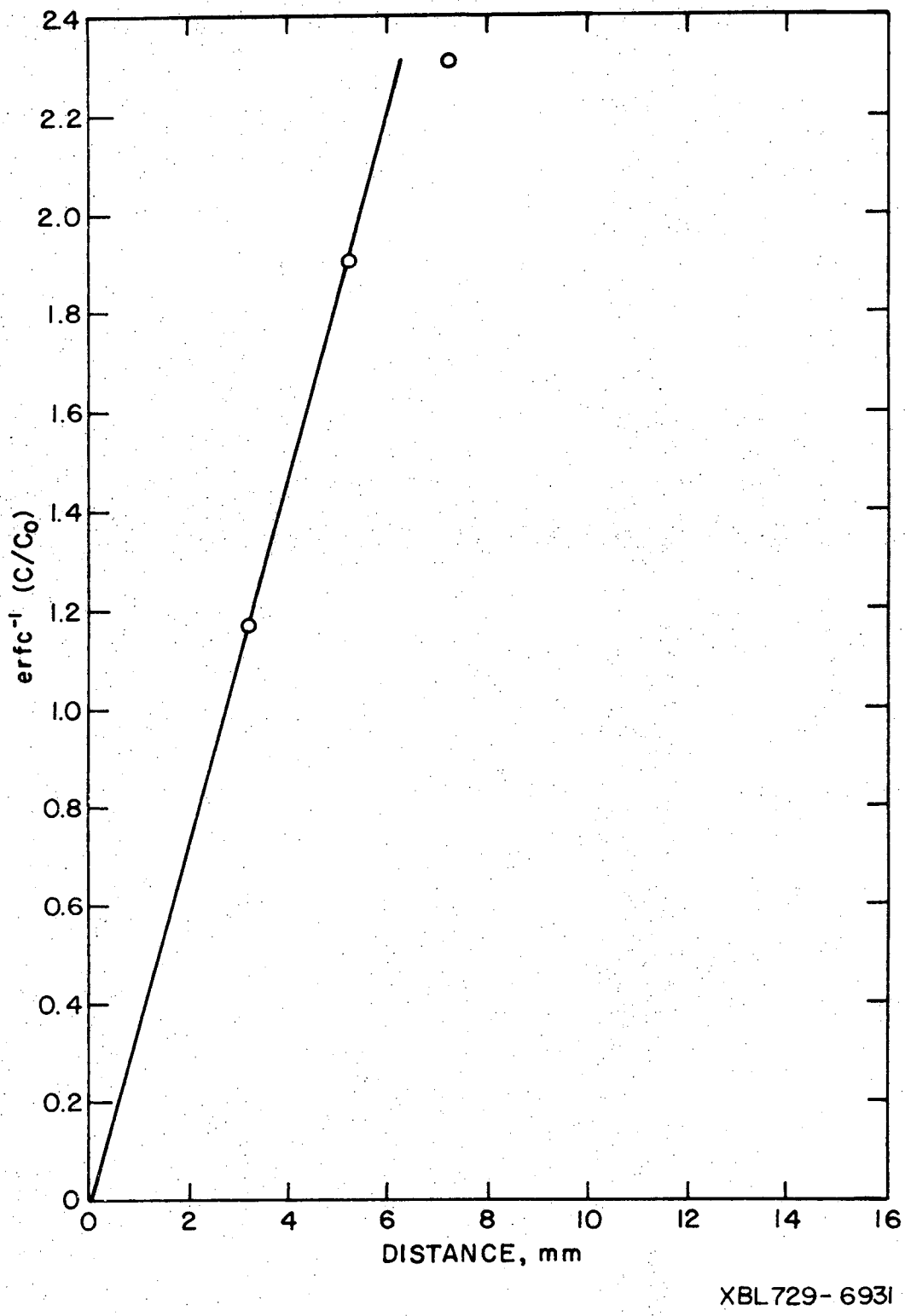

Fig. 11. Inverse complementary error function of concentration ratio as a function of count position for Run 1.

APPENDIX II

Diffusion Run 2

Diffusion Time	8 hours
Diffusion Temperature	1200°C
Pre-Diffusion Interface	28.1 mm
Post-Diffusion Interface	27.9 mm
Pre-Diffusion Lanthanum Length	10.5 mm
Post-Diffusion Lanthanum Length	5.2 mm
Pre-Diffusion Window Width	3.8 mm
Post-Diffusion Window Width	3.9 mm

Results:

Solubility (weight fraction)	0.050
Diffusion Coefficient	4.2×10^{-6} cm^2/sec

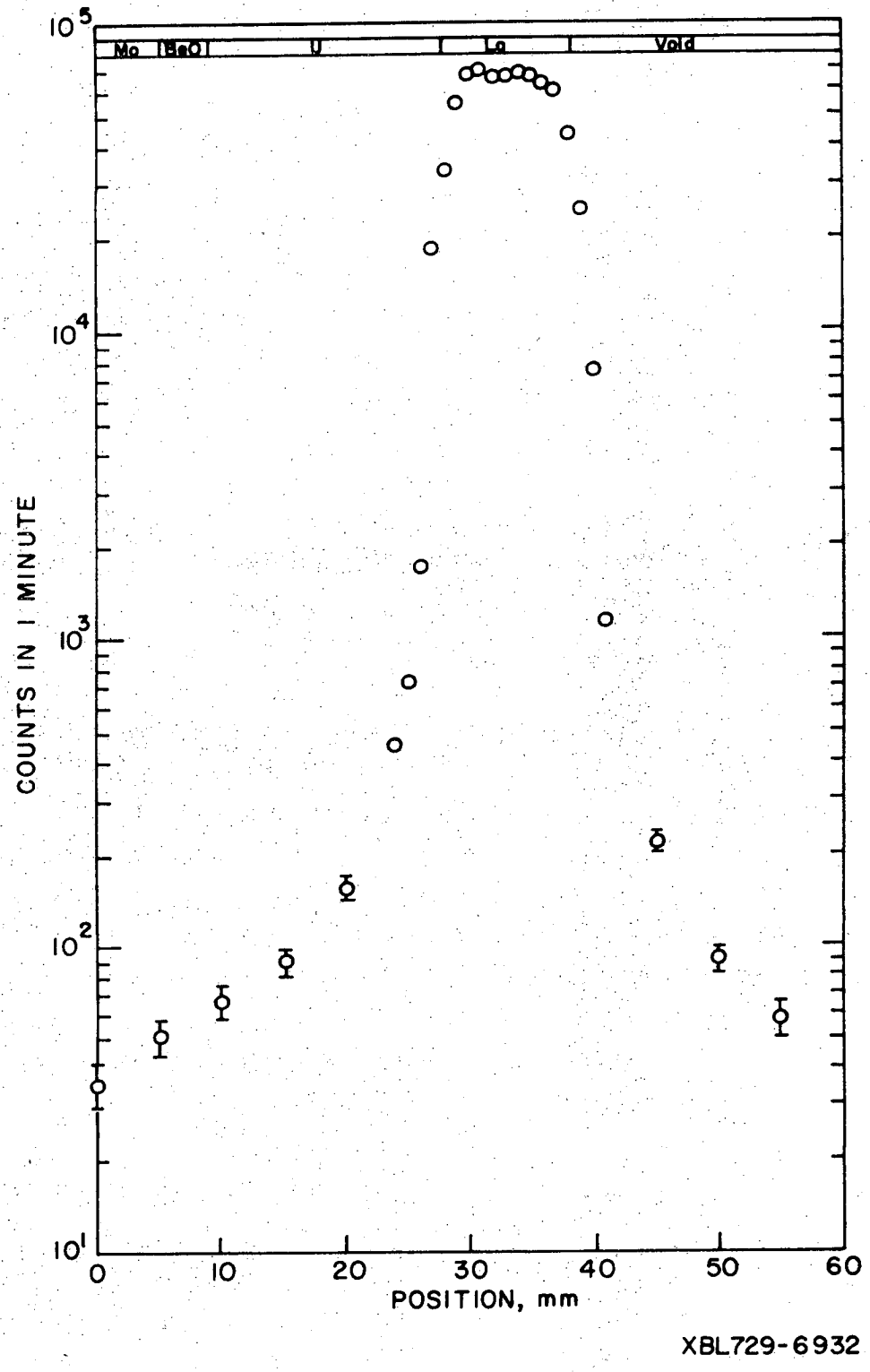

Fig. 12. Pre-diffusion count data for Run 2.

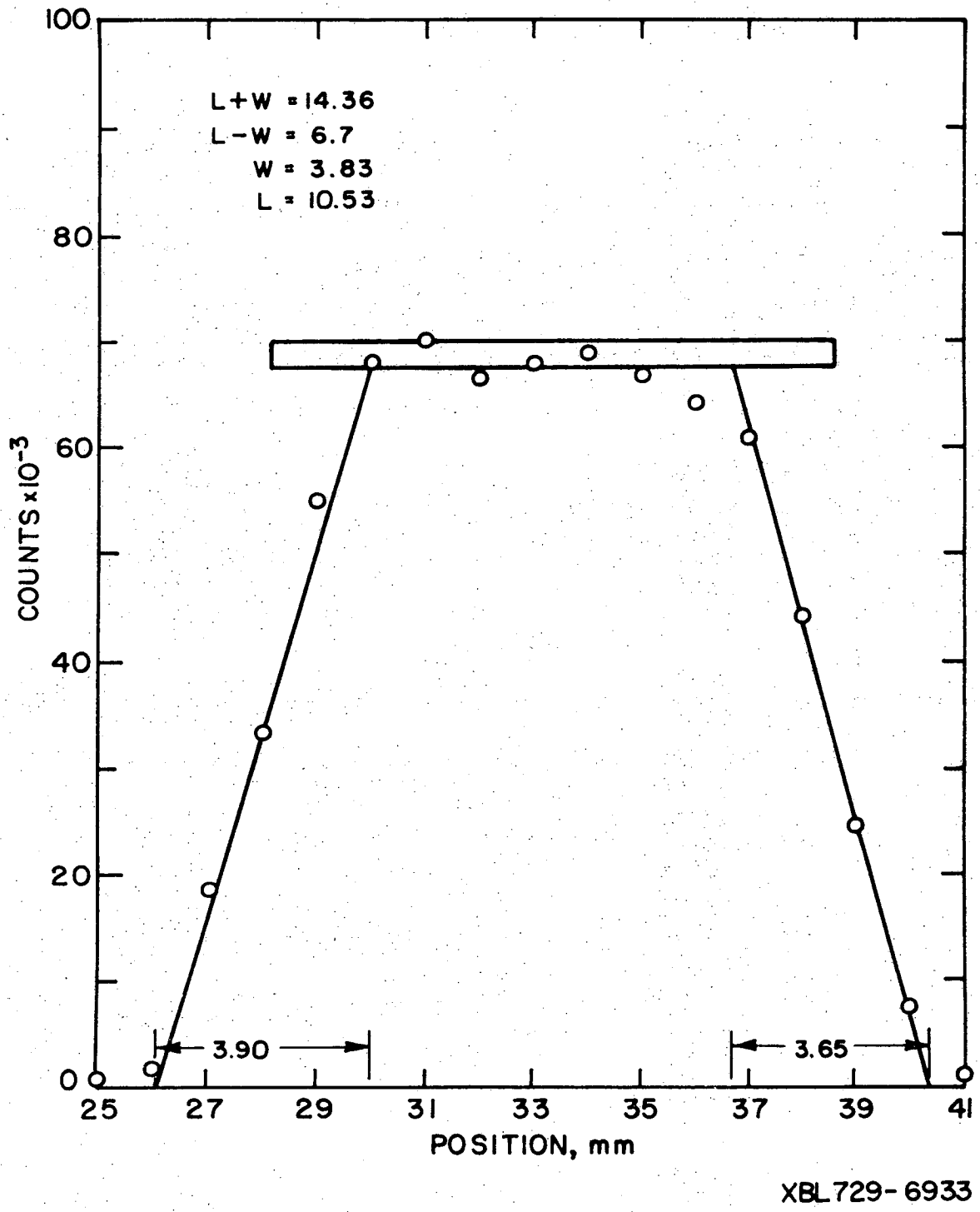

Fig. 13. Estimate of effective window width and lanthanum length using pre-diffusion count data for Run 2.

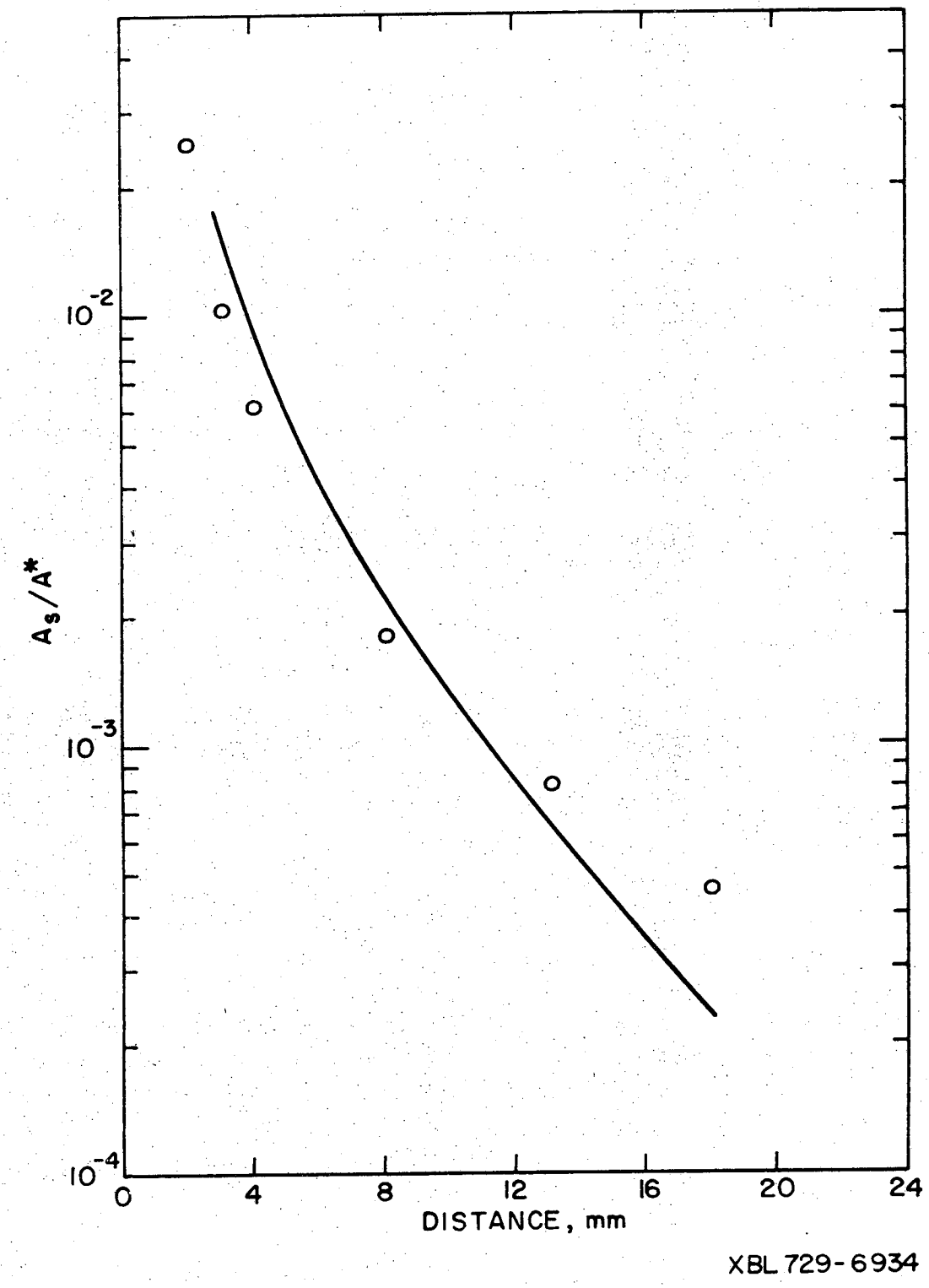

Fig. 14. Scattering correction normalized to maximum count rate of pure lanthanum from pre-diffusion count data for Run 2.

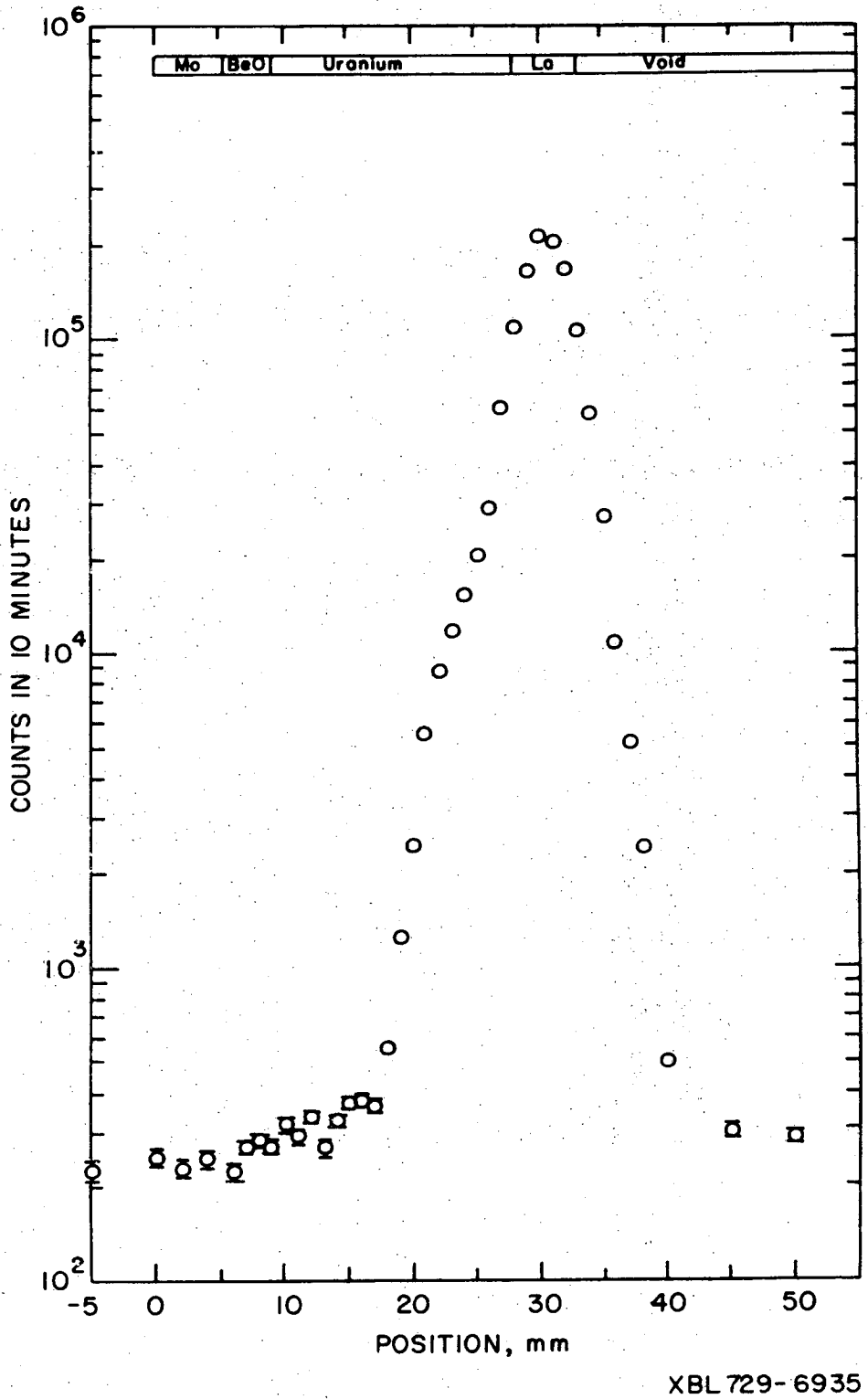

Fig. 15. Post-diffusion count data for Run 2.

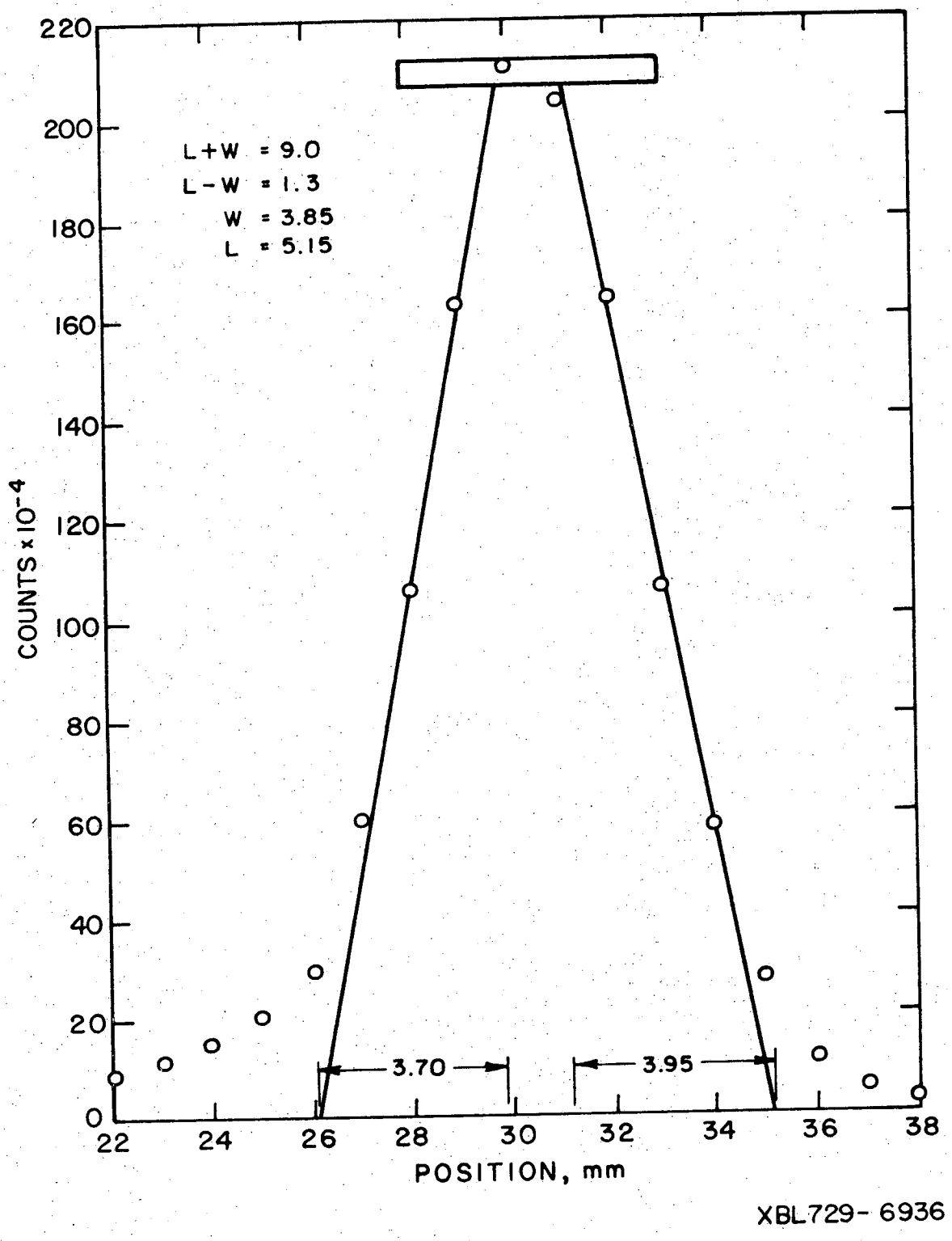

Fig. 16. Estimate of effective window width and lanthanum length using post-diffusion count data for Run 2.

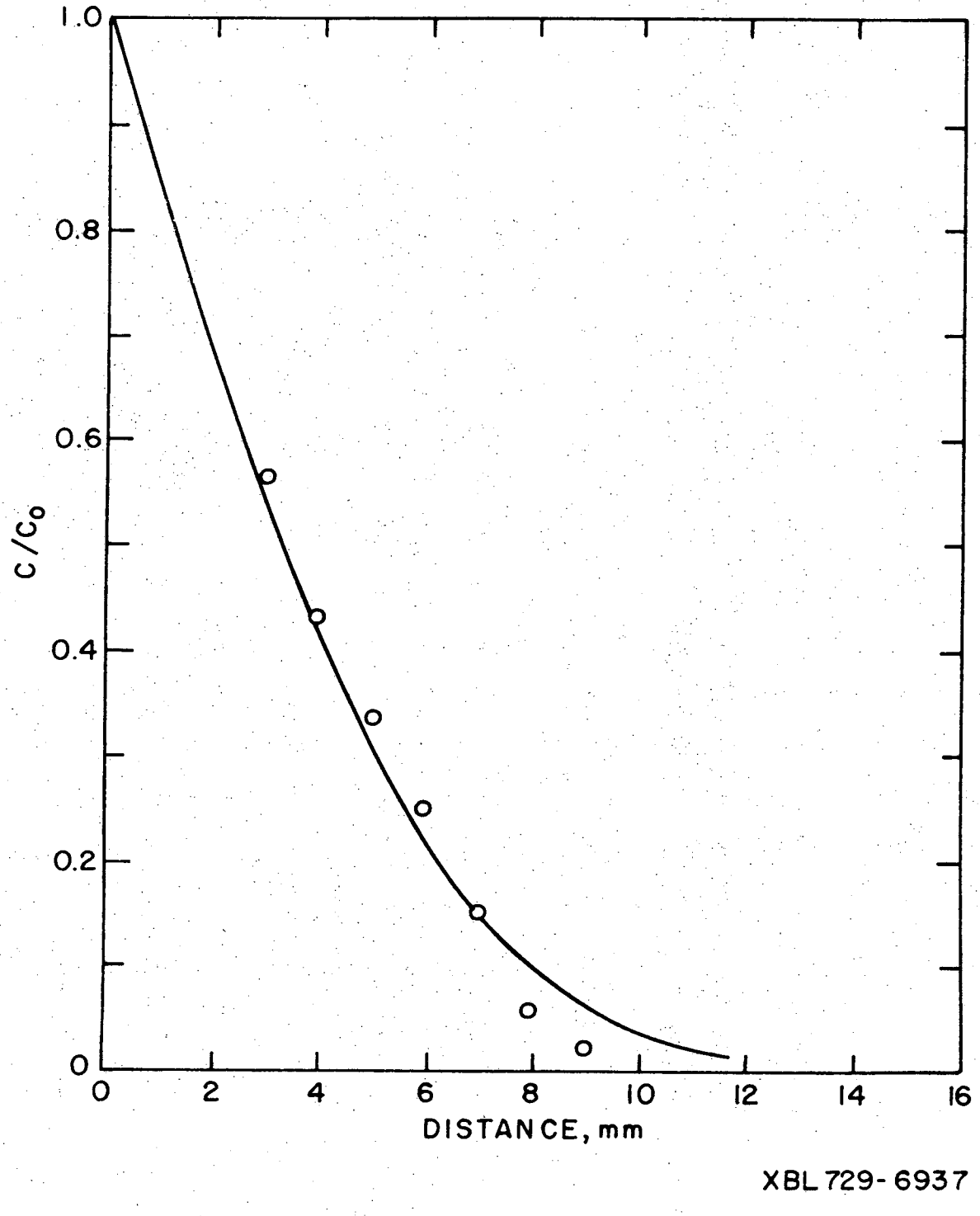

Fig. 17. Normalized concentration as a function of distance from interface for Run 2.

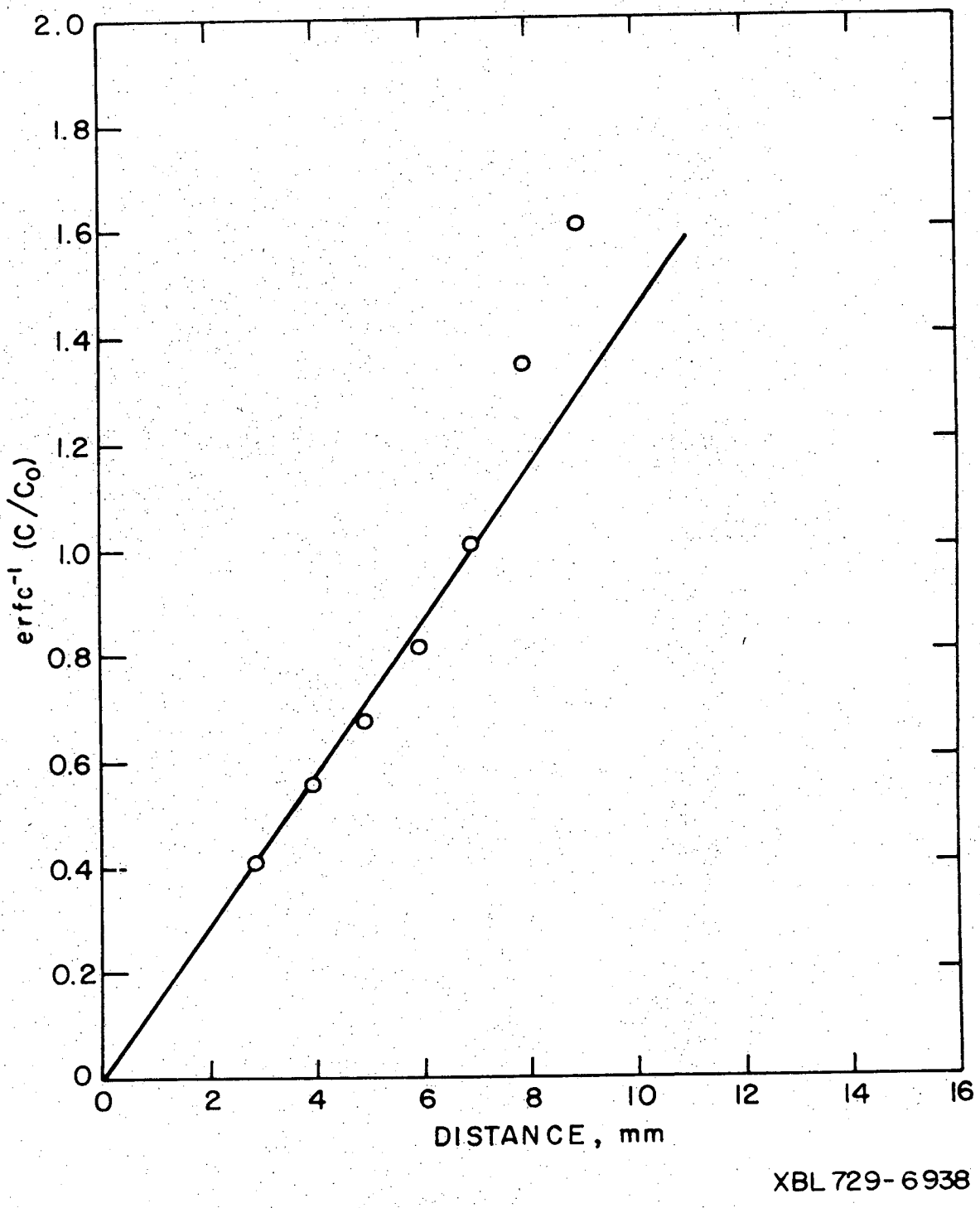

Fig. 18. Inverse complementary error function of concentration ratio as a function of count position for Run 2.

APPENDIX III

Diffusion Run 3

Diffusion Time	8 hours
Diffusion Temperature	1200°C
Pre-Diffusion Interface	26.9 mm
Post-Diffusion Interface	27.6 mm
Pre-Diffusion Lanthanum Length	11.0 mm
Post-Diffusion Lanthanum Length	5.2 mm
Pre-Diffusion Window Width	2.7 mm
Post-Diffusion Window Width	3.9 mm

Results:

Solubility (weight fraction)	0.066
Diffusion Coefficient	1.8×10^{-6} cm^2/sec

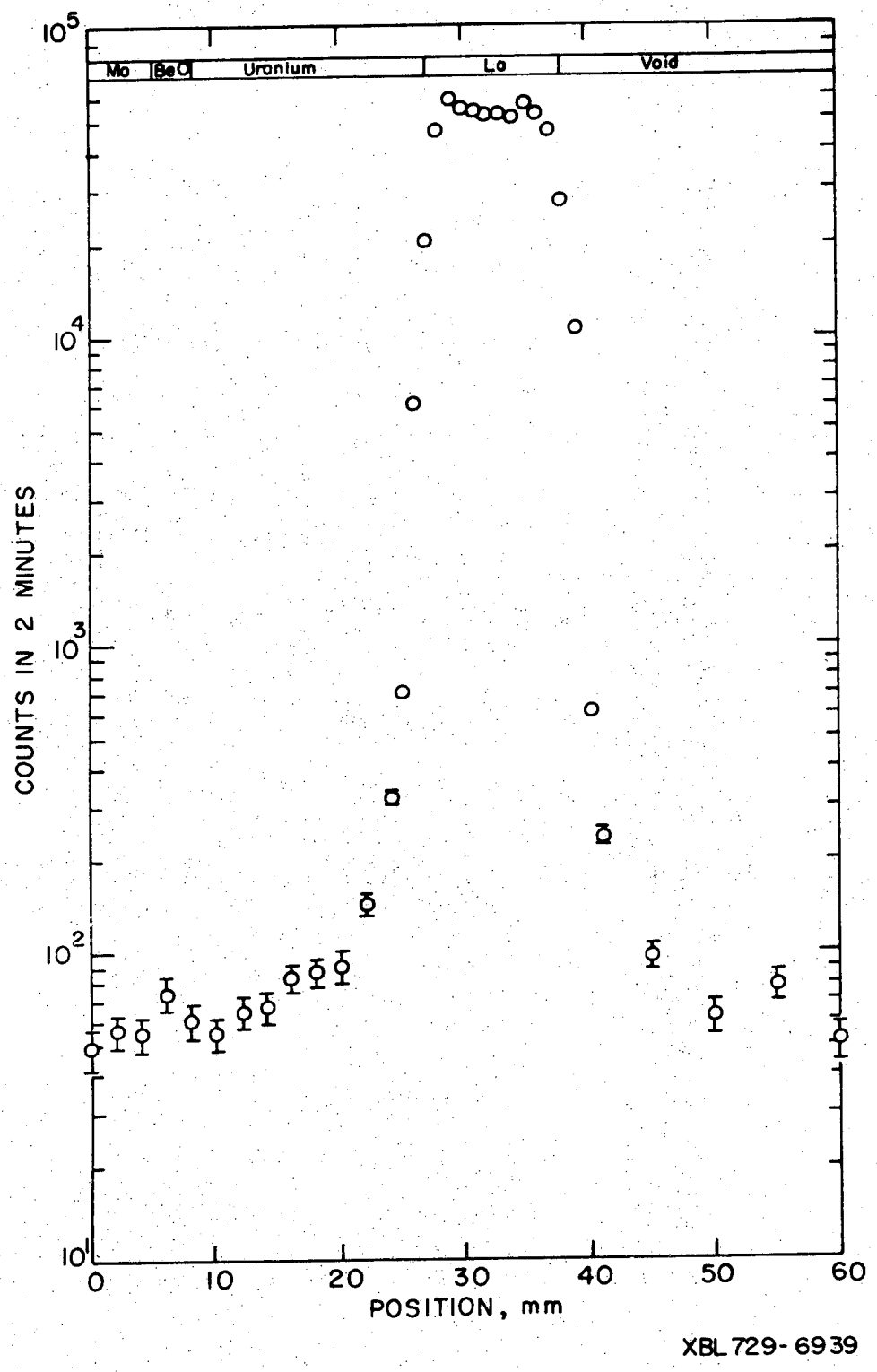

Fig. 19. Pre-diffusion count data for Run 3.

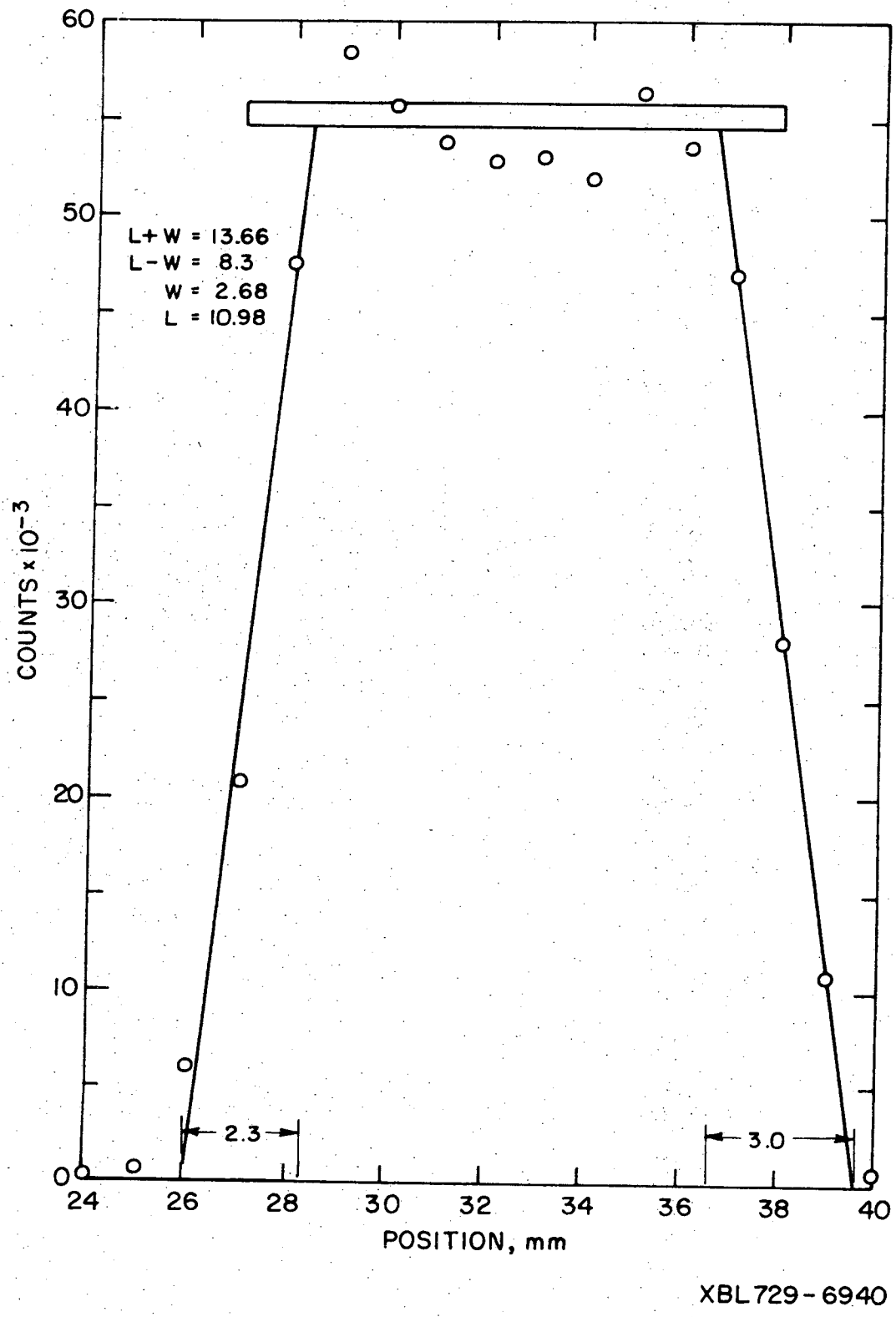

Fig. 20. Estimate of effective window width and lanthanum length using pre-diffusion count data for Run 3.

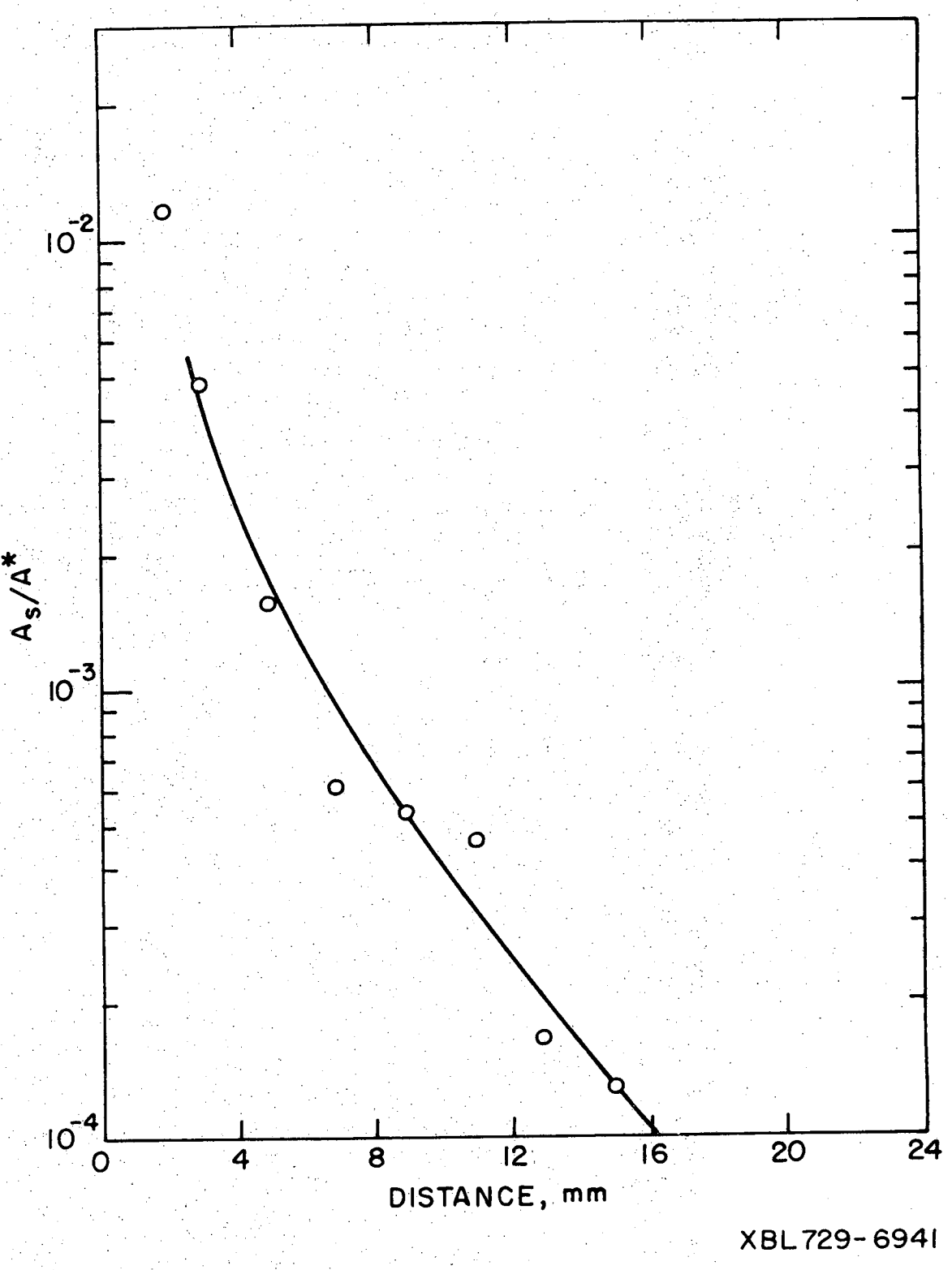

Fig. 21. Scattering correction normalized to maximum count rate of pure lanthanum from pre-diffusion count data for Run 3.

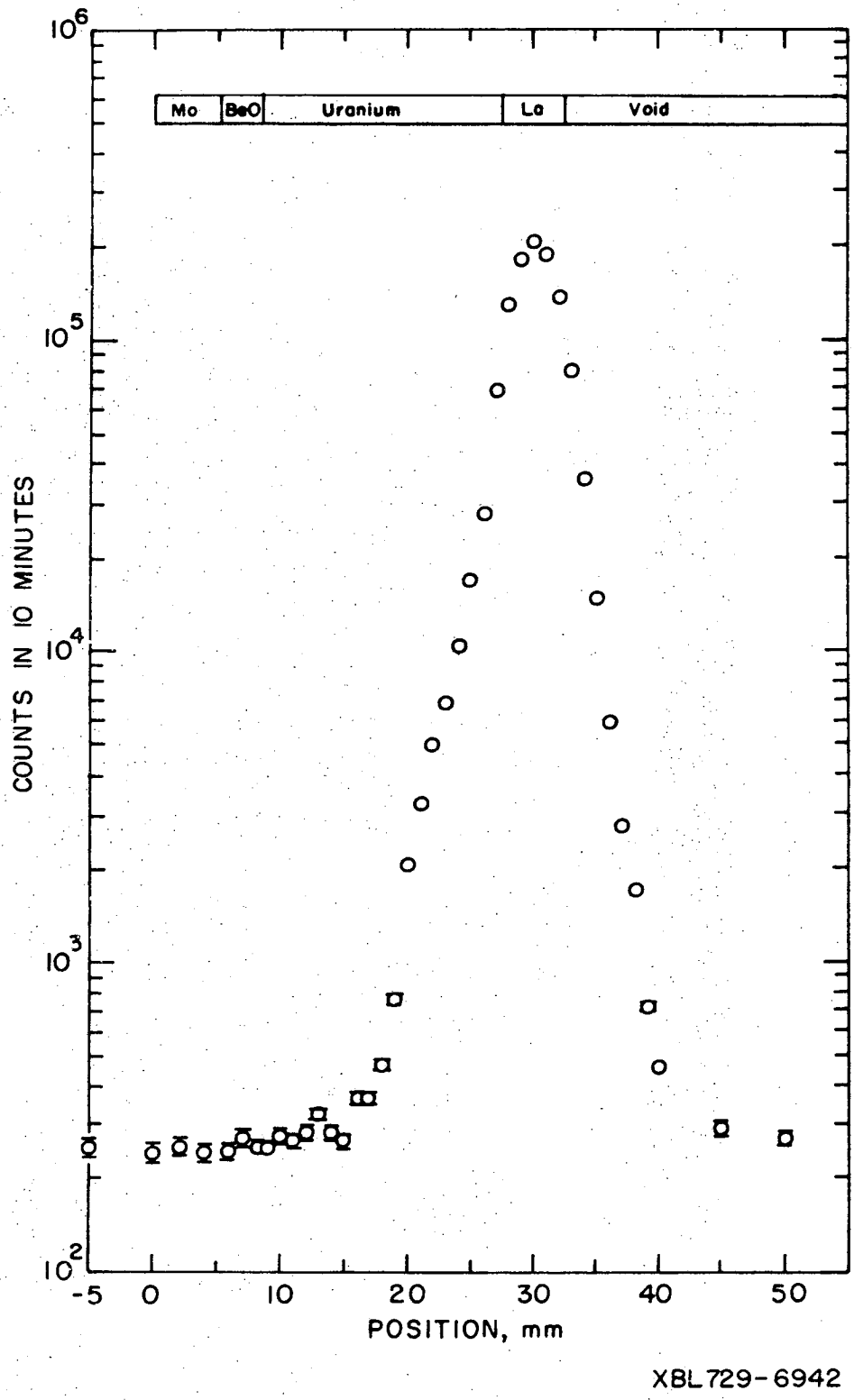

Fig. 22. Post-diffusion count data for Run 3.

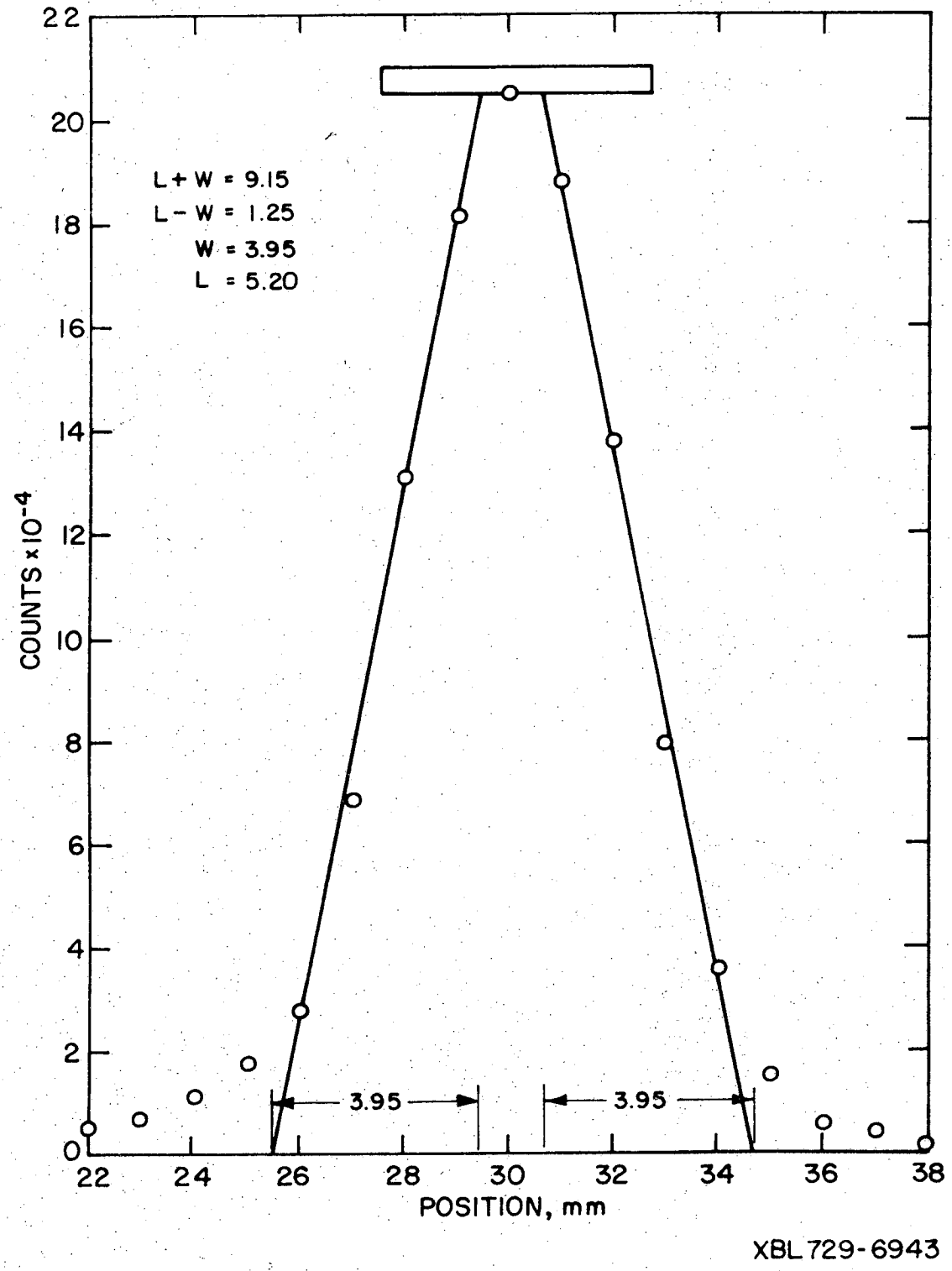

Fig. 23. Estimate of effective window with a lanthanum length using post-diffusion count data for Run 3.

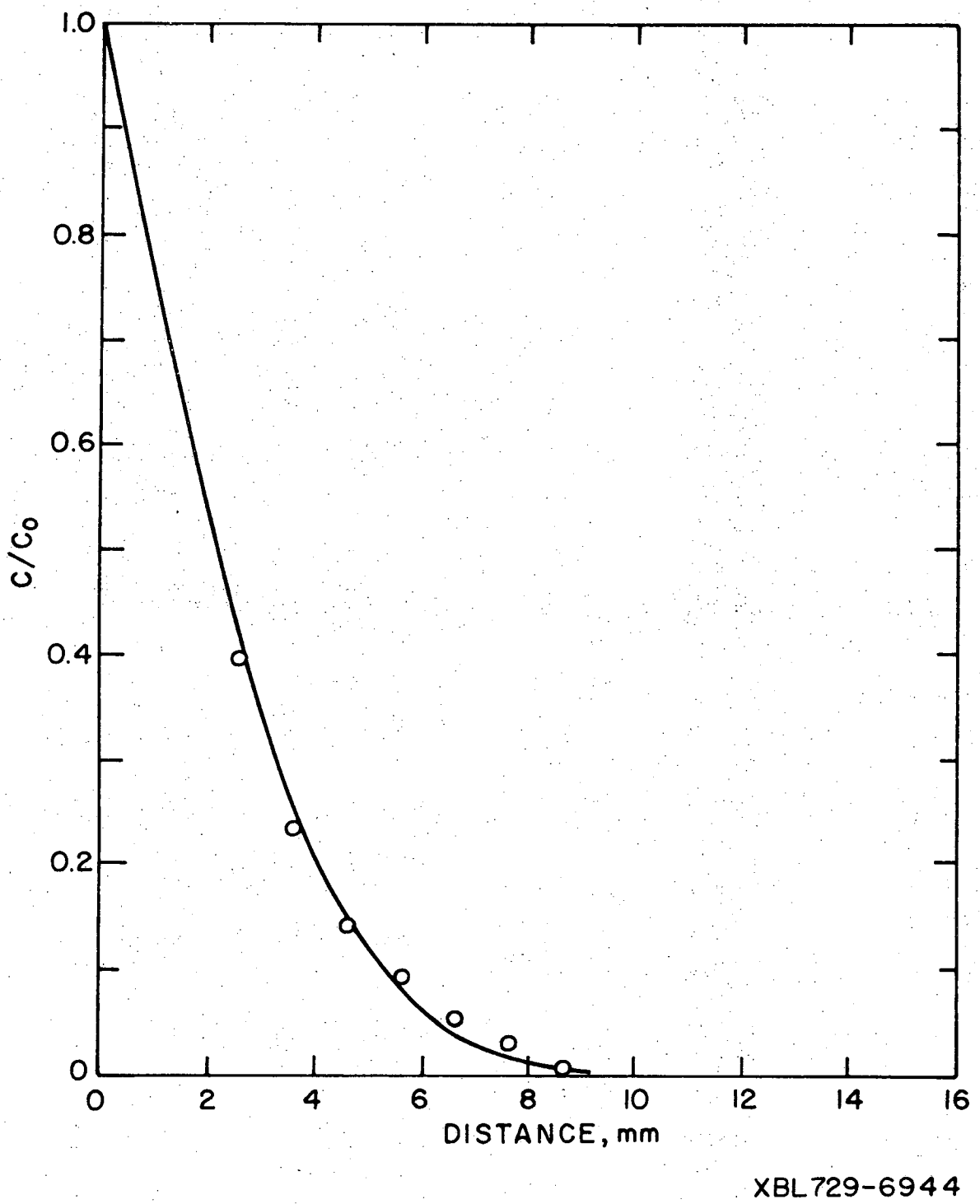

Fig. 24. Normalized concentration as a function of distance from interface for Run 3.

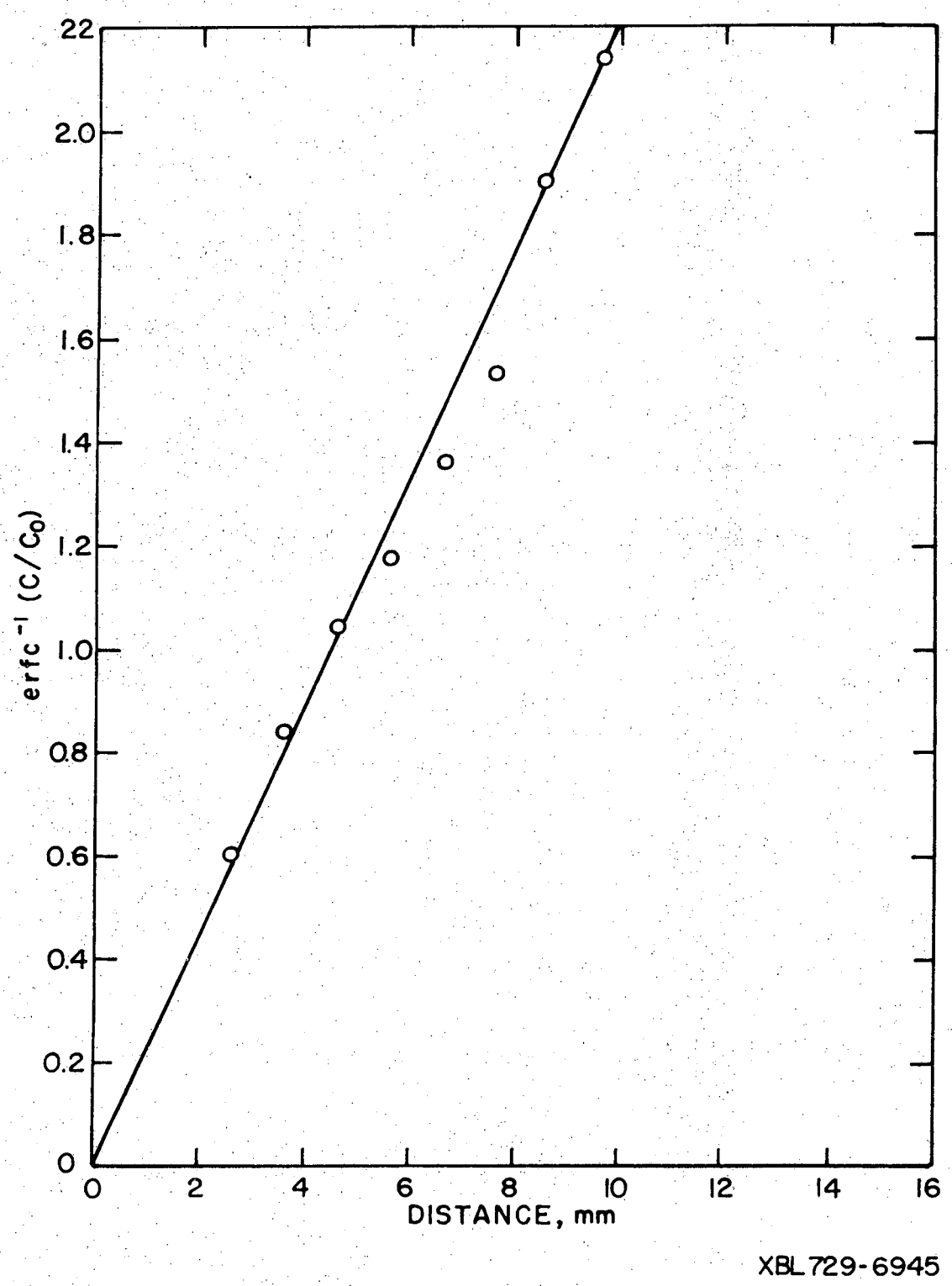

Fig. 25. Inverse complementary error function of the concentration ratio as a function of count position for Run 3.

APPENDIX IV

Diffusion Run

Diffusion Time	16 hours
Diffusion Temperature	1216°C
Pre-Diffusion Interface	39.4 mm
Post-Diffusion Interface	37.2 mm
Pre-Diffusion Lanthanum Length	10.9 mm
Post-Diffusion Lanthanum Length	5.5 mm
Pre-Diffusion Window Width	3.8 mm
Post-Diffusion Window Width	3.9 mm

Results:

Solubility (weight fraction)	0.015
Diffusion Coefficient	5.1×10^{-7} cm^2/sec

Note: Precount curve corrected for 2.4 mm air gap between lanthanum and uranium.

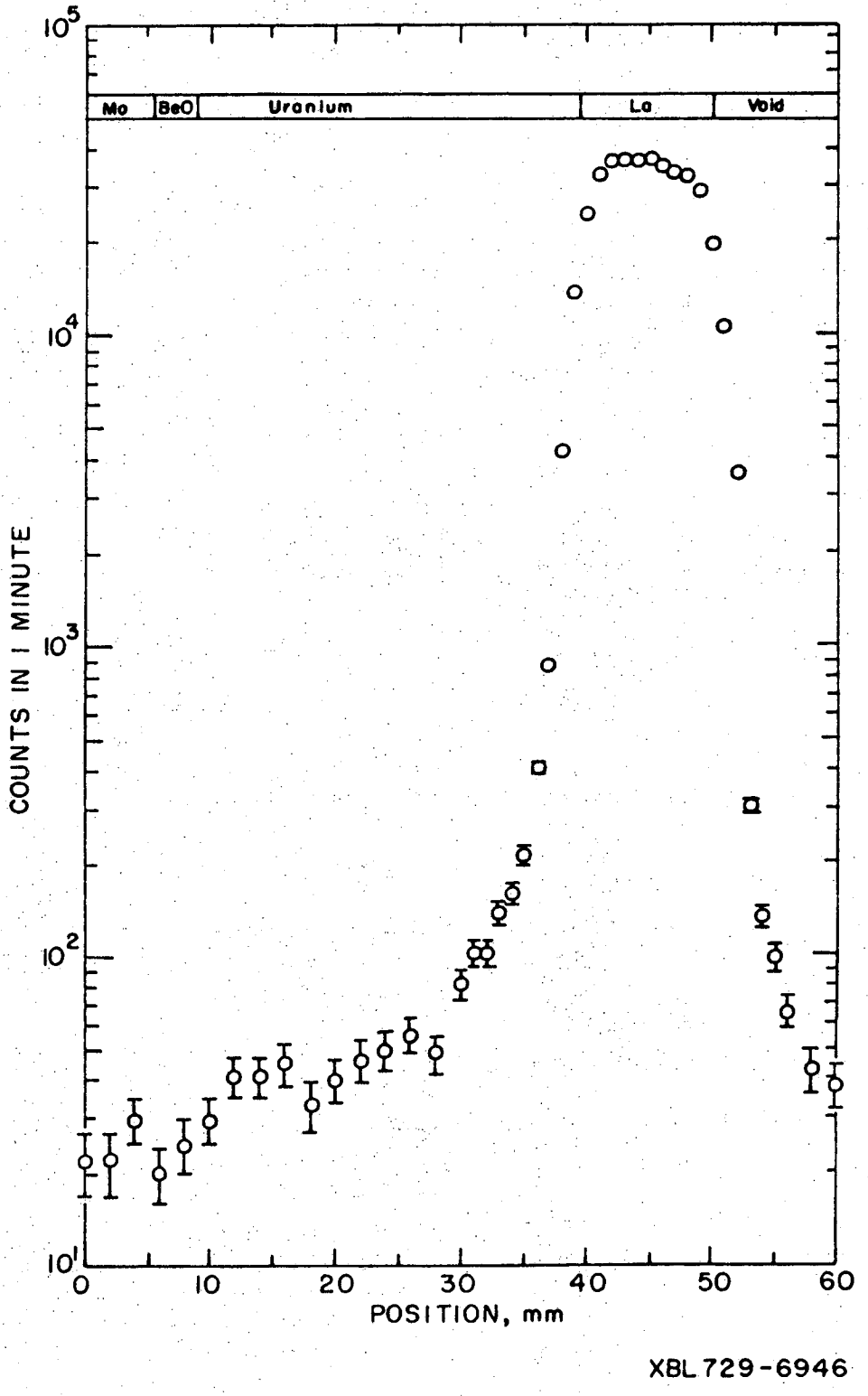

Fig. 26. Pre-diffusion count data for Run 4.

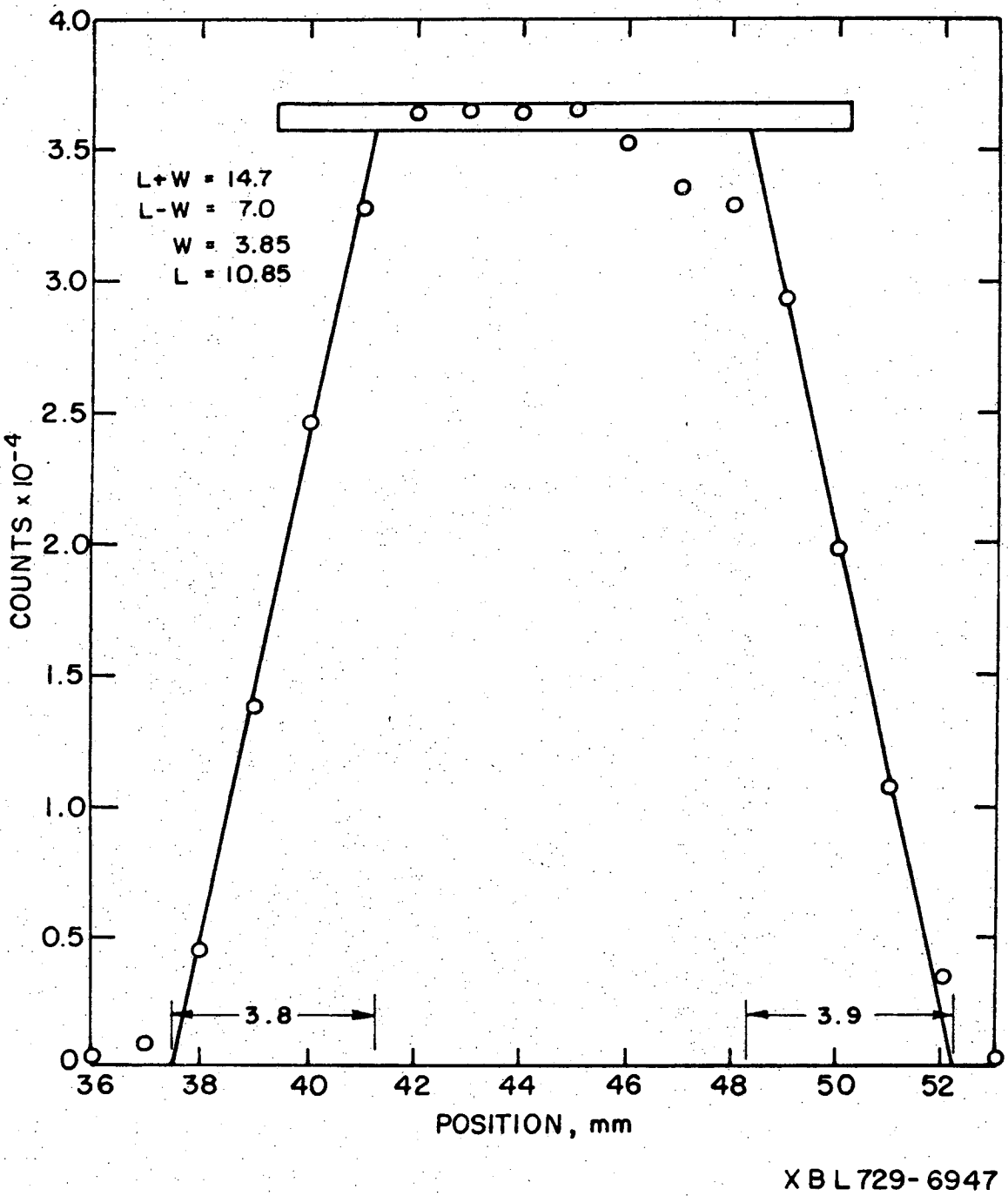

Fig. 27. Estimate of effective window width and lanthanum length using pre-diffusion count data for Run 4.

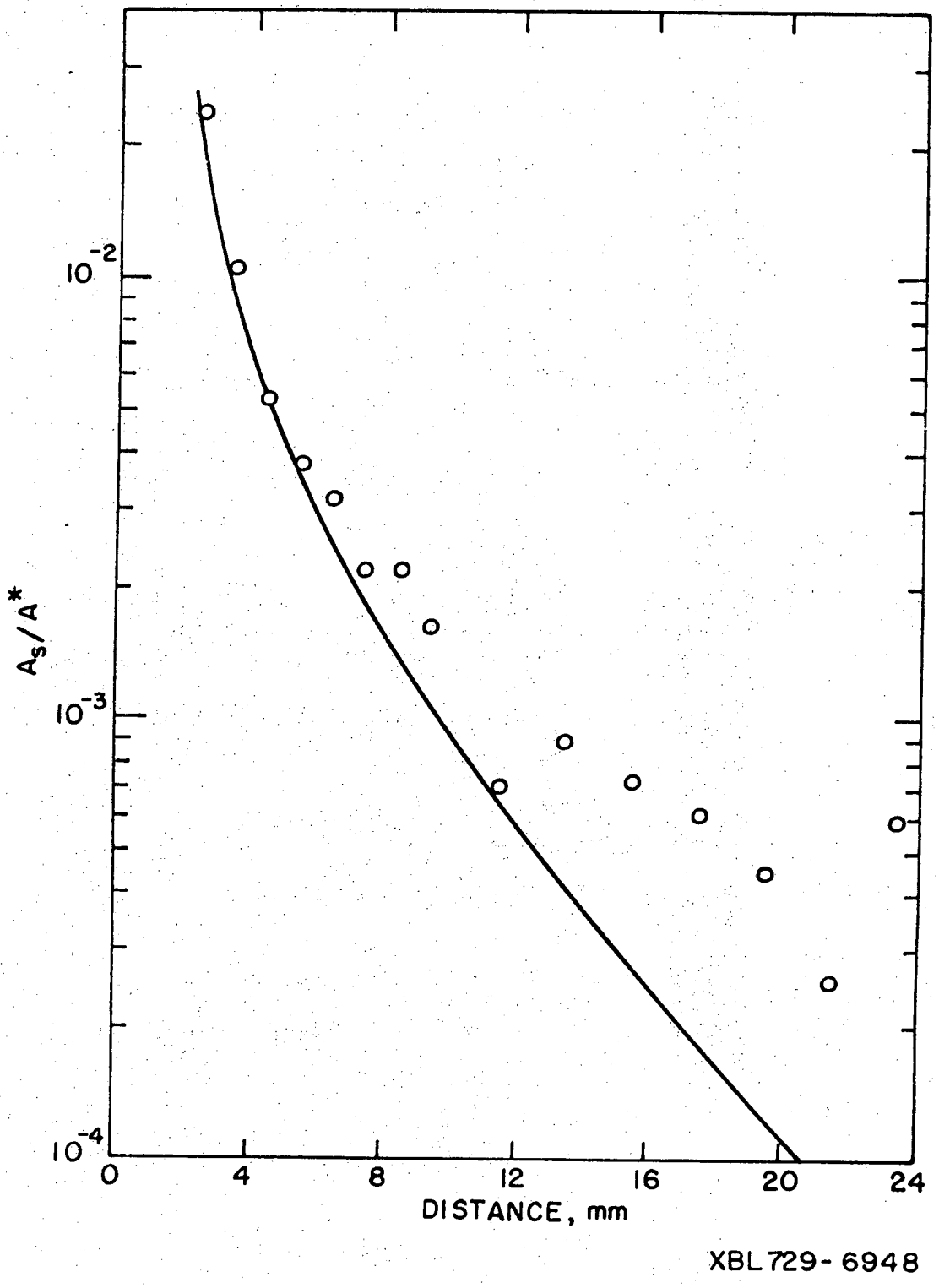

Fig. 28. Scattering correction normalized to maximum count rate of pure lanthanum from pre-diffusion count data for Run 4.

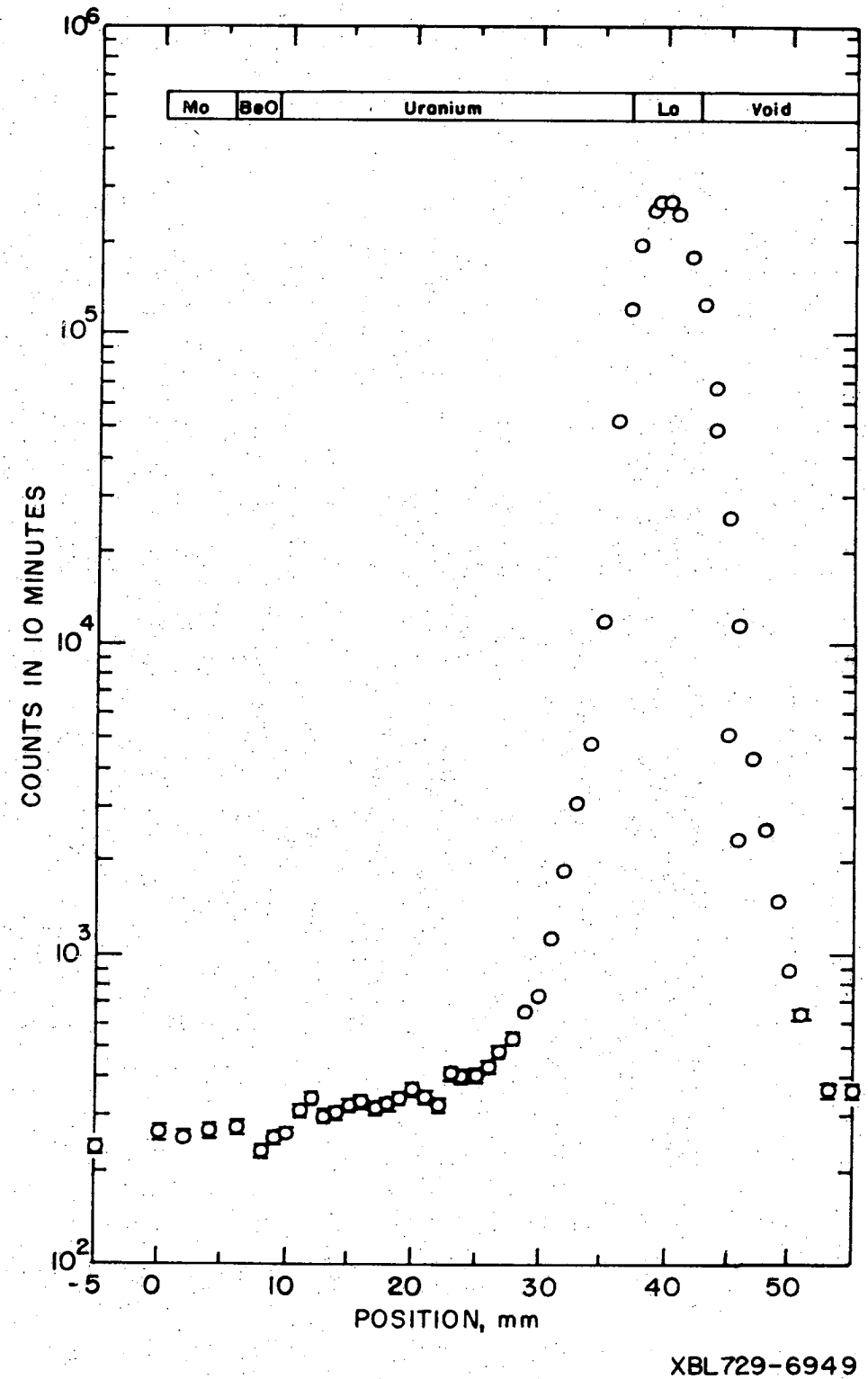

Fig. 29. Post-diffusion count data for Run 4.

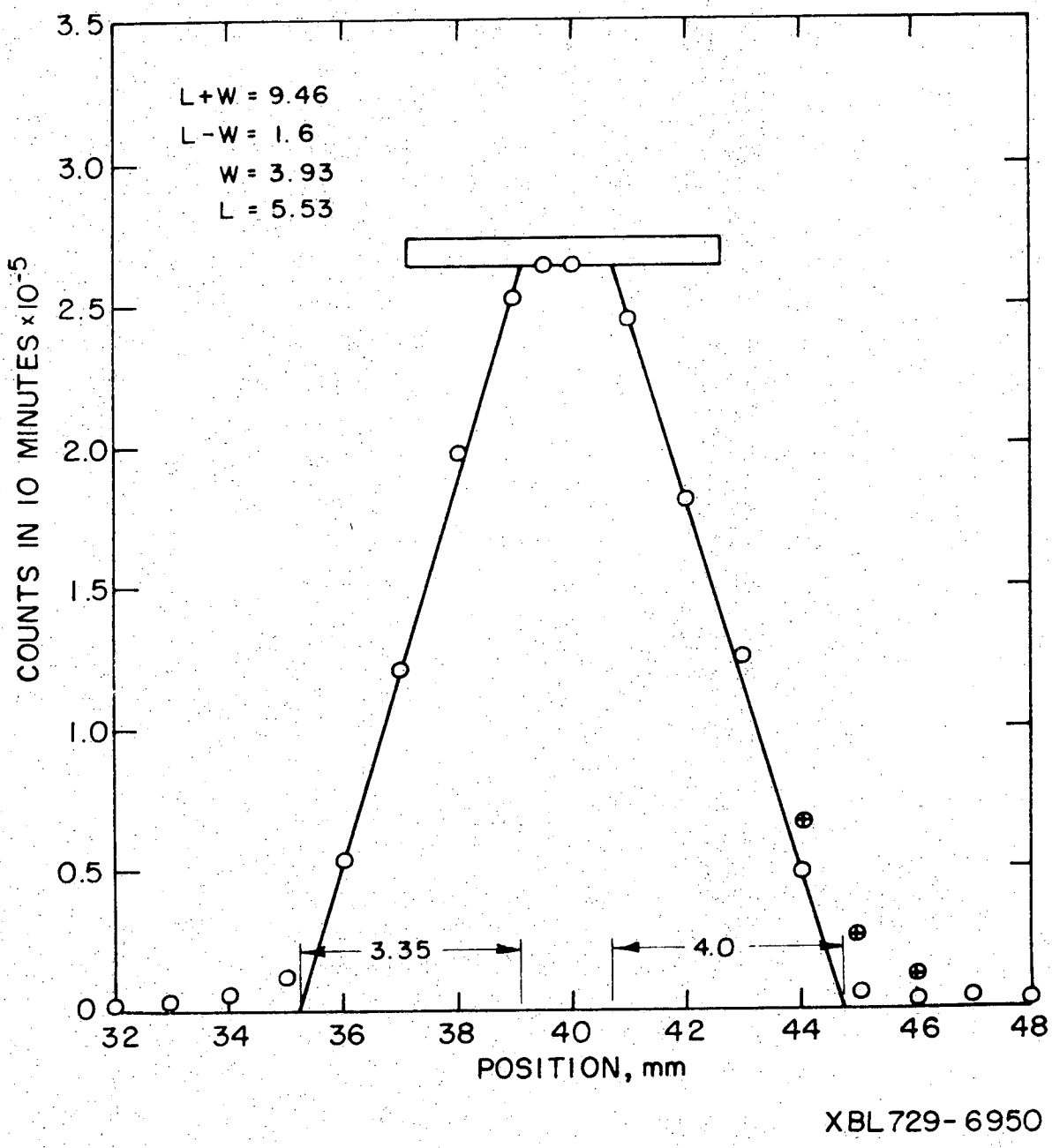

Fig. 30. Estimate of effective window width and lanthanum length using post-diffusion count data for Run 4.

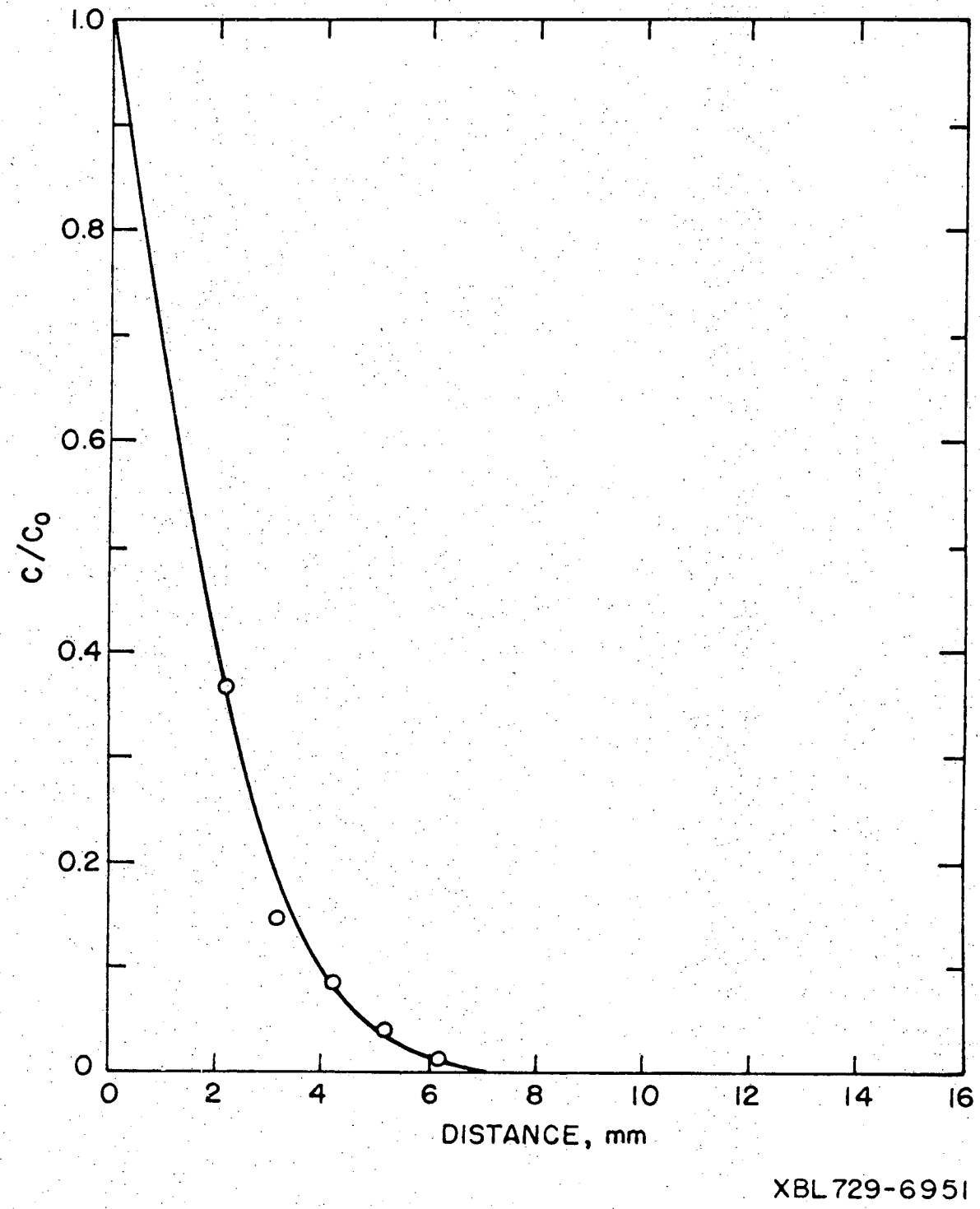

Fig. 31. Normalized concentration as a function of distance from interface for Run 4.

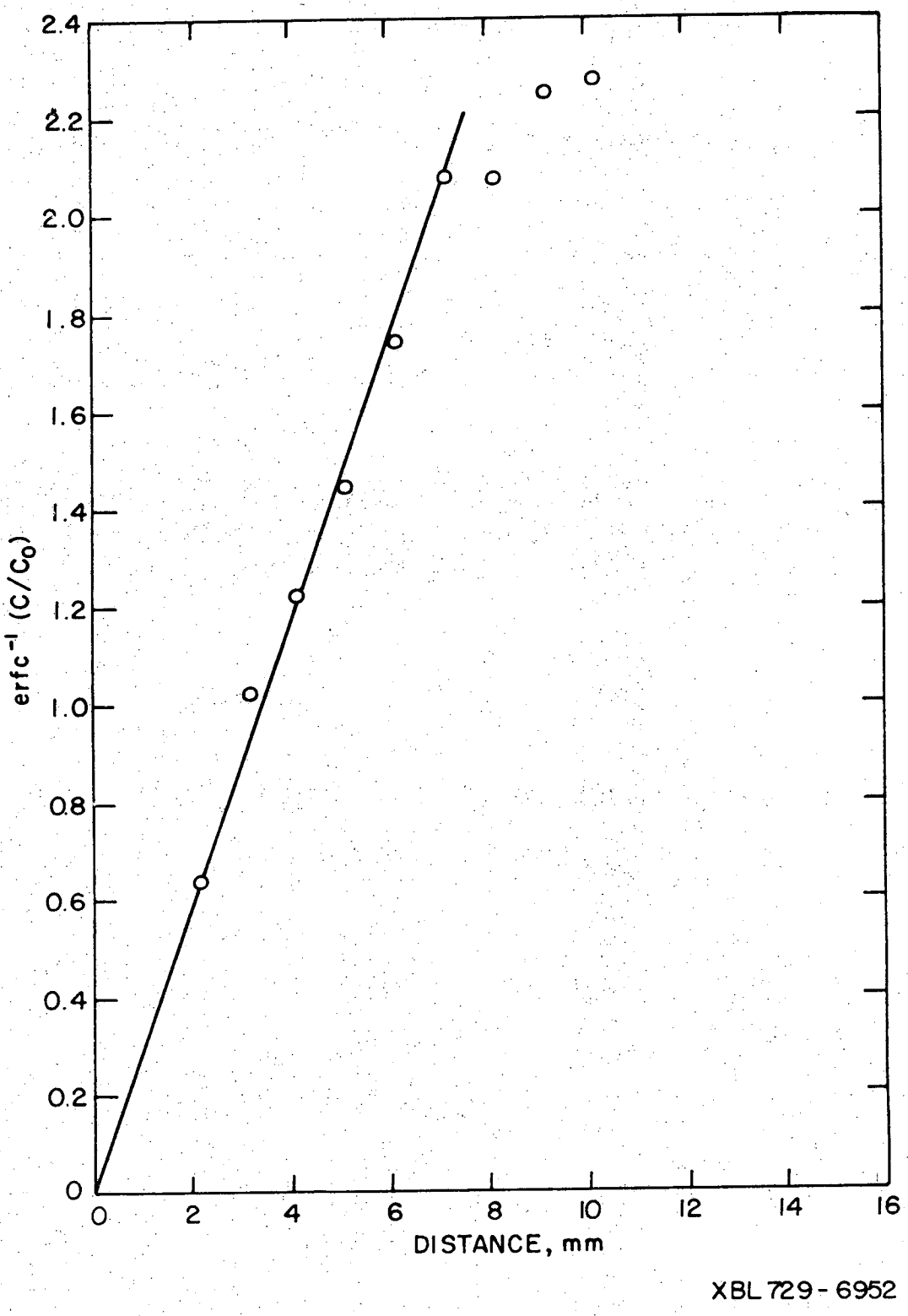

Fig. 32. Inverse complementary error function of concentration ratio as a function of count position for Run 4.

APPENDIX V

Diffusion Run 5

Diffusion Time	4 hours
Diffusion Temperature	1200°C
Pre-Diffusion Interface	22.9 mm
Post-Diffusion Interface	22.7 mm
Pre-Diffusion Lanthanum Length	11.6 mm
Post-Diffusion Lanthanum Length	5.2 mm
Pre-Diffusion Window Width	3.6 mm
Post-Diffusion Window Width	4.5 mm

Results:

Solubility (weight fraction)	0.053
Diffusion Coefficient	8.2×10^{-6} cm^2/sec

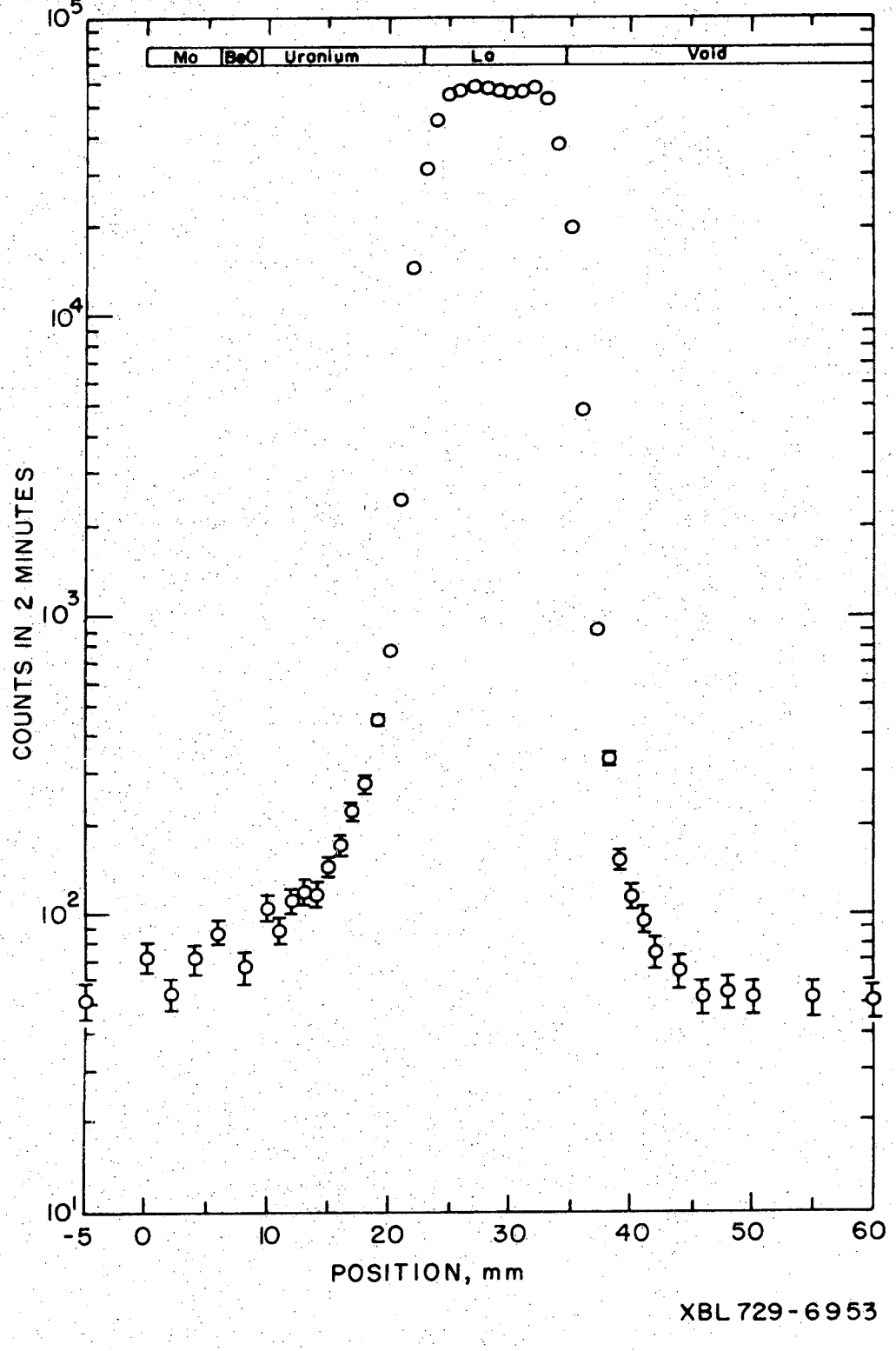

Fig. 33. Pre-diffusion count data for Run 5.

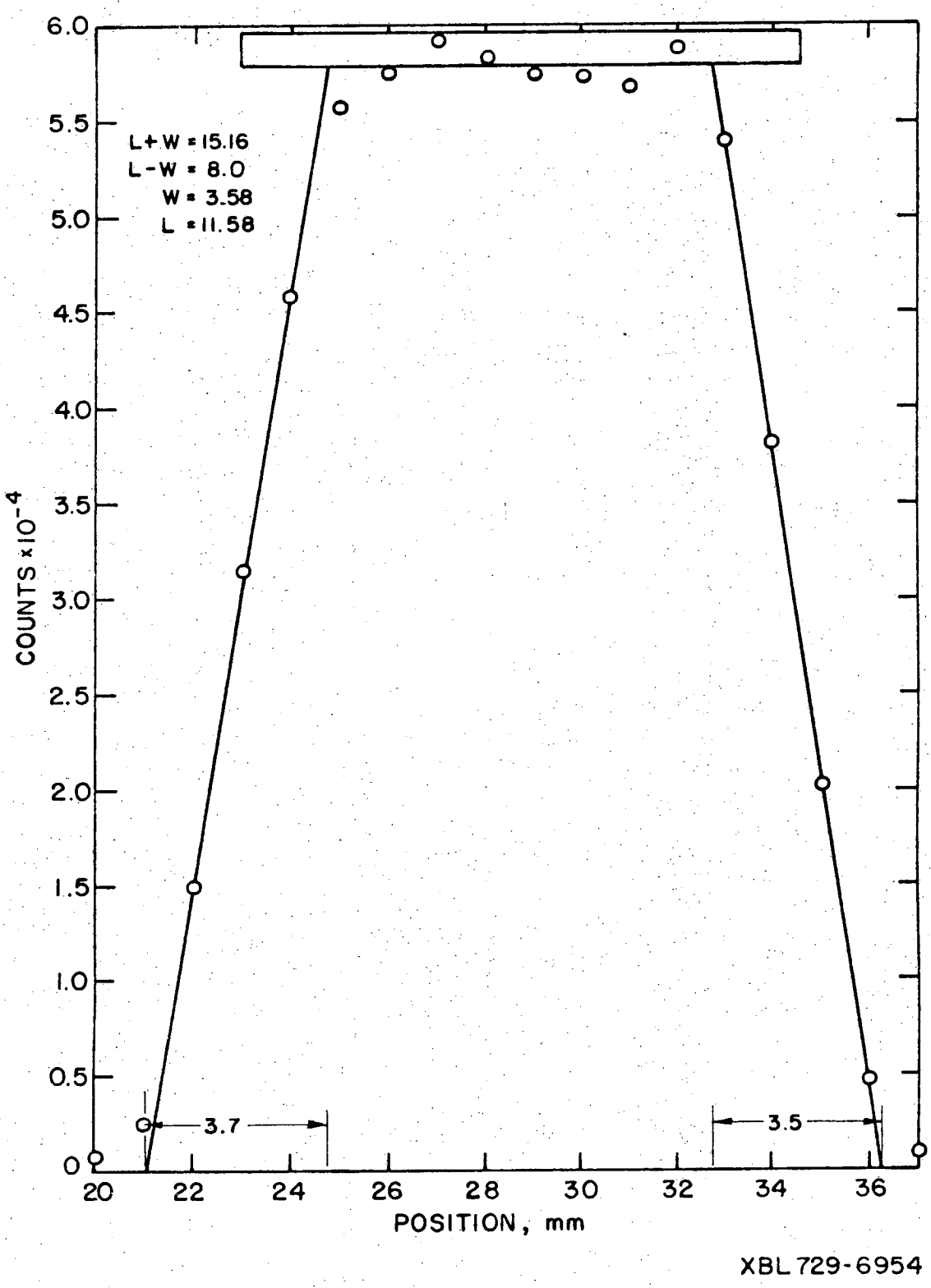

Fig. 34. Estimate of effective window width and lanthanum length using pre-diffusion count data for Run 5.

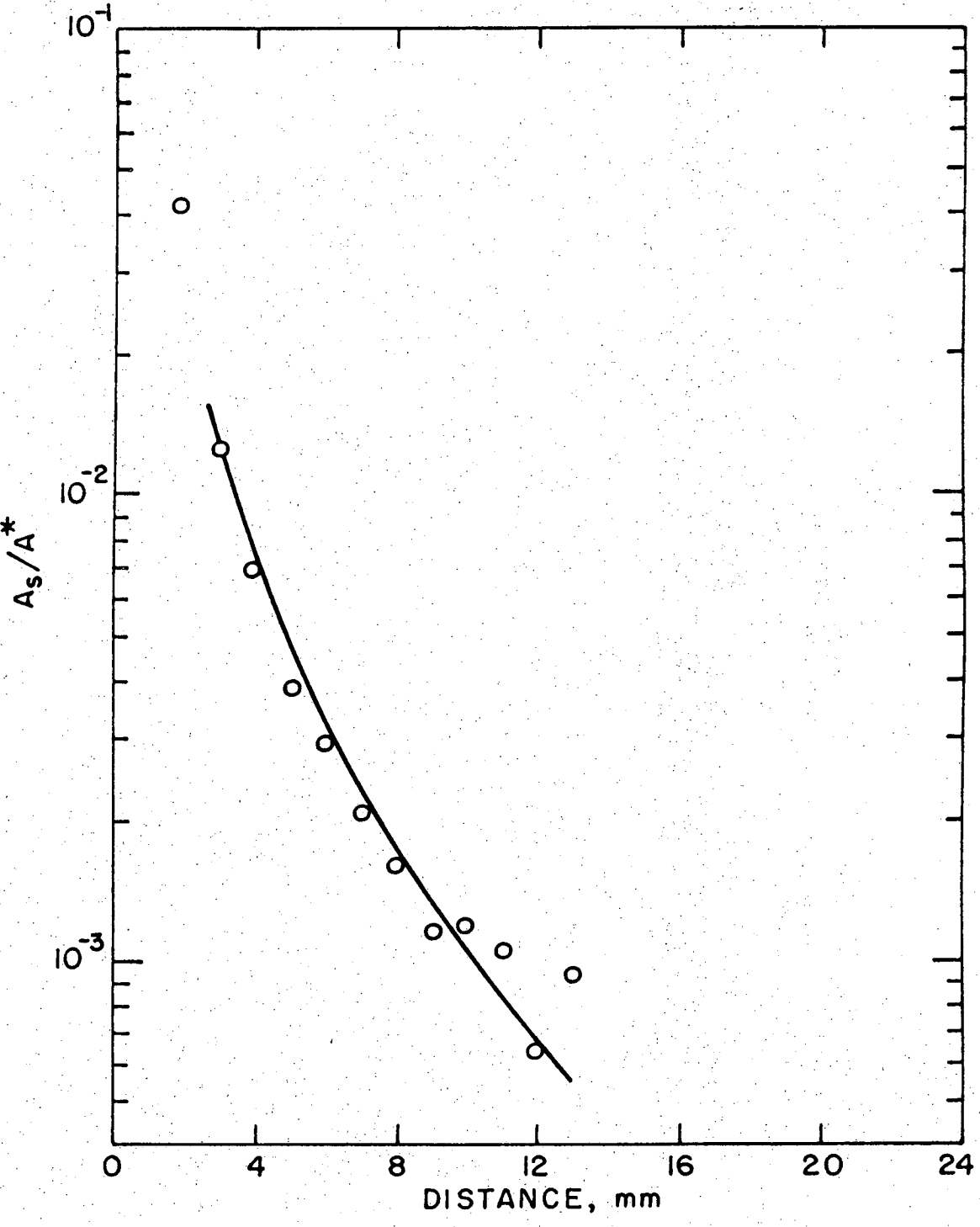

Fig. 35. Scattering correction normalized to maximum count rate of pure lanthanum from pre-diffusion count data for Run 5.

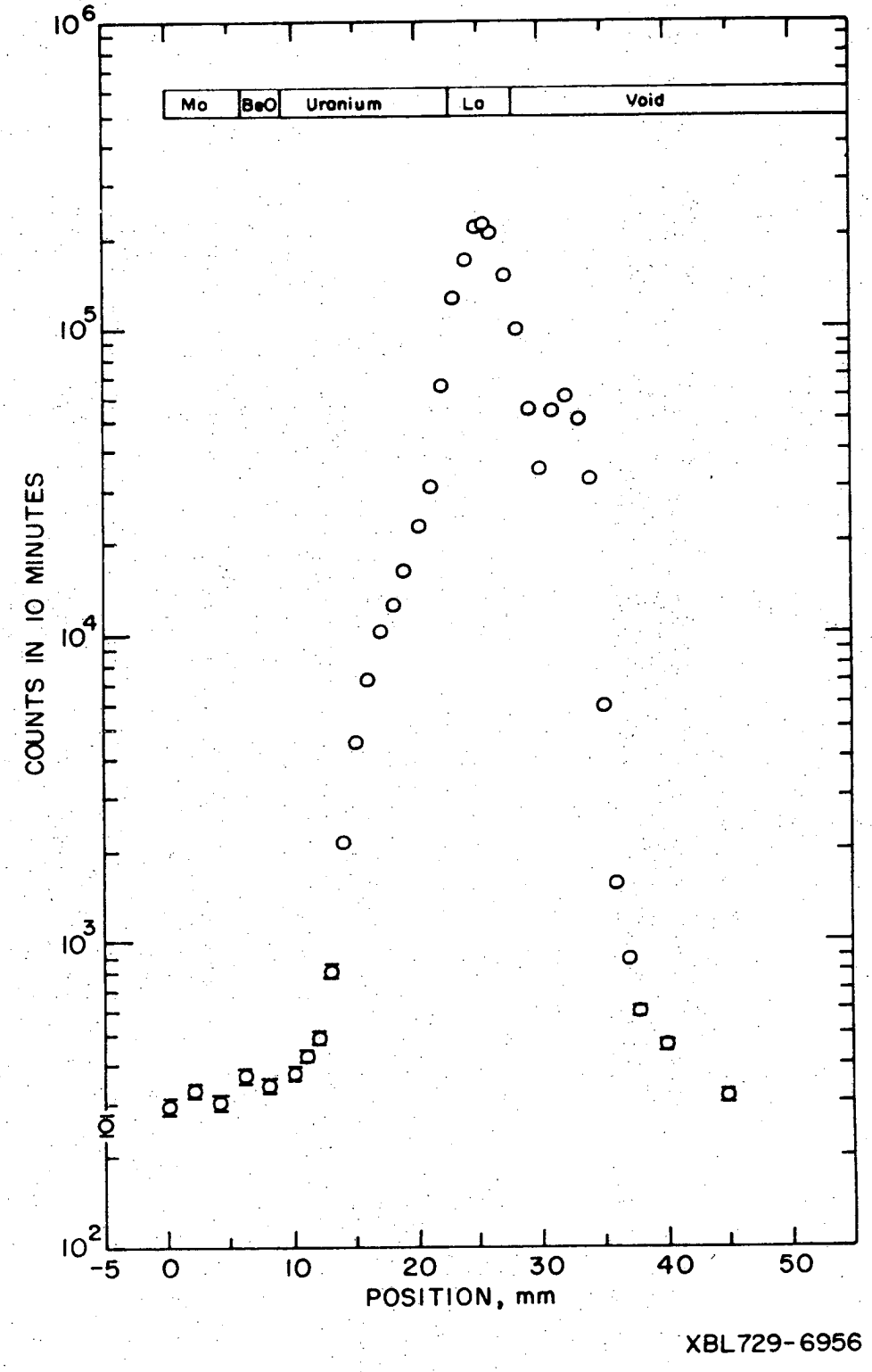

Fig. 36. Post-diffusion count data for Run 5.

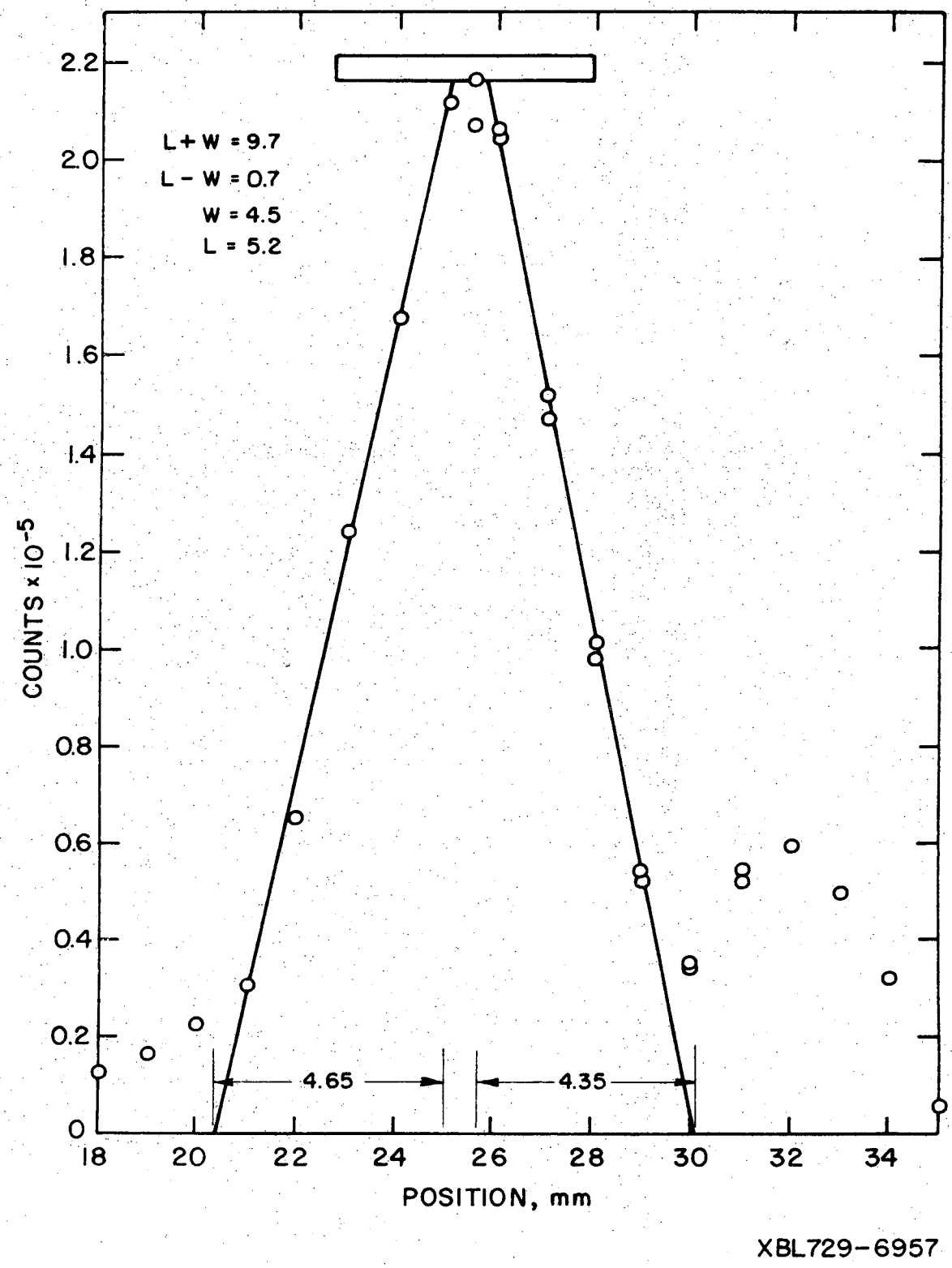

Fig. 37. Estimate of effective window width and lanthanum length using post-diffusion count data for Run 5.

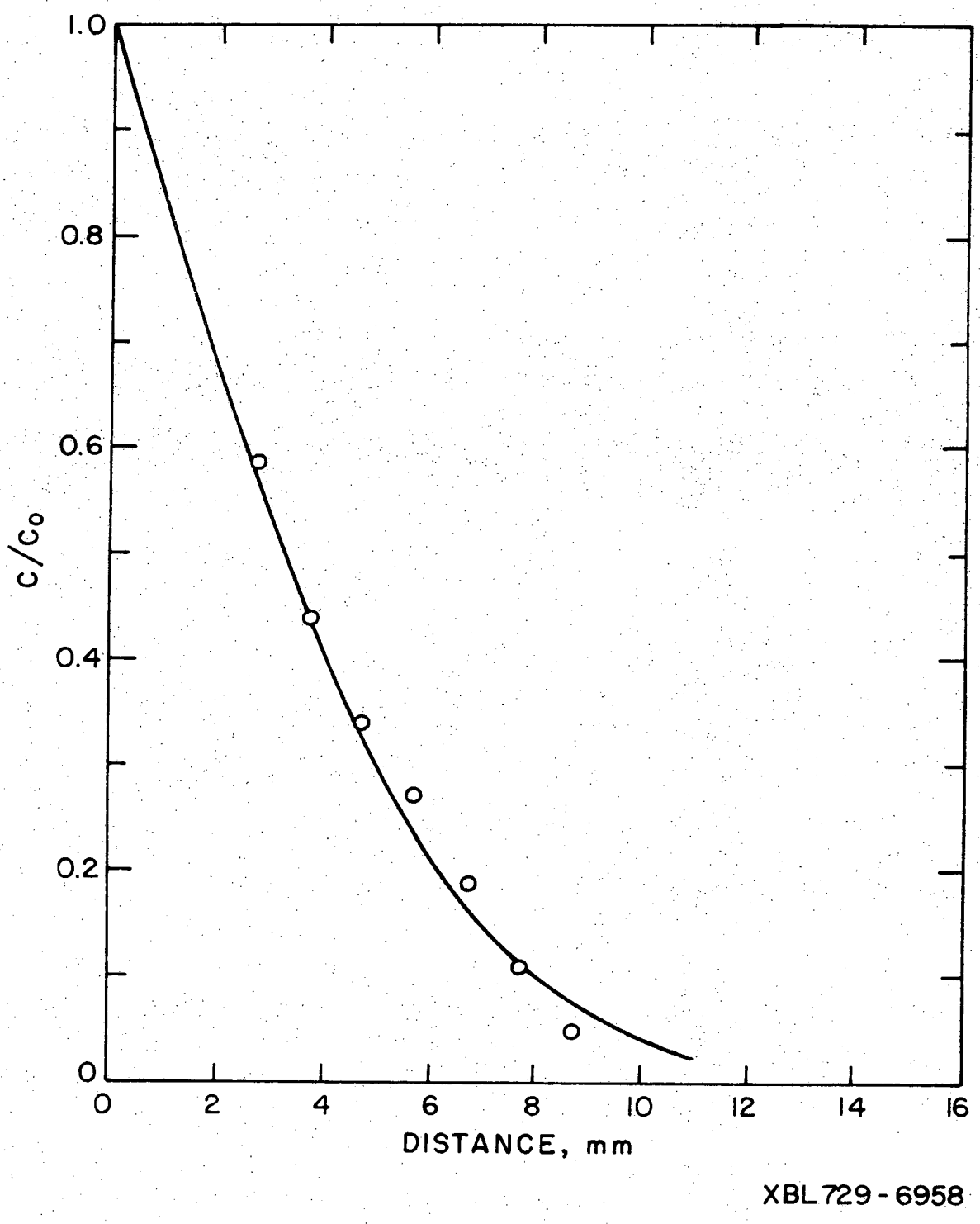

Fig. 38. Normalized concentration as a function of distance from interface for Run 5.

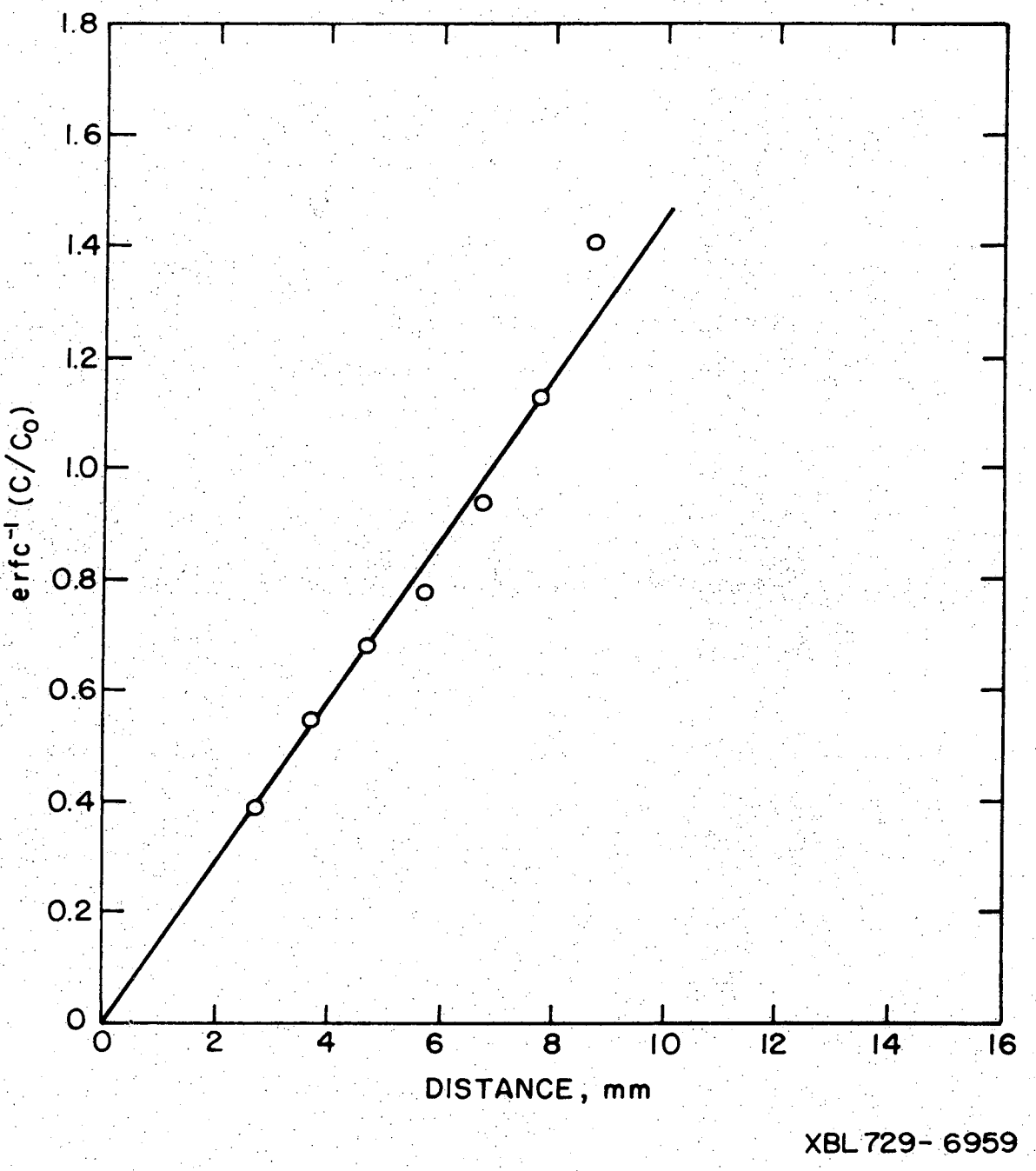

Fig. 39. Inverse complementary error function of the concentration ratio as a function of count position for Run 5.

APPENDIX VI

Diffusion Run 6

Diffusion Time	4 hours
Diffusion Temperature	1200°C
Pre-Diffusion Interface	22.7 mm
Post-Diffusion Interface	9.9 mm
Pre-Diffusion Lanthanum Length	10.8 mm
Post-Diffusion Lanthanum Length	6.1 mm
Pre-Diffusion Window Width	3.8 mm
Post-Diffusion Window Width	3.7 mm

Results: Loss of uranium through tantalum crucible

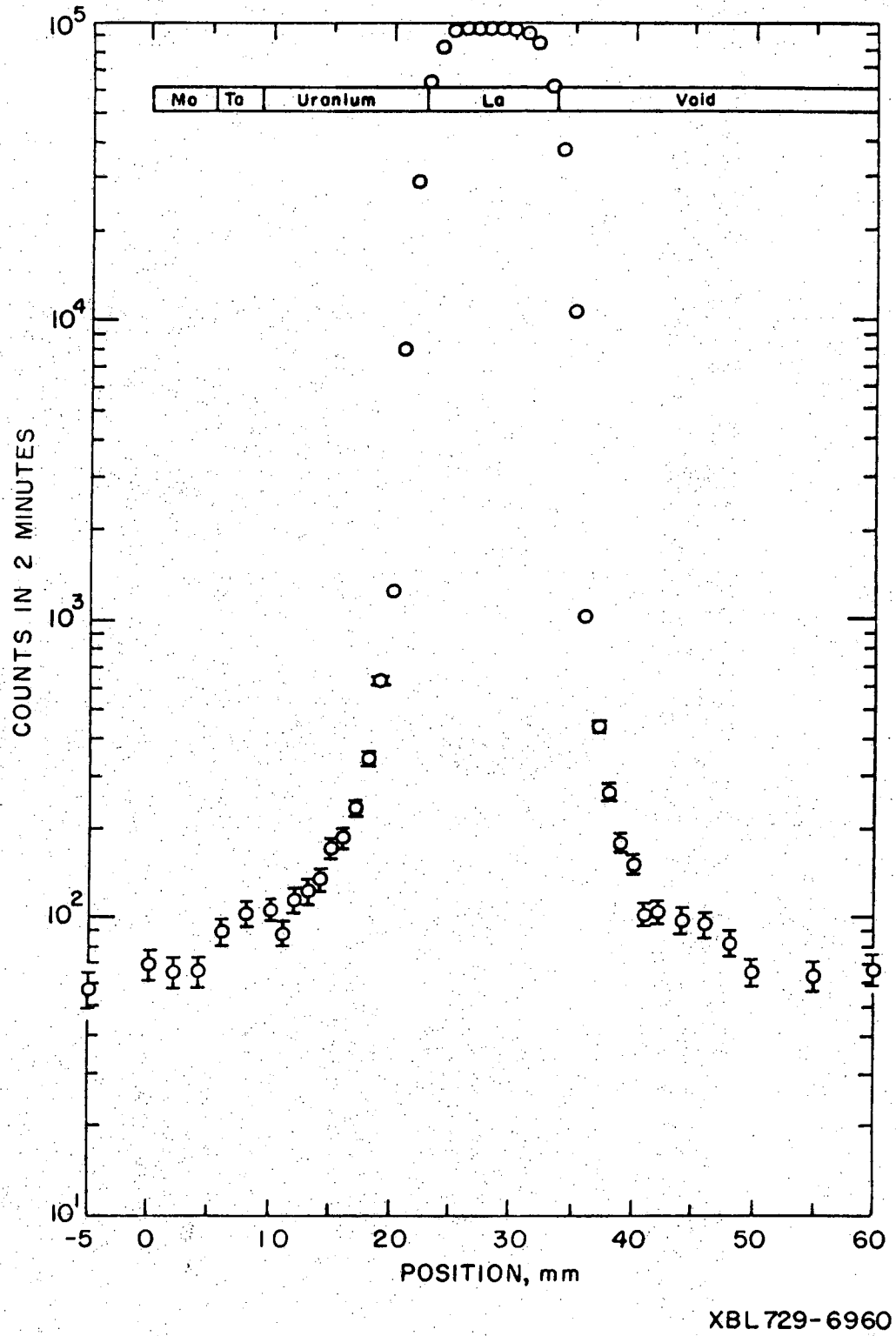

Fig. 40. Pre-diffusion count data for Run 6.

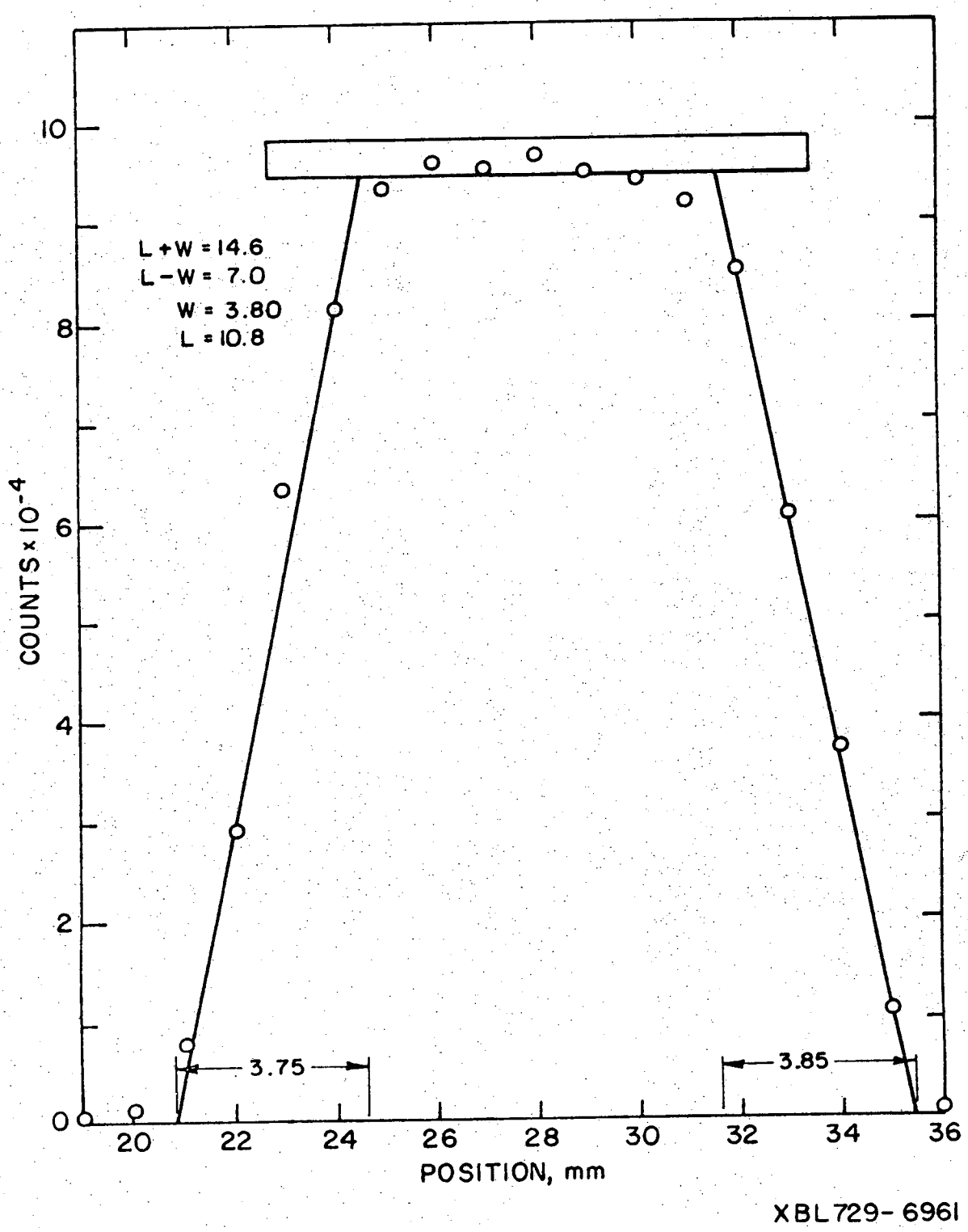

Fig. 41. Estimate of effective window width of lanthanum length using pre-diffusion count data for Run 6.

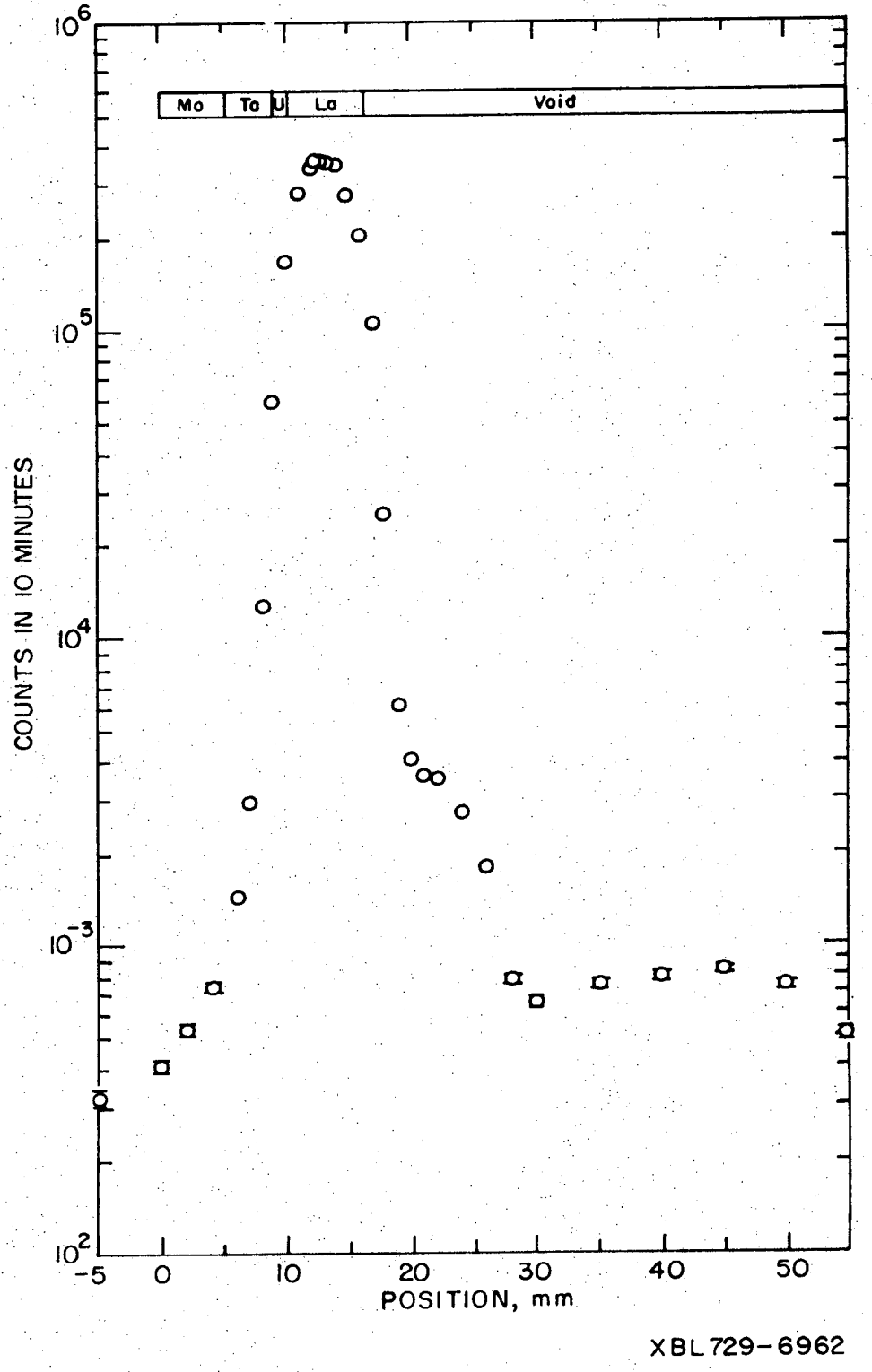

Fig. 42. Post-diffusion count data for Run 6.

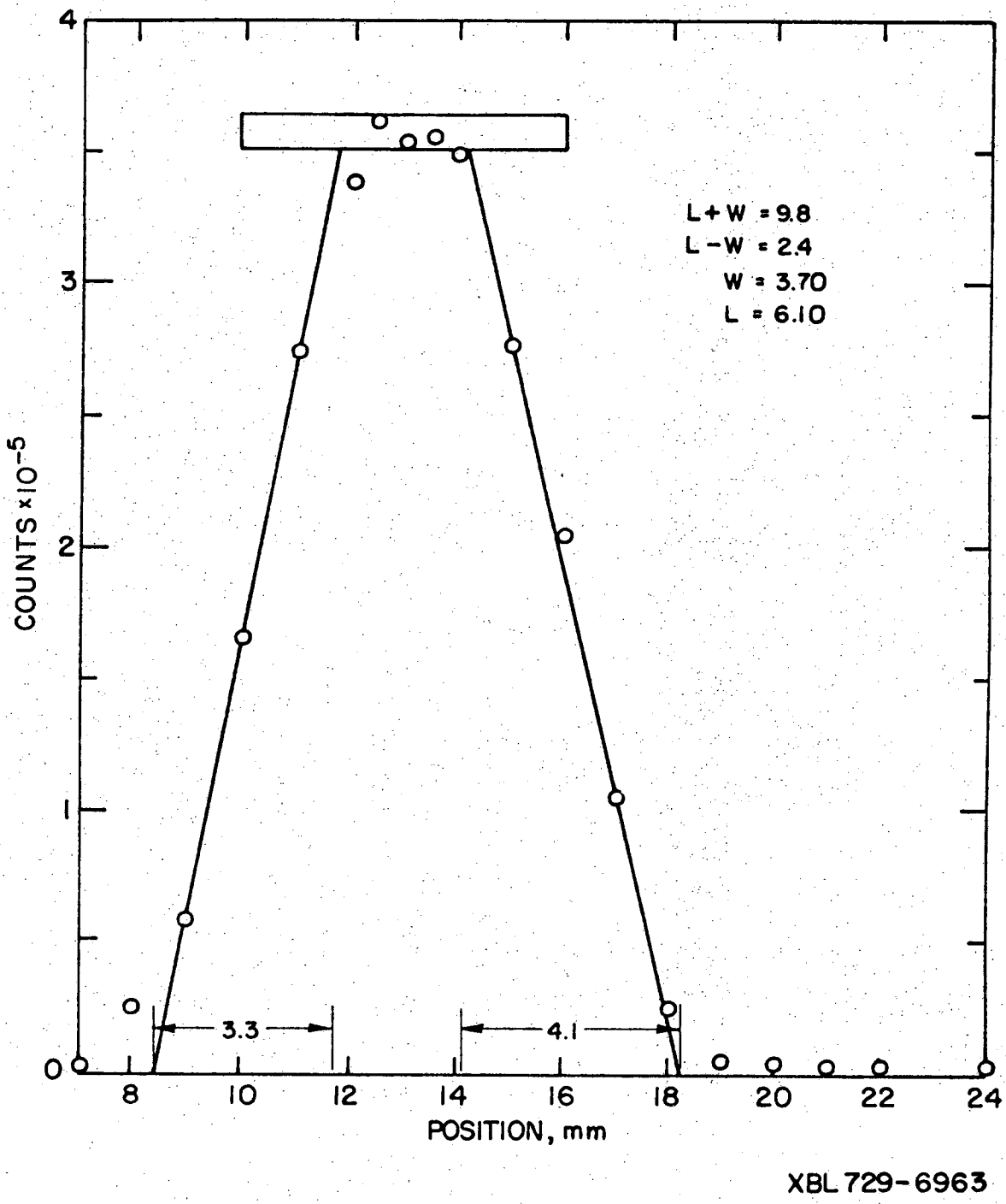

Fig. 43. Estimate of effective window width of lanthanum length using post-diffusion count data for Run 6.

APPENDIX VII

Counting System Calibration

The counting system was calibrated by suing sources with known gamma energies, and determining the cutoff point of the photopeak by examining the count rate of the source as a function of discriminator setting for several input voltages to the preamplifier and several amplifier gain settings. The sources used were cesium 137 (0.663 MeV) and cobalt 60 (1.17 MeV and 1.33 MeV). The voltage across the dynodes of the photo-multplier tube was 800 volts and an amplifier gain of 170 were selected for the counting of the activated lanthanum. The counts of the Cs^{137} and Co^{60} sources as a function of the discriminator setting are shown in Fig. 44. The system calibration curve was derived from Fig. 44 by plotting the discriminator setting which cut off the photopeak of each of the known gamma energies. The system calibration curve is shown in Fig. 45. A discriminator setting of 0.625 which cut off the energies below the photopeak of the lanthanum 140 (~1.4 MeV)[18] was determined from Fig. 45.

The counting system was set to a preamplifier input of 800 volts, an amplifier gain of 170, and a discriminator setting of 625 for the determination of the lanthanum profile in the uranium.

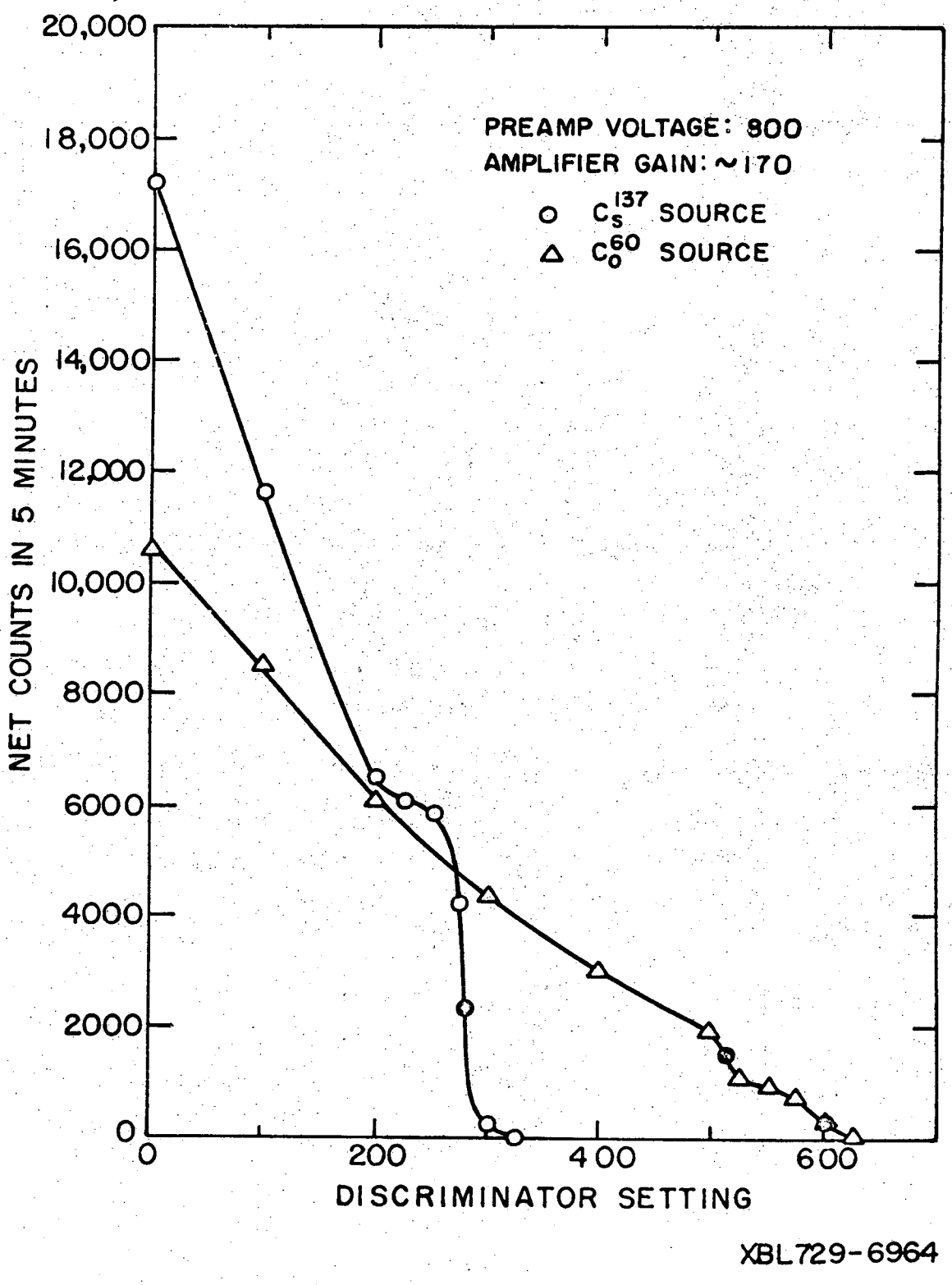

Fig. 44. Counting apparatus discriminator calibration.

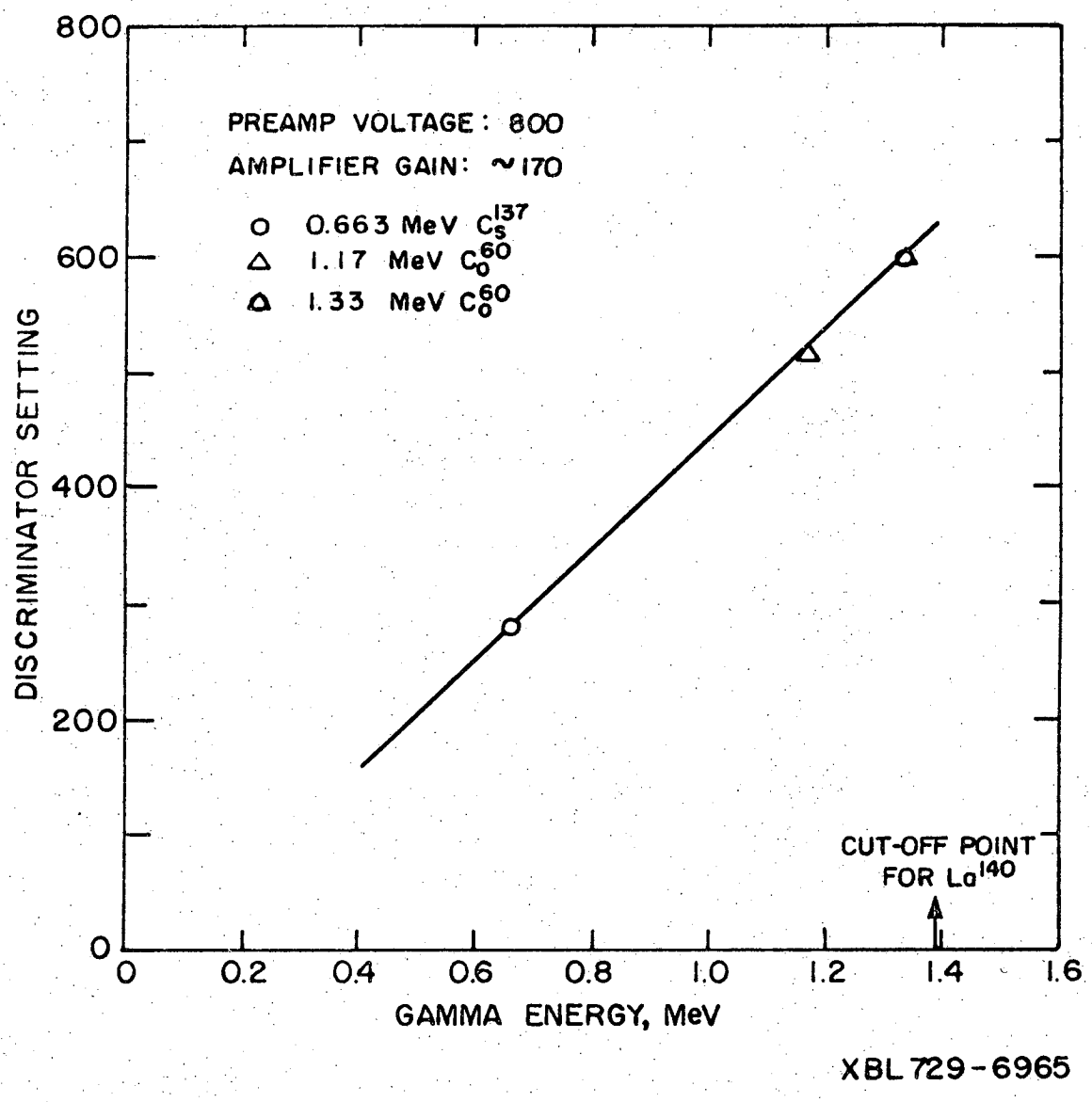

Fig. 45. Counting apparatus discriminator calibration.

APPENDIX VIII

Procedural Changes, Early Test Runs and Results

Procedural Changes During Research

Several procedural changes were initiated over the period covered by the research. The initial method of bringing the evacuated system to atmospheric pressure was to introduce a helium-4% hydrogen gas mixture into the system. The helium outgassing overloads the ion pump during large step changes in the system temperature so dry nitrogen was used to bring the evacuated system to atmospheric pressure. This change in back-fill gas reduced the time required to raise the specimen temperature from 20° to 1300°C from 7 hours to 4 hours without exceeding 10^{-5} torr pressure.

During the diffusion run LeBorgne used approximately 8 cubic feet per hour of the helium-4% hydrogen gas mixture into the system to reduce thermal gradients along the system. A problem encountered using this technique was maintaining a constant flow rate such that the specimen temperature remained constant. A simple thermodynamic analysis indicates that the maximum temperature gradient in the crucible is of the same size in an evacuated system as was measured by LeBorgne in a flowing gas system.

A new encapsulation procedure was developed for containing activated lanthanum during the uranium diffusion experiments.[19] The old encapsulation procedure used by LeBorgne involved electron beam welding either the crucible or the crucible holder closed with the 20 millicuries of activated lanthanum placed on top of the uranium ingot. This procedure required about one-half life of the activated lanthanum before the diffusion experiment, with a concomitant loss of counting precision.

The new encapsulation procedure involves the use of a cap threaded to the top of the molybdenum crucible holder. This capped portion of the crucible holder extends out of the furnace into the cool portion of the vacuum chamber. The threaded cap is at a temperature (~700°C) which is well below the melting point of the lanthanum (926°C) such that the lanthanum vapor from the sample condenses on the cool walls of the crucible holder and does not escape into the test facility.

Two dry runs were performed using the new encapsulation technique. The first run consisted of holding unirradiated lanthanum at 1200°C and 2×10^{-6} torr for 3 hours with no observed loss of lanthanum. The second run consisted of heating slightly activated lanthanum (5 millicuries) to the same temperature and pressure as the previous run. A swipe was taken in the region of the cap threads, the furnace lid and the crucible holder. No activity was detected on any of the swipes. Thus the screw cap encapsulation is regarded as a sealed source. Run #11 used the screw cap method of encapsulation of activated lanthanum for a time of 980 minutes at a temperature of 1185°C and a pressure of 1.1×10^{-6} torr with no release of activated lanthanum as determined by swipes. All runs with the screw cap encapsulation are swipe checked before and after heating the activated lanthanum in the furnace for contamination greater than two times background level.

The early runs used a vibrator fastened to the support plate, and connected to the molybdenum specimen holder by a stainless rod which is pinned to a tantalum rod pinned to the specimen holder. The vibrator operates at a frequency of 120 hertz with an amplitude which can be varied with a 1000 ohm, 25 watt reostat. A preliminary vibrational analysis of

the system indicates the natural frequency of the support system is about 320 Hertz.

The purpose of the vibrator was to eliminate bubbles in the uranium ingot by forcing the bubbles to move upwards through the molten uranium without coalescing to form a large bubble that would impede diffusion of lanthanum in the uranium. However when the tantalum was found to be inadequate as a container for molten uranium, and that even with vibration bubbles would form in the first melt of the uranium in a beryllia crucible (Run #9), vibration was eliminated ruring the uranium melts.

Early Test Runs and Results

A summary of the early test runs is shown in Table IV. There were only small spherical bubbles found in each of the uranium ingots after melting ranging in size from a pinpoint to the order of 0.25 mm in diameter. In all cases, except as noted, less than 15 bubbles were observed under a magnification of 30X. The bubble size and quantity was independent of the amount of vibration during the melt, and independent of the surface treatment of the uranium. Large separations were observed in runs #8 and #9, as shown in Figs. 46 and 47. An interesting bubble formation was found in run #3 which is shown in Fig. 48. Figure 49 shows radiographs of four specimens melted in beryllia crucibles for three hours at 1300°C by LeBorgne.[20,21]

In all of the runs, uranium was lost either by diffusion through the weld region and the walls of the tantalum crucibles, or by flow over the top of the crucibles. Several approaches were made to isolate the cause of the uranium loss. The first solution was to eliminate vibration as a cause of overflow (run #4), which was unsuccessful. The second solution

Table IV. Description of uranium test runs and results.

Run	Date	Temperature °C	Pressure Torr	Time at Temperature Minutes	Vibration Time Minutes	Crucible Material	Crucible Bakeout	Comments
#1	5/28	1296	10^{-5}	180	60	Welded Tantalum	None	Diffusion through weld region
#2	6/22	1310	2.3×10^{-6}	180	60	Welded Tantalum	180 minutes at 1310°C 1×10^{-5} Torr	Diffusion through weld region
#3	7/4	1298	3.0×10^{-5}	180	30	Machined Tantalum	180 minutes at 1302°C 1×10^{-4} Torr	Diffusion through tube and overflow over the top of the tubes
#4	7/17	1300	1.8×10^{-6}	180	0	Welded Tantalum	180 minutes at 1295°C 7×10^{-5} Torr	Diffusion through weld and overflow over tube top
#5	7/24	1303	3.0×10^{-5}	180	60	Closed Welded Tantalum	180 minutes at 1300°C 2×10^{-6} Torr	Diffusion through weld
#6	8/1	1300	1.0×10^{-6}	180	0	Welded Tantalum	180 minutes at 1293°C 1×10^{-5} Torr	Loss of uranium via overflow
	8/10	1250	1 atoms He-4%H_2	1440	0	Closed Welded Tantalum		Unactivated lanthanum used. Loss of uranium by diffusion
#7	8/14	1257	4×10^{-6}	180	0	Closed Welded Tantalum	180 minutes at 1305°C 1×10^{-5} Torr	Diffusion through weld region
#8	8/22	1206	1×10^{-6}	180	0	Closed Machined Tantalum	181 minutes at 1290°C 2×10^{-6} Torr	Large separation of uranium. Diffusion through wall of tube.
#9	8/30	1304	1.0×10^{-6}	180	60	Be O	None used for earlier melt	Overflow of uranium. Large separation of uranium
#10	10/3	1251	1.1×10^{-6}	180	0	Machined Tantalum	None	Premelted uranium used. Diffusion through bottom and walls
#11	10/7	1209	1.3×10^{-6}	45	0	Machined Tantalum	None	Good melt - no signs of uranium leakage
	10/8	1185	1.1×10^{-6}	980	0			Activated lanthanum used apparent overflow

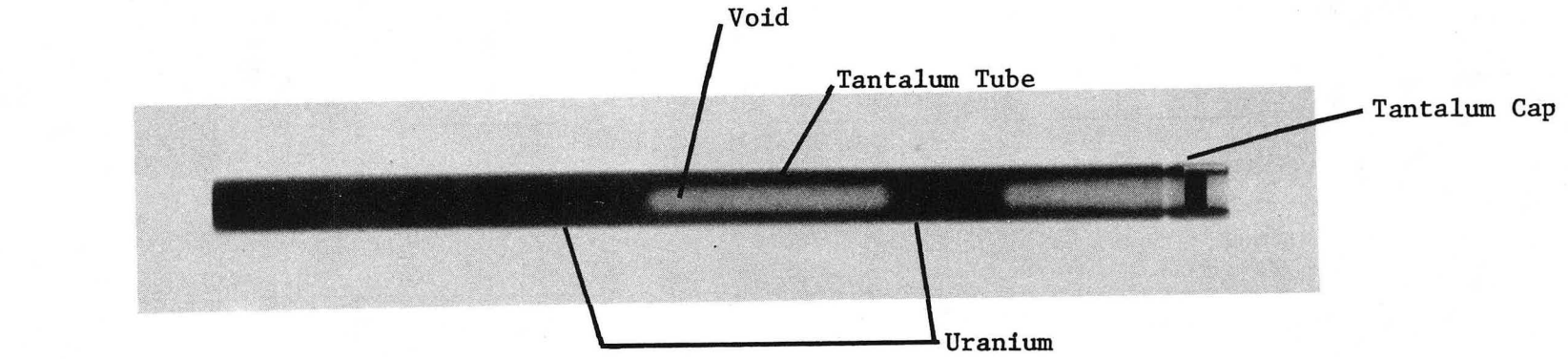

XBB 729-4594

Fig. 46. Radiograph of uranium melted in a closed tantalum capsule (Run #8).

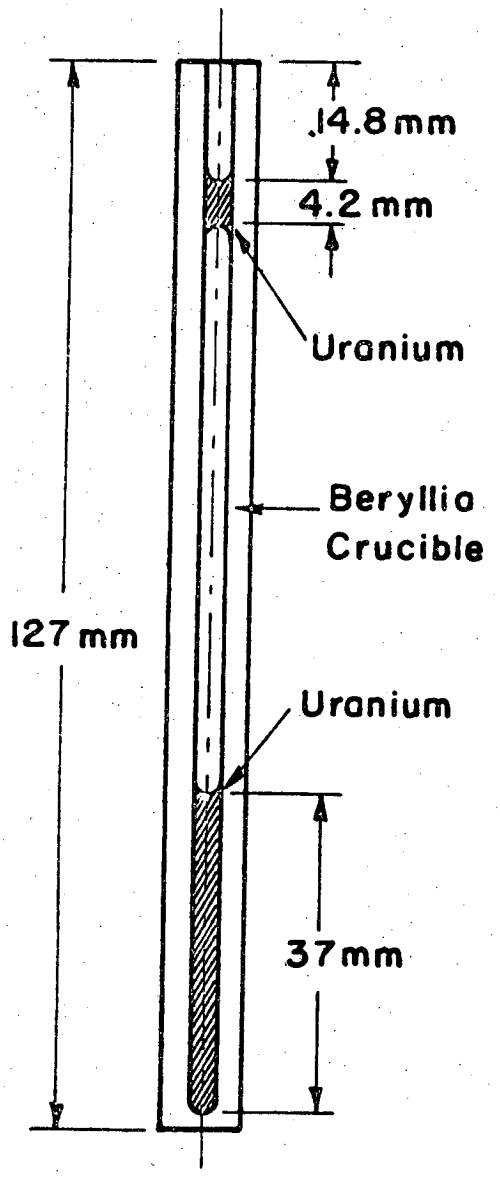

XBL729-6966

Fig. 47. Sketch of uranium melted in a Beryllia crucible using vibration (Run #9).

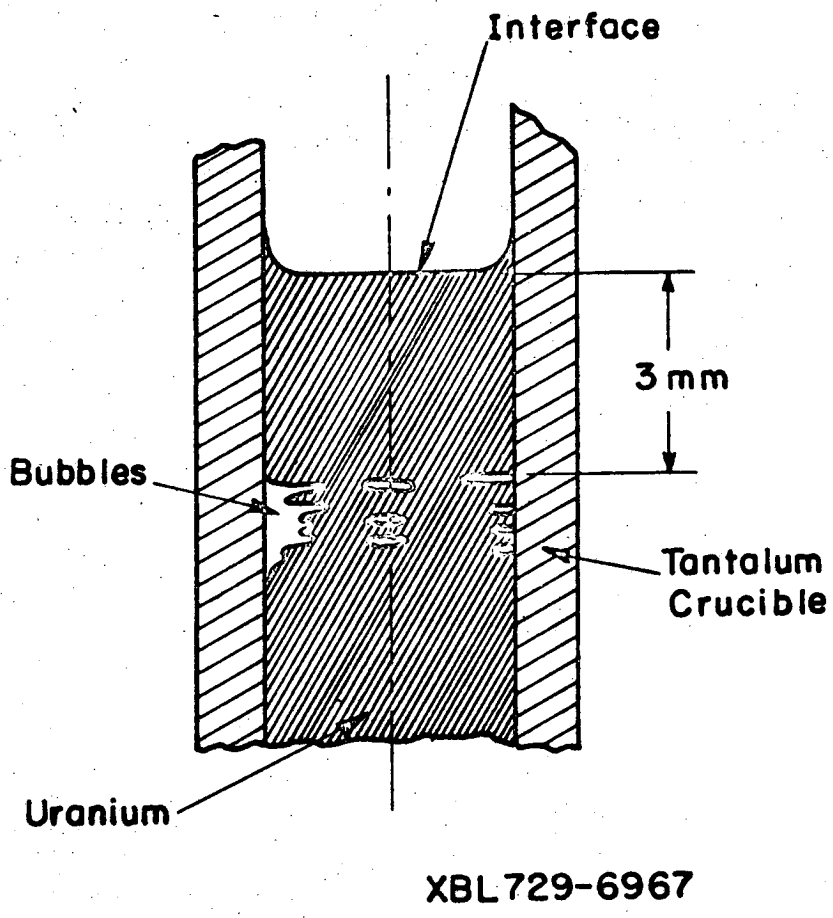

Fig. 48. Sketch of bubble formed in Run 3 as seen through a microscope at 30×.

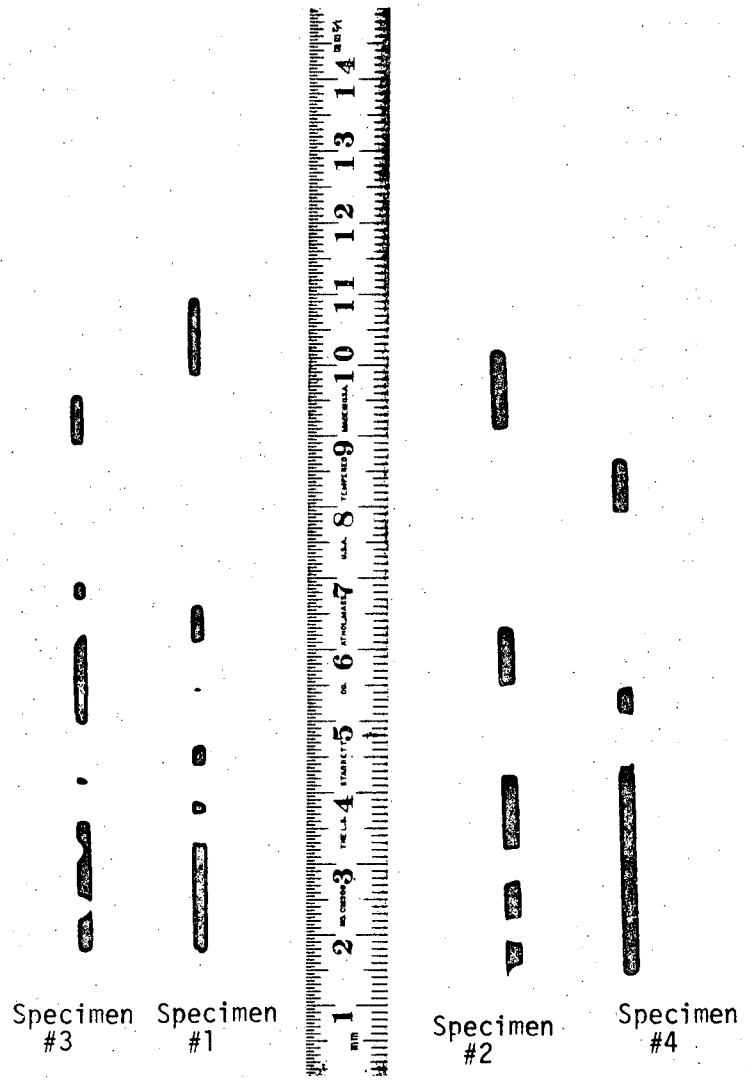

Fig. 49. Radiographs of uranium melted in beryllia crucibles by Le Borgne.

was to weld a cap on the crucible, which prevented overflow, but a loss of uranium by diffusion through the weld occurred (run #5).

The third attempt at solving the loss of uranium by diffusion was to use deep bored, machined tantalum crucibles with a welded cap without vibration. This attempt (run #8) was also a failure as evidence of diffusion at the bottom of the tube was easily observed. Since the gaseous impurities in the uranium may cause the overflow of the uranium, and since the diffusion of uranium through the tantalum was thought to be strongly temperature dependent, a remelt (run #10) of uranium melted at 1300°C in a beryllia crucible by LeBorgne (specimen #1 in Fig. 49) was tried in a machined tantalum crucible at 1250°C. This run was also a failure in that the premelted uranium diffused through the tantalum crucible. A final uranium run was attempted in a tantalum crucible which was not baked out. This run (run #11) was melted at 1200°C for the short time of 45 minutes, and no leakage or diffusion was observed. However, on a remelt at 1185°C for 16 hours with activated lanthanum, evidence from a counting experiment indicated that the uranium overflowed the tantalum crucible.

Bubble Formation in Uranium Ingots

Since a key to the successful measurement of the diffusion of lanthanum in molten uranium is the elimination of bubbles, the formation of the bubbles is of interest. LeBorgne observed a rise in the surface of the original uranium melt caused by bubbles in the uranium of between 3 and 4 centimeters using a 3.2 mm diameter beryllium crucible. If the gas which caused the bubbles was initially an impurity in the uranium, a simple fluid statics analysis will give an order of magnitude estimate of the concentration of the gas in the uranium as function of the gas.

Briefly this analysis gives a gas concentration of:

$$C = \frac{\ell_B}{RT} \times 10^{-6}$$

where ℓ_B is the bubble height, T is the uranium temperature and R is the gas constant. The concentration of gas impurity for several specific gases which could cause a 3.5 cm bubble in the melted uranium is shown in Table V. The increase in bell jar pressure assuming the gas is suddenly released from the uranium and rapidly cooled to 100°C is about 2×10^{-5} torr.

Since a low concentration of gaseous impurities can create a rather large bubble, the concentration of hydrogen, nitrogen and oxygen impurities in the uranium were determined using a vacuum fusion method. Briefly, the uranium specimen is cleaned using an argon sputtering process. The cleaned uranium sample is placed in a molten platinum bath in a graphite crucible at 1900°C. The hydrogen, nitrogen and oxygen impurities are released as free hydrogen and nitrogen and carbon monoxide respectively. The concentration of the released gases are analyzed by a mass spectrometer, and the initial concentration of the impurities in the uranium is determined with a PDP 7 computer. The vacuum fasion analysis was performed by J. Fisher of LLL Livermore to determine the amount of nitrogen, oxygen and hydrogen dissolved in the uranium. The results of this analysis are given in Table V.[22]

For the dissolved gas concentrations measured by Fisher, the estimated bubble height in a 3.2 millimeter diameter tube is approximately 10 cm. The length of the uranium specimens is approximately 5 cm and the length of the tantalum crucibles is about 10 cm. Thus a sudden release of the dissolved gases in the uranium may cause the uranium to overflow the crucible.

Table V. Measured gas impurities in uranium and the amount of the impurities required to cause a 3.5 cm bubble in a 0.32 cm diameter tube

Gas	Measured Concentration (ppm)	Required Concentration (ppm)
Hydrogen	0.10	0.53
Helium	----	1.1
Nitrogen	12.	7.4
Oxygen	9.0	8.5
Xenon	----	34.

Tantalum as a Container for Molten Uranium

The loss of uranium in tantalum crucible has been the major problem area in these diffusion experiments. As noted earlier, some of the uranium loss can be attributed to the overflow of the molten uranium from the crucible. LeBorgne did not have the overflow problem because he used longer crucibles than currently used. However, there is evidence that the uranium also diffused through the tantalum especially in weld regions. J. M. Johnson of LRL-Livermore ran an electron beam microprobe analysis on the welded tantalum crucible used in run #4 described in Table IV. Johnson found that the concentration profile and x-ray images indicate uranium-tantalum diffusion as well as uranium grain boundary attack of the tantalum tube.[23]

LeBorgne used tantalum crucibles to hold molten uranium under virtually identical conditions as the runs described above, except for the use of vibration to eliminate bubbles. LeBorgne did not lose gross amounts of uranium in his experiments, and concluded that tantalum was a satisfactory crucible material. An after-the-fact visual examination of LeBorgne's test specimen indicates some diffusion of the uranium through the tantalum. LeBorgne's crucibles were from a different batch of tantalum than the crucibles used in the above experiments, and the acid cleaning procedure of the current crucibles may have been different than those used by LeBorgne.

Finucane and Smith used tantalum crucibles to contain molten uranium. Finucane's maximum experimental temperatures of the uranium in a tantalum crucible was 1228°C with a test time of minutes. Smith used tantalum crucibles to contain uranium at a temperature of 1480°C for a time of

140 minutes. Neither Finucane nor Smith reported problems containing the uranium in a tantalum crucible.

Other experimenters have had difficulty containing molten uranium with tantalum. McIntosh and Bagley reported that tantalum dissolves slowly in uranium at all temperatures up to 1300°C, and its upper limit as a container material occurs in the region of 1450°C. They report that tantalum becomes permeable to liquid uranium as a result of intergranular diffusion between 1200 and 1250°C. McIntosh and Bagley report a penetration of 10 mils of tantalum by uranium at 1300°C in 90 minutes, 30 mils at 1335°C in 90 minutes, 10 mils at 1300°C in 9 hours, and 5 mils at 1225°C in 4 hours. Wilkinson cites work by Blumenthal where the intergranular corrosion of tantalum by uranium penetrated a 15 mil wall at 1200°C in less than six hours.[24,25] Note that in the current diffusion experiments the penetration is 60 mils at 1200°C in 3 hours. Schramm et al.[26] report that molten uranium attacks tantalum crucibles intergranularly so vigorously even at temperatures only 100-200°C above the uranium melting point that uranium melts drained through the crucibles in a short time.

The excessive diffusion of the uranium in the lanthanum-uranium experiments through the tantalum was initially attributed to temperatures higher than read out on the alumel-chromel thermocouple. The temperatures were checked with an optical pyrometer and found to be in the same region as determined by the thermocouple. Also the effect of the 3 hour bakeout at 1300°C of the tantalum crucible was suspect because of the grain growth associated with the bakeout, which is above the recrystallization temperature of tantalum. However, the bakeout was eliminated in run #10 and diffusion of the uranium through the tantalum still occurred.

Thus, based on the above evidence, the loss of uranium by overflowing the tantalum crucible is much greater than the loss by diffusion. The paucity of information on the variables that influence the diffusion of tantalum by molten uranium is sufficient reason to reject the use of tantalum crucibles to contain molten uranium.

APPENDIX IX

Derivation of Equations for Estimating the Effective Counting Window Width and Lanthanum Length

Consider a counting profile as shown in Fig. 4, where the count rate is plotted as a function of the location of the center of the counting window. When the counter sees only the activated lanthanum the count rate is A^*. Likewise when the counter does not see any activated lanthanum the count rate is A_{bkg}. If the activated lanthanum fills a fraction x/w of the window width the count rate due to the activated lanthanum will be

$$A = (A^*-A_{bkg}) \frac{x}{w} + A_{bkg} \tag{1}$$

for a flat interface. The count rate will be A^* when the counter only sees the activated lanthanum which occurs when the lanthanum interface is half a window width from the center of the window. Thus for a lanthanum length L

$$b = L-w \tag{2}$$

where b is the distance a count rate of A^* is measured. Likewise the count rate will be A_{bkg} when the counter does not see any activated lanthanum which occurs half a window width from the center of the window, or

$$a = L + w \tag{3}$$

where a is the distance that the count rate greater than A_{bkg} is measured. Solving Eqs. (2) and (3),

$$\begin{aligned} L &= \frac{1}{2} (a+b) \\ w &= \frac{1}{2} (a-b). \end{aligned} \tag{4}$$

The count rate as given by Eq. (1) varies linearly with the fraction of the window filled by activated lanthanum. Thus the distances a and b can be determined by extrapolation of straight lines drawn through the count rate points adjacent to the activated lanthanum to the "background" count rate and to the maximum average count rate plateau.

APPENDIX X

Derivation of the Scattering Correction

To estimate the effect of scattering on the measured count rates, consider a rod of activated material with radius a, length L whose interface is located a distance x from the axis of the counting slit of width w as shown in Fig. 50. The flux from an element dy of the activated rod a distance y above the interface is given by

$$I(x) = e^{-\mu_u x} \int_o^L \frac{e^{-\mu_L y}(S\pi a^2 dy)}{4\pi(x+y)^2} = \frac{S a^2 e^{-\mu_u x}}{4} \int_o^L \frac{e^{-\mu_L y}\, dy}{(x+y)^2} \qquad (1)$$

where $\frac{1}{4\pi(x+y)^2}$ is the fraction of photons in the solid angle subtended by a unit area at position x

$S\,\pi a^2 dy$ is the number of photons per unit time emitted by the slice

$e^{-\mu_u x}$, $e^{-\mu_L y}$ are the amount of attenuation due to absorption in the uranium and lanthanum respectively

S is source strength, counts/sec-cm^3

μ is the attenuation coefficient (in lanthanum or uranium)

Now neglecting self absorption in the source ($e^{-\mu_L y} \approx 1$) and integrating

$$I(x) = \frac{Q}{4\pi} \frac{e^{-\mu_u x}}{x(x+L)} \qquad (2)$$

where $Q = \pi a^2 LS$ is the total activity of the source. The average flux over the slit width at the position of the slit is

$$\bar{I}(x) = \frac{1}{w} \int_{x-(1/2)w}^{x+(1/2)w} I(x')dx' = \frac{Q}{4\pi w} \int_{x-(1/2)w}^{x+(1/2)w} \frac{e^{-\mu x'}}{x'(x'+L)}\, dx' \qquad (3)$$

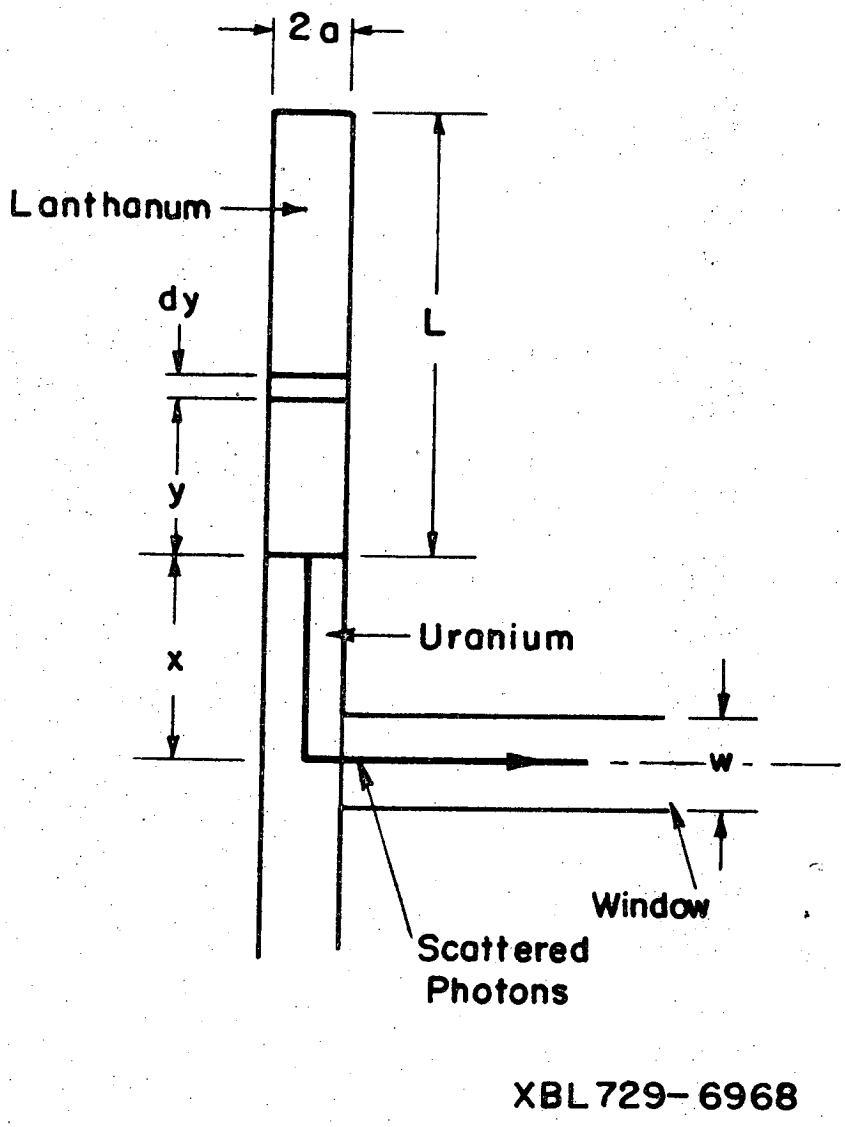

Fig. 50. Model used to compute scattering effect on geometrical counting resolution.

Set $e^{-\mu_u x'}$ constant $= e^{-\mu_u x}$,

$$\bar{I}(x) = \frac{Q\, e^{-\mu_u x}}{4\pi w} \int_{x-(1/2)w}^{x+(1/2)w} \frac{dx'}{x'(x'+L)} \tag{4}$$

Now

$$\bar{I}(x) = \frac{Q\, e^{-\mu_u x}}{4\pi wL} \ln\left[\left(\frac{x-\frac{1}{2}w+L}{x+\frac{1}{2}w+L}\right)\left(\frac{x+\frac{1}{2}w}{x-\frac{1}{2}w}\right)\right] \tag{5}$$

Now if α is the fraction of the 1.6 MeV photon flux at the window which is scattered along the slit and detected, then

$$A_s(x) = \frac{\alpha Q \beta e^{-\mu_u x}}{4\pi wL} \ln\left[\left(\frac{x-\frac{1}{2}w+L}{x+\frac{1}{2}w+L}\right)\left(\frac{x+\frac{1}{2}w}{x-\frac{1}{2}w}\right)\right] \tag{6}$$

where $A_s(x)$ is the count rate due to scattering for distance x from the interface ($x > \frac{1}{2}w$) and β is a constant which converts flux at the detector to count rate. If the lanthanum source fills the window, a count rate A^* is measured where

$$A^* = \beta\, Q\, \frac{w}{L}$$

where $\frac{w}{L}$ is the fraction of the total activity of a rod of length L measured through a width w. Then

$$\frac{A_s(x)}{A^*} = \frac{k'}{w^2}\, e^{-\mu_u x} \ln\left[\left(\frac{x-\frac{1}{2}w+L}{x+\frac{1}{2}w+L}\right)\left(\frac{x+\frac{1}{2}w}{x-\frac{1}{2}w}\right)\right] \tag{7}$$

where $k' = \alpha/4\pi$ is a constant of the detection system.

The constant k' can be estimated from the prediffusion counting profile by

$$k' = \frac{w^2}{n} \sum_{i=1}^{n} \frac{e^{-\mu_u x_i} \left[\frac{A(x_i) - A_{Bkg}}{A^*} \right]}{\ell n \left[\left(\frac{x_i - \frac{1}{2} w + L}{x_i + \frac{1}{2} w + L} \right) \left(\frac{x_i + \frac{1}{2} w}{x_i - \frac{1}{2} w} \right) \right]} \qquad (8)$$

where n is the number of positions counted in the premelt profile.

A comparison of the calculated scattering correction factor with the measured values of the net count rate normalized to the maximum count rate for the prediffusion data of runs 1 through 5 are shown in Appendices I through V, respectively.

APPENDIX XI

Effect of the Use of a Window with Non Zero Width to Determine the Concentration in a Medium of a Solute with Complementary Error Function Distribution

Assume the distribution of a solute in a medium is given by

$$\frac{C}{C_o} = \operatorname{erfc}\left(\frac{x}{2\sqrt{Dt}}\right) \tag{1}$$

with D the diffusion coefficient, t the diffusion time, C the concentration of the solute at distance x from the interface and C_o the interface concentration assumed invarient with time. For an element of width w centered around x the average concentration of the solute is

$$\frac{\bar{C}}{C_o} = \frac{1}{w}\int_{x-\frac{w}{2}}^{x+\frac{w}{2}} \operatorname{erfc}\left(\frac{x'}{2\sqrt{Dt}}\right) dx' \tag{2}$$

Rearranging, equation (2) can be written as

$$\frac{\bar{C}}{C_o} = \frac{1}{2P}\int_{P(\eta-1)}^{P(\eta+1)} \operatorname{erfc}(u)\,du \tag{3}$$

where

$$P = \frac{w}{4\sqrt{Dt}} \quad \text{and} \quad \eta = 2\,\frac{x}{w}$$

The correction factor for using a non zero window to determine the concentration of the solute at a point in the medium is, for $P(\eta-1) \geq 0$,

$$F = \frac{C}{\bar{C}} = \frac{C}{C_o} \cdot \frac{C_o}{\bar{C}} = \frac{\operatorname{erfc}(P\eta)}{\frac{1}{2P}\int_{P(\eta-1)}^{P(\eta+1)} \operatorname{erfc}(u)\,du} \tag{4}$$

Using the error function relationships found in the Appendix of Carslaw and Jaeger,[10] or in AMS 55,[12] the denominator of equation (4) can be written as

$$\frac{1}{2P}\int_{P(\eta-1)}^{P(\eta+1)} \operatorname{erfc}(u)\,du = \frac{1}{2P\sqrt{\pi}}\left[e^{-[P(\eta-1)]^2} - e^{-[P(\eta+1)]^2}\right]$$

$$+\left(\frac{\eta+1}{2}\right)\operatorname{erfc}\left[P(\eta+1)\right]-\left(\frac{\eta-1}{2}\right)\operatorname{erfc}\left[P(\eta-1)\right] \tag{5}$$

Combining equations (4) and (5) the correction factor F is shown as a function of η for several values of P in Fig. 51, and as a function of P for several values of η in Fig. 52.

These curves can be used to correct data for a given experiment, or, perhaps even better, they can be used to design a more meaningful diffusion experiment. For an experiment checking for an expected order of magnitude diffusion coefficient, the element length and test time can be varied so that

$$P = \frac{w}{2(Dt)^{1/2}}$$

can be made small so the measuring precision which determines the maximum product $P\eta$ will give an arbitrarily small error from the element length effect at the maximum $P\eta$.

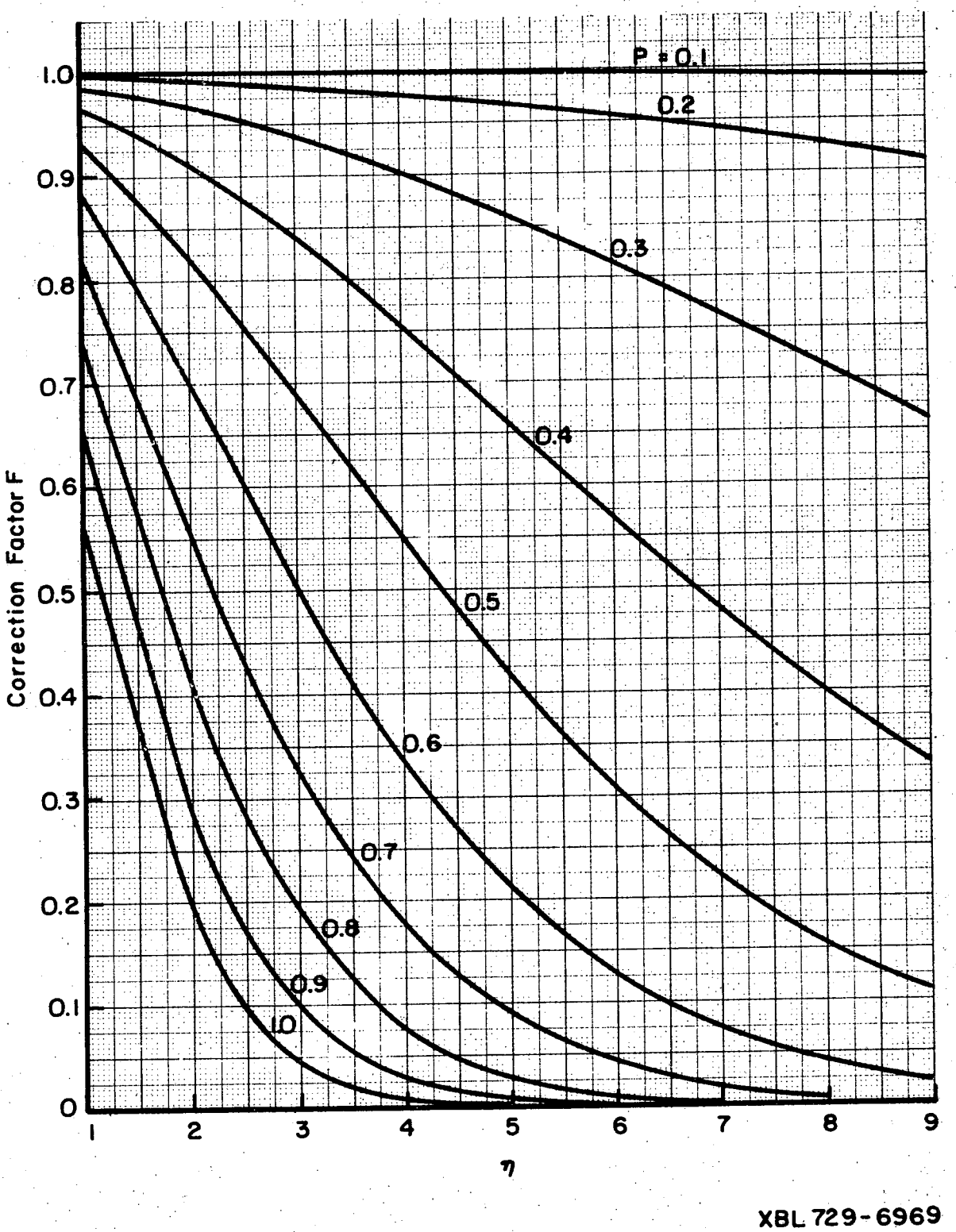

Fig. 51. Correction factor for use of a non zero width window to find the concentration of a solute at a point on a medium where the concentration is a complementary error function distribution.

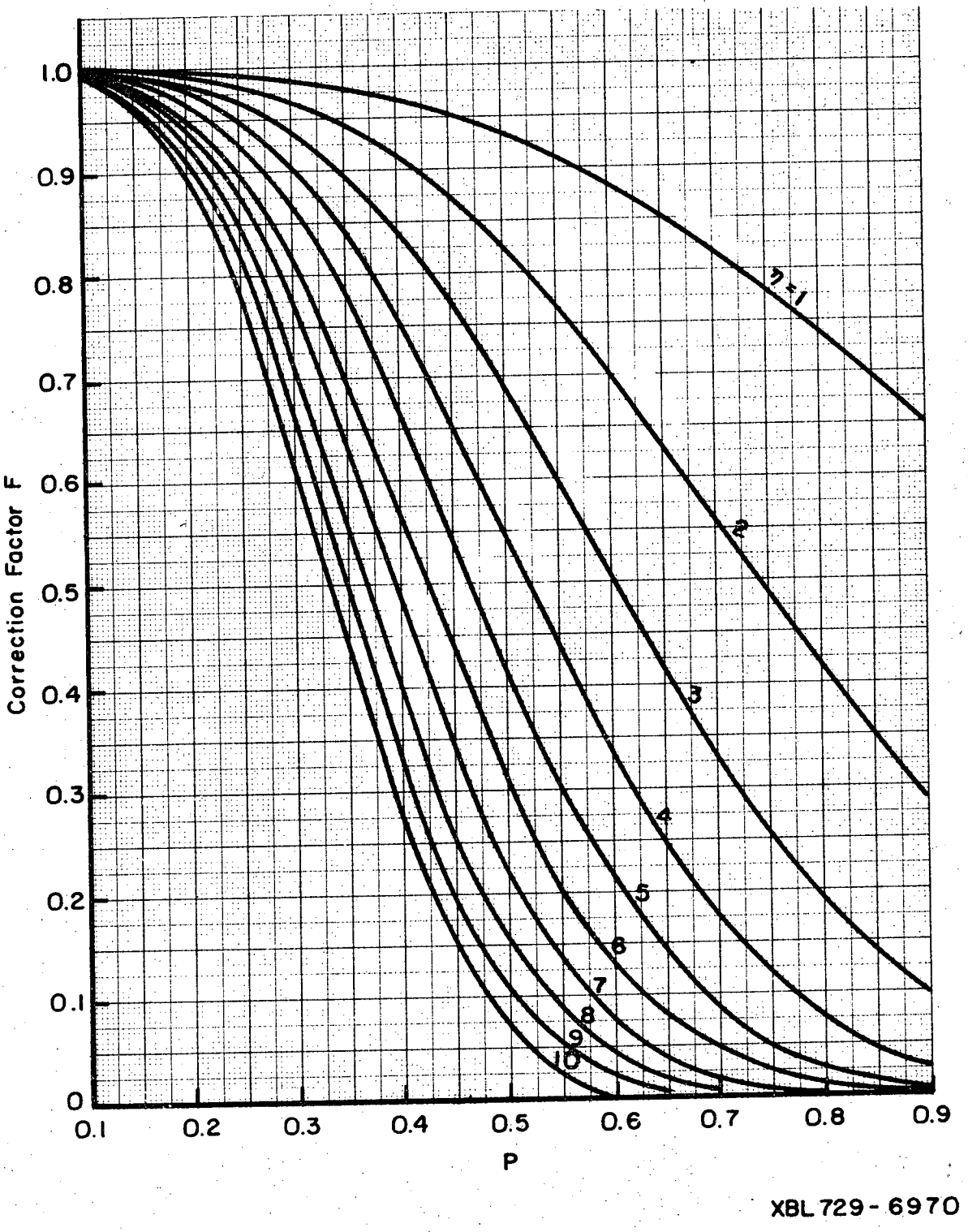

Fig. 52. Correction factor for use of a non zero width window to find the concentration of a solute at a point in a medium where the concentration is a complementary error function distribution.

APPENDIX XII

An Estimate of the Gap Size, Vertical Flow and Diffusion of Lanthanum at the Uranium-Beryllia Crucible Interface During Start-Up and the Diffusion Run

A. Gap Size Estimate and Effect on Measured Saturation Concentration of Lanthanum in Molten Uranium

Assume that during cooling of the pre-diffusion melt the beryllia crucible has cooled to room temperature while the uranium remains completely molten. Upon solidification the change in volume of the uranium relative to its volume as a liquid at the melting point is

$$\frac{\delta V}{V} = 1 - \frac{\rho_\ell}{\rho_s} = \frac{2\delta}{r} + \frac{\delta \ell}{\ell} \qquad (1)$$

where ℓ and r are the dimension of the liquid uranium melt and ρ_ℓ and ρ_s are the densities of the liquid and solid uranium respectively. Assuming the change in uranium volume during solidification and cool-down as isotropic such that

$$\frac{\delta r}{r} = \frac{\delta \ell}{\ell}$$

then the gap between the ingot of solid uranium and the beryllia crucible is given by

$$\delta r = \frac{r}{3}\left(1 - \frac{\rho_L}{\rho_s}\right) \qquad (2)$$

The maximum gap will occur if the crucible temperature increases suddenly to 1200°C from 20°C during the diffusion melt start-up, while the uranium ingot remains at room temperature. This gap is

$$\delta r = \left[\left(\alpha\Delta T\right) + \frac{1}{3}\left(1 - \frac{\rho_L}{\rho_s}\right)\right] r \qquad (3)$$

where $\alpha\Delta T$ is the linear expansion of the beryllia.

The density of liquid uranium is cited by Finucane as

$$\rho = 19.083 - 16.01 \times 10^{-4}\ T$$

where ρ is in grams per cubic centimeter and T is in degrees C. For liquid uranium at the melting point (1132°C), ρ = 17.27 g/cc and for solid uranium at 20°C, ρ = 19.06 g/cc. Lillie[27] cites the linear expansion of beryllia as 11.3×10^4 microunits per unit at 1200°C. Thus the maximum possible radial gap between the 3.18 millimeter inner diameter of the beryllia crucible and the uranium ingot is

$$\delta r = 0.068 \text{ millimeter}$$

If we assume the gap is filled with lanthanum, then the counting apparatus will count the lanthanum in solution in the uranium plus the activated lanthanum in the gap. Thus the measured activity is

$$A_m = A^* \frac{\delta r}{d} + A_o \qquad (4)$$

where A_o is the activity of the lanthanum in the saturated solution, and A^* is the activity of the pure lanthanum, and d is the diameter of the uranium ingot. Rewriting,

$$\frac{A_m}{A_o} = \frac{\delta r}{d}\frac{A^*}{A_o} + 1 = \frac{\rho_u S + \rho_L}{\rho_u S} \cdot \frac{\delta r}{d} + 1 \qquad (5)$$

where ρ_u and ρ_L are the densities of the uranium and lanthanum respectively, and S is the solubility limit of lanthanum in uranium expressed as a weight fraction. For the maximum gap described above, with S = 0.0081 as given by Haefling and Daane, and the density of 6.19 and 19.06 grams per cubic centimeter for lanthanum and uranium respectively,

$$\frac{A_m}{A_o} = 1.88$$

Thus the measured saturated concentration of lanthanum in uranium will be less than twice as high than the actual saturated concentration.

B. Vertical Flow Estimate of Lanthanum Submerged in Molten Uranium

Now assuming there is a gap effect, an estimate of the time required for the low density lanthanum to rise to the surface of the high density uranium is in order. Assume that the lanthanum behaves as a solid sphere in an infinite high density medium. Note this assumption ignores boundary layer effects of the lanthanum against the crucible and viscosity effects in the lanthanum sphere. These effects may have a large effect on the real time for the lanthanum to rise to the surface. Also assume the lanthanum does not diffuse into the uranium while it is rising to the surface, or react with the beryllia crucible. The effect of diffusion into the uranium or the crucible will tend to increase an apparent diffusion coefficient.

The force balance on the low density sphere is

$$\frac{\rho_L r^3}{g} \frac{d^2x}{dt^2} = r^3\rho_U - \frac{3}{4} C_D \frac{r^2\rho_U}{2g} \left(\frac{dx}{dt}\right)^2 \qquad (6)$$

where C_D is the drag coefficient of the sphere through the dense fluid, r is the radius of the sphere, ρ_L is the density of the sphere, and ρ_u is the density of the fluid. For small Reynolds numbers, Re < 1

$$C_D = \frac{24}{Re} = 24\left(\frac{2r\rho_u}{\mu_u g} \cdot \frac{dx}{dt}\right)^{-1} \tag{7}$$

where μ_u is the viscosity of the dense fluid. Thus the force balance can be written as

$$\frac{d^2x}{dt^2} + \frac{9}{2}\frac{g}{r^2}\left(\frac{\rho_u}{\rho_L}\right)\left(\frac{\mu_u}{\rho_u}\right)\frac{dx}{dt} = g\left(\frac{\rho_u}{\rho_L}\right) \tag{8}$$

The solution to the force balance can be written as

$$x(t) = C_1 + \frac{2}{9}\left(\frac{\rho_u}{\mu_u}\right)r^2 t + C_2 \exp\left[-\frac{9}{2}\left(\frac{\rho_u}{\rho_L}\right)\left(\frac{\mu_u}{\rho_u}\right)\frac{gt}{r^2}\right] \tag{9}$$

For the initial conditions that $\dot{x}(0) = x(0) = 0$, the above equation becomes

$$x(t) = \frac{4r^4}{81g}\left(\frac{\rho_u}{\mu_u}\right)^2\left(\frac{\rho_L}{\rho_u}\right)\left\{\frac{9}{2}\left(\frac{\rho_u}{\rho_L}\right)\left(\frac{\mu_u}{\rho_u}\right)\frac{gt}{r^2} - 1 + \exp\left[-\frac{9}{2}\left(\frac{\rho_u}{\rho_L}\right)\left(\frac{\mu_u}{\rho_u}\right)\frac{gt}{r^2}\right]\right\} \tag{10}$$

The above equation can be used to estimate the time required for lanthanum in the gap at the bottom of the crucible to rise a distance x from the bottom for a given melt temperature. The velocity and the Reynolds number of the sphere are respectively

$$\dot{x}(t) = \frac{2}{9}r^2\left(\frac{\rho_u}{\mu_u}\right)\left\{1 - \exp\left[-\frac{9}{2}\left(\frac{\rho_u}{\rho_L}\right)\left(\frac{\mu_u}{\rho_u}\right)\frac{gt}{r^2}\right]\right\} \tag{11}$$

$$Re(t) = \frac{4}{9}\frac{r^3}{g}\left(\frac{\rho_u}{\mu_u}\right)^2 \left\{ 1 - \exp\left[-\frac{9}{2}\left(\frac{\rho_u}{\rho_L}\right)\left(\frac{\mu_u}{\rho_u}\right)\frac{gt}{r^2}\right]\right\} \qquad (12)$$

For the ratio

$$\frac{9}{2}\left(\frac{\rho_u}{\rho_L}\right)\left(\frac{\mu_u}{\rho_u}\right)\frac{tg}{r^2} > 3$$

the Reynolds number and the distance moved by the lanthanum as a function of time can be approximated with less than 5% error by

$$x(t) = \frac{4r^4}{81g}\left(\frac{\rho_u}{\mu_u}\right)^2\left(\frac{\rho_L}{\rho_u}\right)\left\{\frac{9}{2}\left(\frac{\rho_u}{\rho_L}\right)\left(\frac{\mu_u}{\rho_u}\right)\frac{gt}{r^2} - 1\right\} \qquad (13)$$

$$Re = \frac{4}{9}\frac{r^3}{g}\left(\frac{\rho_u}{\mu_u}\right)^2 \qquad (14)$$

At 1200°C the following properties will be assumed:

ρ_u = 17.27 g/cc

μ_u = 0.09 g/cm-sec

$\rho_L = (6.24 - 2.37\times10^{-4}T) \pm 0.01$, T in °K [23]

= 5.89 g/cc

For a maximum radius of 0.0034 centimeters, the above approximation are appropriate for times greater than 5×10^{-7} seconds. The Reynolds number is a maximum for the maximum lanthanum particle size, so that

$Re < 4.4 \times 10^{-1}$

so that the movement of the lanthanum is within the Stoke's flow regime.

For times greater than 2×10^{-5} seconds the distance the lanthanum rises is, within an error of less than 1%

$$x(t) = \frac{2}{9}\left(\frac{\rho_u}{\mu_u}\right) r^2 t = 42.6\ r^2 t \tag{15}$$

$$\dot{x}(t) = \frac{2}{9}\left(\frac{\rho_u}{\mu_u}\right) r^2 = 42.6\ r^2 \tag{16}$$

C. Radial Diffusion of Lanthanum in the Uranium-Beryllia Gap into the Molten Uranium Ingot

Consider the effect of diffusion from a gap filled with lanthanum surrounding an initially lanthanum free uranium ingot. For an infinitely long cylinder with no axial gradient the diffusion equation is

$$\frac{\partial c}{\partial t} = D\left[\frac{1}{r}\ \frac{\partial}{\partial r}\ \left(r\ \frac{\partial c}{\partial r}\right)\right] \tag{17}$$

Assuming that initially there is no lanthanum in the uranium and that the concentration of lanthanum at the surface remains constant at the saturation concentration of lanthanum in uranium, the initial and boundary conditions can be written as

$$\begin{aligned} C(r,0) &= 0 \\ C(a,t) &= C_o \end{aligned} \tag{18}$$

where C_o is the saturated concentration and a is the radius of the ingot. From Carslaw and Jaeger, the concentration of lanthanum in the uranium as a function of time and position is given by

$$\frac{C(r,t)}{C_o} = 1 - 2\sum_{n=1}^{\infty} e^{-\beta_n^2 T}\ \frac{J_o(r\beta_n/a)}{\beta_n J_1(\beta_n)} \tag{19}$$

where β_n, $n = 1,2,\cdots$ are roots of

$$J_o(\beta) = 0 \tag{20}$$

$J_o(x)$, $J_1(x)$ are the zeroth and first order of the Bessel function of the first kind. Note that T is a dimensionless time defined as

$$T = \frac{Dt}{a^2}$$

where D is the diffusion coefficient of lanthanum in molten uranium. The average concentration of lanthanum in the molten uranium can be found from

$$\frac{\bar{C}(t)}{C_o} = \frac{2}{a^2} \int_o^a \frac{r\, C(r,t)}{C_o}\, dr \tag{21}$$

So that

$$\frac{\bar{C}(t)}{C_o} = 1 - 4 \sum_{n=1}^{\infty} \frac{e^{-\beta_n^2 T}}{\beta_n^2} \tag{22}$$

Carslaw and Jaeger have curves of the average and center concentrations as a function of the dimensionless time T. For example, for an average concentration of 0.5, the dimensionless time is 0.06 and the center concentration is 0.03, i.e.

$$\frac{\bar{C}(t)}{C_o} = 0.5; \quad \frac{C(0,t)}{C_o} = 0.03, \quad \frac{Dt}{a^2} = 0.06$$

Thus for a 0.318 centimeter diameter uranium ingot the time required to achieve an average concentration of lanthanum in the molten uranium of 50% of the saturation concentration is

$$t = \frac{.0015}{D} \quad \text{seconds} \tag{23}$$

For a diffusion coefficient of between 10^{-7} centimeter squared per second and 10^{-4} centimeters squared per second the time required for a 50% average saturated concentration is between roughly 15 seconds and 4 hours.

APPENDIX XIII

Thermodynamic Stability of Lanthanum Dissolved In Uranium In a Beryllia Crucible at 1200°C

The formation reactions of lanthana and beryllia are

$$\frac{4}{3}\,La(s) + O_2(g) = \frac{2}{3}\,La_2O_3(s) \qquad (1)$$

$$2\,Be(s) + O_2(g) = 2\,BeO(s) \qquad (2)$$

with ΔG_1^o and ΔG_2^o the standard free energy change of lanthana and beryllia respectively. Subtracting Eq. (2) from Eq. (1)

$$\frac{4}{3}\,La(s) + 2\,BeO(s) = \frac{2}{3}\,La_2O_3(s) + 2\,Be(s) \qquad (3)$$

with the standard free energy change

$$\Delta G_3^o = \Delta G_1^o - \Delta G_2^o$$

The equilibrium constant for the reaction

$$\frac{4}{3}\,La(\text{liq. sol'n}) + 2\,BeO(s) = \frac{2}{3}\,La_2O_3(s) + 2\,Be(\text{liq. sol'n}) \qquad (4)$$

is

$$K = e^{-\Delta G_3^o/RT}$$

Consider a solution initially containing an atom fraction x_{La}^o of lanthanum dissolved in uranium. From Eq. (3), for every gram atom of lanthanum removed from the solution, 1.5 gram atoms of beryllium are produced. Therefore if x_{La} is the final concentration of lanthanum in the solution, then

$$x_{Be} = \frac{3}{2}(x_{La}^o - x_{La})$$

is the final concentration of beryllium in the solution.

The equilibrium concentration of the various species when the lanthanum and beryllium are in solution is determined by the law of mass action for reaction (4).

$$K = \frac{a_{Be}^{2}\, a_{La_2O_3}^{2/3}}{a_{La}^{4/3}\, a_{BeO}^{2}}$$

where a_i is the activity of component i. For an activity coefficient γ_i such that

$$a_i = \gamma_i x_i$$

where x_i is the atom fraction of component i,

$$K^{3/4} = \frac{a_{Be}^{3/2}}{a_{La}} = \frac{\gamma_{Be}^{3/2}}{\gamma_{La}} \cdot \frac{x_{Ba}^{3/2}}{x_{La}}$$

assuming the beryllia and the lanthana are immiscible in the solution and in each other such that

$$a_{La_2O_3} = a_{BeO} = 1 \ .$$

Thus

$$\frac{\gamma_{La}}{\gamma_{Be}^{3/2}}\ K^{3/4} = \frac{1.5^{3/2}(x_{La}^{o}-x_{La})^{3/2}}{x_{La}}$$

$$= 1.5^{3/2}(x_{La}^{o})^{1/2}\ \frac{(1-f)^{3/2}}{f}$$

where

$$f = \frac{x_{La}}{x_{La}^{o}} = \text{fraction of lanthanum remaining.}$$

Thus

$$\frac{(1-f)^{3/2}}{f} = \frac{1}{1.5^{3/2}(x_{La}^{o})^{1/2}} \frac{\gamma_{La}}{\gamma_{BeO}^{3/2}} K^{3/4}$$

The activity of the lanthanum in the uranium is the same as the activity of the lanthanum in the lanthanum, i.e.,

$$a_{La}^{(U)} = a_{La}^{(La)} = 1 = \gamma_{La} x_{La}$$

where x_{La} is the solubility of lanthanum in uranium. From Haefling and Daane the solubility of lanthanum in uranium at 1200°C is 0.81 wt.%, or an atom fraction of 0.0139. Thus

$$\gamma_{La} = \frac{1}{x_{La}} = 72$$

Likewise for the atom fraction solubility of beryllium in uranium of 0.05 as cited in Hansen and Anderko,[29]

$$\gamma_{Be} = 20$$

Thus,

$$\frac{(1-f)^{3/2}}{f} = 3.73\, K^{3/4}$$

From Darras and Loriers,[30] with

$$\Delta G_3^{o} = 2.3 \text{ kcal/mole}$$

at 1200°C, the equilibrium constant for Eq. (3) becomes

$$K = 0.456$$

$$\frac{(1-f)^{3/2}}{f} = 2.1$$

Thus the fraction of lanthanum remaining in solution in the uranium at 1200°C is 0.29 of the initial amount of lanthanum in solution.

Since ΔG_3^o is positive, which implies that work must be done on the system for the reaction described by Eq. (3) to take place, the reaction may not take place. However, if the reaction does take place the lanthanum is not stable in solution in uranium contained in beryllia crucible at 1200°C, and the diffusion coefficient of lanthanum in molten uranium measured experimentally using beryllia crucibles is less than the true diffusion coefficient. Also the measured solubility of lanthanum in uranium at 1200°C measured using counting of the activity of activated lanthanum may be greater than the true solubility.

APPENDIX XIV

An Estimation of the Diffusion and Concentration Of Lanthanum Dissolved in Liquid Uranium Into and Reacting with a Beryllia Crucible

Consider the uranium-lanthanum solution just below the lanthanum uranium interface where the lanthanum concentration is maintained at an atom fraction of 0.0139 by the presence of the liquid lanthanum above the interface. Assume that at this position the inner surface is converted completely to lanthana by the reaction

$$\frac{4}{3}\ \text{La (sol'n)} + 2\ \text{BeO(s)} = \frac{2}{3}\ \text{La}_2\text{O}_3\text{(s)} + 2\ \text{Be (sol'n)}$$

Since the density of lanthana is 6.51 grams per cubic centimeter, and its molecular weight is 326, the concentration of the lanthanum in the ceramic at the uranium-beryllia interface is

$$C_L^o = \frac{2\times 6.51}{326} = 0.04\ \frac{\text{gram atoms La}}{\text{cc La}_2\text{O}_3}$$

Assume that during the diffusion run the lanthanum diffuses into the beryllia. Assuming that the penetration distance of the lanthanum into the beryllia crucible is small compared to the inner radius of the crucible, the lanthanum concentration profile in the beryllia is approximately

$$\frac{C_{La}(y)}{C_{La}^o} = \text{erfc}\left(\frac{y}{2\sqrt{D_L t}}\right)$$

where D_L is the diffusion coefficient of lanthanum ions in the beryllia-lanthana solid solution.

Now consider a unit height of the beryllia crucible just below the lanthanum-uranium interface. At time t after diffusion starts the total amount of lanthanum in the beryllia is given by

$$La_{BeO} = (2\pi a)\int_o^\infty C_{La}(y)dy = (2\pi a)\ 2\sqrt{D_L t}\ C^o_{La}\int_o^\infty \text{erfc}(u)dy$$

$$= 4\pi a\ \sqrt{D_L t}\ C^o_{La}\ \text{ierfc}\ (0)$$

$$= 4a\ \sqrt{\pi D_L t}\ C^o_{La}$$

from Appendix XI, where a is the crucible inner radius.

Since the lanthanum concentration in the uranium just below the lanthanum-uranium interface is at the saturation value x_{La} for all time, the total lanthanum per unit height in the uranium is given by

$$La_U = \frac{\rho_U}{238}\ x_{La}\pi a^2$$

Thus the ratio of lanthanum in the beryllia to that in the uranium at the lanthanum-uranium interface is

$$\frac{La_{BeO}}{La_U} = 4 \times 238\ \frac{C^o_{La}}{\rho_u x_{La}}\sqrt{\frac{D_L t}{\pi a^2}}$$

For $\rho_u = 19$, $C^o_{La} = 0.04$ and $x_{La} = 0.0139$,

$$\frac{La_{BeO}}{La_U} \approx 81\sqrt{\frac{D_L t}{a^2}}$$

Now assuming the diffusion coefficient of lanthanum into the beryllia at 1200°C is of the same order as that given by Condits and Hashimoto[31] for beryllium diffusing into beryllia, then

$$D_L \sim 10^{-12} \text{ cm}^2/\text{sec}$$

The inner radius of the beryllia crucible is roughly 0.16 centimeters. For a diffusion time of 16 hours (5.8×10^4 seconds),

$$\frac{La_{BeO}}{La_U} \approx 0.12$$

The penetration depth of the lanthanum in beryllia can be defined as the distance which contains 99.999% of the lanthanum in the beryllia. This distance occurs when

$$\frac{y_P}{2\sqrt{D_L t}} = 2.92$$

Thus, for the diffusion runs the penetration depth is roughly 14 microns, which is small compared to the inner radius of the beryllia crucible.

REFERENCES

1. Tennyson Smith, Diffusion of Cerium and Zirconium in Molten Uranium, J. Electrochem. Soc. 106, 1046 (1959).

2. A. M. Weinberg and E. P. Wigner, The Physical Theory of Neutron Chain Reactors (University of Chicago Press, 1958).

3. Edmond LeBorgne, Lanthanum Diffusion in Molten Uranium, UCRL-19072, October 1969.

4. D. A. Morgan and J. A. Kitchener, Solutions in Liquid Iron, Part 3--Diffusion of Cobalt and Carbon, Trans. Faraday Soc. 50, 51 (1954).

5. A. W. Castleman, Jr. and J. J. Conti, On Diffusion in Liquid Metals, BNL-14077, 1970.

6. R. B. Bird, J. O. Hirschfelder and C. F. Curtiss, The Equation of State and Transport Properties of Gases and Liquids, Handbook of Physics (McGraw-Hill, 1958).

7. D. R. Olander and A. D. Pasternak, Mass Transfer and Transport Properties in Fused Salt and Liquid Metal Systems, in Proceedings of the Symposium on Reprocessing of Nuclear Fuels, Ames, Iowa, 1969 (CONF-690801) p. 467.

8. A. D. Pasternak and D. R. Olander, Diffusion in Liquid Metals, A.I.Ch.E. Journal 13, 1052 (1967).

9. D. R. Olander, Mutual Diffusion in Dilute Binary Systems, A.I.Ch.E. Journal 9, 207 (1963).

10. H. S. Carslaw and J. C. Jaeger, Conduction of Heat in Solids, (Oxford, 1959).

11. J. S. Finucane, Viscosity of Uranium Metal and Some Uranium Chromium Alloys, UCRL-16988, May 1969.

12. Walter Gautschi, Error Function and Fresnel Integrals in Handbook of Mathematical Functions, AMS 55, National Bureau of Standards, August 1966.

13. I. A. Stegun and Ruth Zucker, Automatic Computing Methods for Special Functions, Journal of Research of the National Bureau of Standards, Vol. 74B, No. 3, 1970.

14. J. F. Haefling and A. H. Danne, The Immiscibility Limits of Uranium with the Rare Earth Metals, Trans. Met. Soc. AIME 215, 336 (1959).

15. H. M. Eikenberry and G. A. Graman, Solidification Mechanism of Uranium Ingots, NLCO-1077, August 1971.

16. G. R. Pulliam and E. S. Fitzsimmons, Reactions of Cerium and Lanthanum with Ceramic Oxides, ISC-659, 1955.

17. A. B. McIntosh and K. Q. Bagley, Selection of Canning Materials for Reactors Cooled by Sodium/Potassium and Carbon Dioxide, J. Inst. Metals 84, 251 (1956).

18. H. F. Hsu and S. H. Wang, Gamma Ray Spectroscopy and Radioactive Decay, Experiment 2, U.C. Berkeley NE 201 Report, October 1968.

19. D. R. Olander, Encapsulation Procedures for La^{140} in E-192, Berkeley Nuclear Engineering Department Memorandum, Sept. 28, 1970.

20. Edmond LeBorgne and D. R. Olander, Diffusion in Liquid Uranium; Log Book, August 4, 1969.

21. Jack L. Hile, Radiographic Inspection Uranium Rods Items: 1 through 4, LRL Livermore Memorandum, Sept. 3, 1970.

22. J. W. Fisher, Verbal Presentation of Results of Vacuum Diffusion Experiment.

23. J. M. Johnson, Electron Beam Microprobe Analysis of Metallography Samples 1929 and 1930, LRL Livermore Memorandum, Oct. 20, 1970.

24. W. D. Wilkinson, Uranium Metallurgy Vol. II (Interscience, 1962).

25. B. Blumenthal, Refining Uranium by Melting and Liquation, ANL-5348, 1955.

26. C. H. Schramm, P. Gordon and A. R. Kaufmann, The Alloy Systems Uranium-Tungsten, Uranium-Tantalum and Tungsten-Tantalum, Trans. AIME, J. of Metals, 188, 195 (1950).

27. J. Lillie, Some Properties of Beryllium Oxide, UCRL-6457, May 1961.

28. L. J. Wittenberg, D. Ofte and W. G. Rohr, The Viscosity and Density of Molten Lanthanum, Cerium and Praseodymium Metals, Rare Earth Research II, Proceedings of the Third Conference on Rare Earth Research, April 21-24, 1963 (Gordon and Breach, New York, 1964).

29. Max Hansen and Kurt Anderko, Constitution of Binary Alloys, 2nd edition (McGraw Hill, 1958) 299.

30. R. Darras and H. Loriers, Diagrammes de Variations D'Energie Libre de Formation des Composes Metalliques, CEA Report 1582, 1960.

31. R. H. Condit and Y. Hashimoto, Self Diffusion of Beryllium in Polycrystalline Beryllium Oxide, J. Am. Ceram. Soc. 50, (8)423 (1967).

TECHNICAL INFORMATION DIVISION
LAWRENCE BERKELEY LABORATORY
UNIVERSITY OF CALIFORNIA
BERKELEY, CALIFORNIA 94720